

# Angles from $B$ Decays with Charm

G. Cavoto,<sup>1</sup> R. Fleischer,<sup>2</sup> T. Gershon,<sup>3,4,5</sup> A. Soni,<sup>6</sup> [conveners]

K. Abe,<sup>3</sup> J. Albert,<sup>7</sup> D. Asner,<sup>8</sup> D. Atwood,<sup>9</sup> M. Bruinsma,<sup>10</sup> S. Ganzhur,<sup>11</sup> B. Iyutin,<sup>12</sup>  
Y.Y. Keum,<sup>13</sup> T. Mannel,<sup>14</sup> K. Miyabayashi,<sup>15</sup> N. Neri,<sup>16</sup> A.A. Petrov,<sup>17</sup> M. Pierini,<sup>18</sup> F. Polci,<sup>1</sup>  
M. Rama,<sup>19</sup> F. Ronga,<sup>3</sup> L. Silvestrini,<sup>1</sup> A. Stocchi,<sup>20</sup> M.H. Schune,<sup>20</sup> V. Sordini,<sup>1,20</sup>  
M. Verderi,<sup>21</sup> C. Voena,<sup>1</sup> G. Wilkinson,<sup>22</sup> J. Zupan,<sup>23,24</sup>

<sup>1</sup> *Università di Roma La Sapienza, Dipartimento di Fisica and INFN, I-00185 Roma, Italy*

<sup>2</sup> *CERN, Department of Physics, Theory Division, CH-1211 Geneva 23, Switzerland*

<sup>3</sup> *High Energy Accelerator Research Organization (KEK), Tsukuba, Japan*

<sup>4</sup> *Department of Physics, University of Tokyo, Tokyo, Japan*

<sup>5</sup> *Department of Physics, University of Warwick, Coventry, CV4 7AL, UK*

<sup>6</sup> *Physics Department, Brookhaven National Laboratory, Upton, New York 11973, USA*

<sup>7</sup> *California Institute of Technology, Pasadena, California, 91125, USA*

<sup>8</sup> *Carleton University, Ottawa, Ontario, K1S 5B6, Canada*

<sup>9</sup> *Dept. of Physics and Astronomy, Iowa State University, Ames, Iowa 50011, USA*

<sup>10</sup> *University of California at Irvine, Irvine, California 92697, USA*

<sup>11</sup> *DSM/Dapnia, CEA/Saclay, F-91191, Gif-sur-Yvette, France*

<sup>12</sup> *Massachusetts Institute of Technology, Cambridge, MA 02139, USA*

<sup>13</sup> *Department of Physics, National Taiwan University, Taipei, 106 Taiwan, ROC*

<sup>14</sup> *Theoretische Physik 1, Fachbereich Physik, Universität Siegen, D-57068, Siegen, Germany*

<sup>15</sup> *Nara Women's University, Nara, Japan*

<sup>16</sup> *Università di Pisa, Dipartimento di Fisica, Scuola Normale Superiore and INFN, I-56127  
Pisa, Italy*

<sup>17</sup> *Dept. of Physics and Astronomy, Wayne State University, Detroit, Michigan 48201, USA*

<sup>18</sup> *University of Wisconsin, Madison, Wisconsin 53706, USA*

<sup>19</sup> *Laboratori Nazionali di Frascati dell'INFN, I-00044, Frascati, Italy*

<sup>20</sup> *Laboratoire de l'Accélérateur Linéaire, F-91898 Orsay, France*

<sup>21</sup> *Ecole Polytechnique, LLR, F-91128 Palaiseau, France*

<sup>22</sup> *University of Oxford, 1, Keble Road, Oxford OX1 3NP, UK*

<sup>23</sup> *J. Stefan Institute, Jamova 39, P.O.Box 3000, Ljubljana, Slovenia*

<sup>24</sup> *Department of Physics, Carnegie Mellon University, Pittsburgh, PA 15213, USA*

## Abstract

Proceedings of the CKM 2005 Workshop (WG5), UC San Diego, 15-18 March 2005.

# WG5: Angles from $B$ Decays with Charm

## Charge:

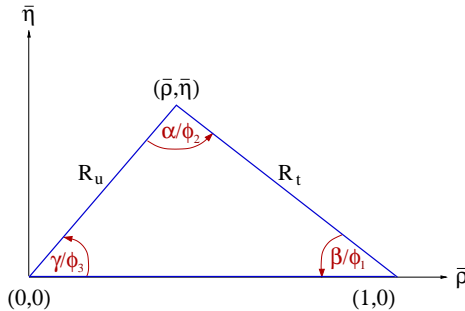
The main goal is the measurement of the angles  $\gamma$  and  $\beta$  from  $B$  decays involving  $D$  or charmonium mesons. The limitations and ways to overcome them will be discussed, as well as new approaches and high statistics projections.

## Introduction

This report is a summary of the activities of Working Group 5 of the CKM2005 Workshop on the Unitarity Triangle (UT), which took place in San Diego, California, from 15–18 March 2005. The main goal of this Working Group was the determination of the UT angles  $\beta/\phi_1$  and  $\gamma/\phi_3$  from  $B$  meson decays into final states with charm. These determinations play a key role for the experimental testing of the Kobayashi–Maskawa (KM) mechanism of CP violation, which has already reached an impressive level thanks to the great efforts of the BaBar and Belle collaborations at the SLAC and KEK  $B$  factories, respectively.

The outline of this report is as follows: after this introduction, a table is provided, listing the talks at the San Diego meeting. An executive summary provides a brief overview of the activities of the Working Group. This summary describes the current status, both experimental and theoretical, and includes an outlook to the future reach of the measurements. More detailed information and references can be found in the the collated contributions at the end of the document.

## Dictionary:



$$\alpha \equiv \phi_2 = \arg \left[ -\frac{V_{td}V_{tb}^*}{V_{ud}V_{ub}^*} \right]$$

$$\beta \equiv \phi_1 = \arg \left[ -\frac{V_{cd}V_{cb}^*}{V_{td}V_{tb}^*} \right]$$

$$\gamma \equiv \phi_3 = \arg \left[ -\frac{V_{ud}V_{ub}^*}{V_{cd}V_{cb}^*} \right]$$

## Talks given in Working Group 5 at the San Diego meeting.

sin( $2\beta$ ) in Charmonium Modes and Discussion of Experimental Analysis Techniques	
T. Mannel	Theory of the golden mode
T. Browder	Review of charmonium kaon analysis in Belle
D. Lange	Review of charmonium kaon analysis in BaBar
W.T. Ford	Experimental approaches in BaBar $CP$ measurements
A. Kusaka	Vertexing technique in Belle
K. Sumisawa	Background suppression in Belle
Measurements related to $\beta$	
M. Verderi	cos( $2\beta$ ) with $B_d \rightarrow J/\psi K^*$ Experimental Review
K. Miyabayashi	$CP$ in $b \rightarrow c\bar{c}d$ review
R. Jesik	$B_s \rightarrow J/\psi\phi$ status at Tevatron
T. Gershon	Feasibility of $\beta$ measurement with $B_d \rightarrow D\pi^0$
M. Bruinsma	$B \rightarrow$ double charm status in BaBar
B. Iyutin	$B_s \rightarrow$ double charm status at CDF
J. Albert	$\gamma$ from $B \rightarrow D^{(*)}D^{(*)}$
Measurements of sin( $2\beta + \gamma$ )	
S. Ganzhur	BaBar status and prospects for $CP$ asymmetry measurements
F. Ronga	Belle status and prospects for $CP$ asymmetry measurements
C. Voena	Extraction of $2\beta + \gamma$ from $B \rightarrow D^{(*)}\pi$
M. Baak	$B \rightarrow D^*\rho$ feasibility study
F. Polci	$2\beta + \gamma$ from $B \rightarrow D^+ K_S \pi^-$
V. Sordini	$2\beta + \gamma$ from $B \rightarrow D^0 K^{(0/+)}$
Y.Y. Keum	$\gamma$ with PQCD
G. Wilkinson	$B_s \rightarrow D_s K$ etc. at LHCb
C. Ferretti	$\Lambda_b \rightarrow J/\psi \Lambda^0$ feasibility study at ATLAS
$\gamma$ from $B \rightarrow DK$ decay modes	
D. Atwood	Combined strategies for $\gamma$
K. Trabelsi	Belle status and prospects
M. Rama	BaBar status and prospects
Y. Grossman	Methods to extract $\gamma$ with $B \rightarrow DK$ modes
A. Petrov	Charm input for $\beta$ and $\gamma$ measurement, theory
D. Asner	Charm input for $\beta$ and $\gamma$ measurement, experiment
R. Fleischer	$\gamma$ from $B_c$ decays
$\gamma$ from $B \rightarrow DK$ with $D$ Dalitz analysis	
J. Zupan	Theory introduction
K. Abe	Belle status and prospects
M.H. Schune	BaBar status and prospects
N. Neri	Statistical treatment in BaBar $DK$ Dalitz analysis
D. Asner	Experimental Input from CLEO-c
Q. Zeng	$D \rightarrow \pi^+ \pi^- \pi^0$ feasibility study
A. Soni	WG5 summary talk

Links to these talks are available at [http://ckm2005.ucsd.edu/WG/WG5/allWG5\\_sessions.php](http://ckm2005.ucsd.edu/WG/WG5/allWG5_sessions.php)

## Executive Summary

The leading decay of hadrons containing the  $b$  quark is via the  $b \rightarrow c$  transition. Therefore,  $B$  decays to final states containing either charm or charmonia are abundant, and provide fertile ground for investigations of the phenomenology of the  $B$  system, including properties of the CKM matrix. For example, the flavour-specific semileptonic decays  $b \rightarrow c l \nu$  are used to measure  $B$ - $\bar{B}$  mixing properties (in both  $B_d$  and  $B_s$  systems) such as the mass difference  $\Delta m$  and the parameter of  $CP$  violation in mixing,  $|q/p|$ . Furthermore,  $b \rightarrow c$  transitions to final states consisting of two vector mesons can be used to measure polarization, search for triple-product correlations, and, most notably for the decay  $B_s \rightarrow J/\psi \phi$ , to measure the lifetime difference  $\Delta\Gamma_s/\Gamma_s$ . In addition, the  $b \rightarrow c$  transition is the principal tool to investigate the properties of heavy baryons and hyperons. While the activity of this working group has touched on these areas, the charge restricts the scope to the – nonetheless wide – subject area of measurements of angles of the Unitarity Triangle.

Table 1 lists some of the modes of interest. These modes include measurements of weak phases using both mixing-induced and direct  $CP$  violation. At the top of the list is the so-called “golden mode,”  $B_d \rightarrow J/\psi K_S$ . This mode allows a theoretically clean measurement of  $\sin(2\beta)$ . Although there is a penguin contribution, this amplitude has, dominantly, the same weak phase as the leading tree diagram, and therefore does not cause significant pollution of the result. There has been some recent activity to try to quantify the level of theoretical uncertainty, due to subleading terms in both mixing and decay amplitudes, with the outcome that it is below the level of the current experimental systematic errors – about 0.01 on  $\sin(2\beta)$  – and likely to be much smaller.

Table 1: Quark level transitions of interest. For each, an alternative transition which gives the same final state quarks is given, and whether this alternative is penguin (P), or tree (T) is noted. The CKM suppression, including the phase, of the alternative transition is noted, where for penguin amplitudes short-distance dominance is assumed (only the top quark in the loop is accounted for). Where the alternative is a tree diagram, interference can only occur if the ultimately final state can be produced by both intermediate sets of quarks, which contain  $c\bar{u}$  and  $\bar{c}u$ , respectively.

Transition	Alternative	CKM Suppression	Typical decays
$b \rightarrow c\bar{c}s$	$b \rightarrow sc\bar{c}$ (P)	1	$B_d \rightarrow J/\psi K_S, B_s \rightarrow J/\psi \phi, \dots$
$c\bar{c}d$	$dc\bar{c}$ (P)	$R_t e^{i\beta}$	$B_d \rightarrow J/\psi \pi^0, B_d \rightarrow D^{(*)+} D^{(*)-}, \dots$
$c\bar{u}d$	$u\bar{c}d$ (T)	$\lambda^2 R_u e^{i\gamma}$	$B_d \rightarrow D\pi^0, B_d \rightarrow D^{(*)\pm} \pi^\mp, B_s \rightarrow DK^{(*)}, \dots$
$c\bar{u}s$	$u\bar{c}s$ (T)	$R_u e^{i\gamma}$	$B_{u,d} \rightarrow DK^{(*)}, B_s \rightarrow D\phi, B_s \rightarrow D_s^{(*)\pm} K^\mp \dots$

On the experimental side, this mode is equally golden, with large product branching fractions and a very clean signal when reconstructed via  $J/\psi \rightarrow l^+ l^-$ ,  $K_S \rightarrow \pi^+ \pi^-$  ( $l = e, \mu$ ). The precision of the current results from BaBar and Belle, consequences of the excellent performances of the PEP-II and KEKB accelerators, is such that the systematic errors are no longer very small compared to the statistical errors. Detailed understanding of the uncertainties due to vertexing, resolution, flavour tagging, and so on, will thus continue become more and more important. To reduce these errors, there is particular benefit from the continued operation of both  $B$  factories, since the two collaborations use somewhat different techniques, and much is being learned from discussions and comparisons. The precision of the – already rather mature –

$\sin(2\beta)$  measurements should continue to improve in line with the accumulated luminosity over the next few years. In addition, comparisons of  $\sin(2\beta)$  measured with different final states of the  $b \rightarrow c\bar{c}s$  transition (eg.  $J/\psi K_S, \eta_c K_S, \chi_{c0} K_S$ ) can test some new physics models.

Measurements of  $\sin(2\beta)$  provide constraints corresponding to two bands in the  $(\bar{\rho}, \bar{\eta})$  plane. To remove this ambiguity,  $\cos(2\beta)$  should be measured. In general, where there is interference between  $CP$ -even and  $CP$ -odd final states there will be sensitivity to the cosine of the weak phase. Several methods based on this concept exist in the literature. For example, in the decay  $B_d \rightarrow J/\psi K^*$ , where  $K^* \rightarrow K_S \pi^0$ , different partial waves contributing to the vector-vector final state have different  $CP$  properties, and their interference allows measurement of  $\cos(2\beta)$ . In order to perform this measurement, the relative magnitudes and phases of the contributing partial waves need to be determined, which can be achieved with angular analysis. Furthermore, to determine the sign of  $\cos(2\beta)$ , an ambiguity in the solutions for the strong phase has to be resolved. This can either be taken from theory, under certain assumptions, or (as performed by BaBar) can be extracted from data by exploiting the interference between  $K^*(892) \rightarrow K\pi$  and the contribution from the broad  $K-\pi$  S-wave in the same invariant mass region of  $B \rightarrow J/\psi K\pi$ . Results to date prefer the Standard Model solution  $\cos(2\beta) > 0$ , albeit with rather large uncertainties. Recently, a new method has been proposed, which utilizes the interference pattern in  $D \rightarrow K_S \pi^+ \pi^-$  decay following  $B_d \rightarrow D\pi^0$  (and similar decays). [This method was first discussed in WG5 at CKM2005.] In this case the decay model is fixed from studies of flavour tagged  $D$  mesons (from  $D^{*\pm} \rightarrow D\pi^\pm$ ) decay, and the ambiguity is removed by using Breit-Wigner line-shapes. This method also allows to test the Standard Model prediction that the weak phase measured in  $b \rightarrow c\bar{u}d$  transitions should be the same as that in  $b \rightarrow c\bar{c}s$  decays (ie.  $2\beta$ ). Results from this method are consistent with the Standard Model, and  $\cos(2\beta) < 0$  is now ruled out with greater than 95% confidence.

In the limit of tree dominance, and within the Standard Model,  $B_d$  decays via the  $b \rightarrow c\bar{c}d$  transition also probe  $\sin(2\beta)$ . However, the situation is encumbered by the penguin amplitude, which is not dominated by a single weak phase (the contributions with  $t, c$  and  $u$  quarks in the loop appear at the same level of CKM suppression, so the assumption of short-distance dominance is not well justified). Studies of decays dominated by the  $b \rightarrow d$  penguin amplitude, may provide more information about this contribution. If there is found to be a non-negligible effect due to the weak phase of the penguin, then direct  $CP$  violation may arise, allowing an additional probe of the weak phases involved. To date, measurements of time-dependent  $CP$  violation in  $b \rightarrow c\bar{c}d$  transitions have been performed using  $J/\psi\pi^0, D^+D^-, D^{*\pm}D^\mp$  and  $D^{*+}D^{*-}$ , all of which are consistent with tree-dominance and with the Standard Model. Future updates will reduce the statistically dominated errors on these results, and additional channels may also be added.

The decay  $B_d \rightarrow D^{(*)\pm}\pi^\mp$  can proceed either via the doubly-Cabibbo-suppressed  $b \rightarrow u\bar{c}d$  transition, or by  $B_d-\bar{B}_d$  mixing followed by the Cabibbo-favoured  $\bar{b} \rightarrow \bar{c}u\bar{d}$  transition. The interference of these two amplitudes results in sensitivity to  $\sin(2\beta + \gamma)$ , and the size of the interference effect depends on the ratio of the magnitudes of the two amplitudes (usually denoted  $R_{D^{(*)}\pi}$ ). Although the  $D^{(*)\pm}\pi^\mp$  final states are abundant, the smallness of  $R_{D^{(*)}\pi}$  makes the  $CP$  violation effect hard to measure and, since it must be extracted from a large number of events, sensitive to systematic errors. Furthermore, while there are two observables for each final state, there are also two hadronic parameters ( $R_{D^{(*)}\pi}$  and  $\delta_{D^{(*)}\pi}$ , the strong phase difference between the decay amplitudes), and therefore it is difficult to cleanly extract the weak phase information, although approaches based on, eg., SU(3) symmetry exist. A further complication arises due to

multiple ambiguous solutions. Nonetheless, these modes are being actively pursued experimentally. Both BaBar and Belle have results with  $D^\pm\pi^\mp$  and  $D^{*\pm}\pi^\mp$ ; BaBar have also investigated  $D^\pm\rho^\mp$ . Both experiments have used partial reconstruction techniques (in addition to the conventional full reconstruction) to increase the signal yields in the  $D^{*\pm}\pi^\mp$  channel. Although rather different techniques have been employed, most notably to deal with the troublesome possibility of  $CP$  violation effects on the flavour tagging side of the  $\Upsilon(4S) \rightarrow B\bar{B}$  event, the results are consistent at the current level of precision, which is starting to probe the region where  $CP$  violation effects are expected to be found. Future updates are therefore of great interest, although it will be difficult to continue reducing the systematic uncertainty.

Some related modes may also prove useful to measure  $2\beta + \gamma$ .  $B_d \rightarrow D^{*\pm}\rho^\mp$  has a vector-vector final state, and the interfering amplitudes result in an increased number of observables, so that all parameters can, in principle, be extracted from the data. However, this mode is experimentally challenging, *eg.* the polarization measurement is sensitive to systematic effects, and recent results suggest that the  $CP$  violation effect may be even smaller than previously expected. Larger effects are expected to be found in modes mediated by the  $b \rightarrow c\bar{u}s$  &  $b \rightarrow u\bar{c}s$  transitions, such as  $B_d \rightarrow DK^{(*)}$  and  $B_d \rightarrow D^{(*)\pm}K_S\pi^\mp$  (note that for time-dependent  $CP$  violation effects to arise, the kaon must be reconstructed in a strangeness nonspecific final state). These techniques are currently limited by statistics and, in the latter case, due to lack of knowledge of the resonant structure of the three-body decay. Another interesting mode is  $B_s \rightarrow D_s^{(*)\pm}K^\mp$ . In this case the  $B_s$  mixing phase  $\phi_s$  replaces  $2\beta$ , so the time-dependence probes  $\phi_s + \gamma$ . Since  $R_{D_s^{(*)}K}$  is expected to be reasonably large, there will be sufficient observables to extract all parameters from the data. The problem of multiple solutions remains, however, this can be addressed firstly using additional observables which arise if  $\Delta\Gamma_s/\Gamma_s$  is not small, and secondly using U-spin symmetry, which translates  $s \leftrightarrow d$ , and thus relates  $B_s \rightarrow D_s^{(*)\pm}K^\mp$  to  $B_d \rightarrow D^{(*)\pm}\pi^\mp$ . This symmetry can be applied in various different ways, and mechanisms exist to quantify the uncertainty due to its breaking. This approach looks very promising for the LHCb experiment.

The decays  $B_{u,d} \rightarrow D^{(*)}K^{(*)}$  provide the cleanest method to determine  $\gamma$ . The method employs the interference between  $b \rightarrow c\bar{u}s$  and  $b \rightarrow u\bar{c}s$  when the final state is accessible to both  $D^0$  and  $\bar{D}^0$  mesons. The theoretical uncertainty is completely negligible, and effects due to mixing and  $CP$  violation in the neutral  $D$  sector can be taken into account if they are discovered. As before, there are important hadronic parameters: the ratio of the magnitudes of the two amplitudes and the strong phase difference between them (these are usually denoted  $r_B$  and  $\delta_B$ ), that can be extracted from the data. It is important to emphasise again that this method applies to any final state which is accessible to both  $D^0$  and  $\bar{D}^0$ , and one important way to progress is to add more decay modes. The theoretical framework exists to do so, both for exclusive and inclusive final states. To this end, it is crucial to develop experimental techniques to optimally combine the results from the different modes and obtain the best sensitivity on  $\gamma$ .

The  $B$  decay modes which have been exploited to date are  $B_u^\pm \rightarrow DK^\pm$ ,  $D^*K^\pm$  and  $DK^{*\pm}$ , and in each case the  $D$  decay modes to  $CP$  eigenstates (principally  $K^+K^-$  for  $CP$ -even and  $K_S\pi^0$  for  $CP$ -odd), doubly-Cabibbo-suppressed final states ( $K^\mp\pi^\pm$ ), and multibody final states ( $K_S\pi^+\pi^-$ ) have been used. Although fairly large samples of  $CP$  eigenstate decays have now been accumulated, the statistics are still not sufficient to probe the small  $CP$  violation effect expected ( $r_B \sim O(0.1)$ ). Larger effects are expected using the doubly-Cabibbo-suppressed final state; however no significant signals in  $B_u^\pm \rightarrow [K^\mp\pi^\pm]_D K^\pm$ , and related modes, have yet been observed.

One of the major developments of the  $B$  factories over the past few years has been the use of the multibody decay  $D \rightarrow K_S \pi^+ \pi^-$ . The rich interference pattern across the Dalitz plot results in regions which are highly sensitive to  $\gamma$ ; in addition this mode is reasonably clean experimentally, due to its large product branching fraction and clean signal. However, in order to perform an unbinned fit (necessary to extract the maximum possible information from the data) it is necessary to make an assumption about the strong phase variation across the Dalitz plot (achieved using a sum of resonant amplitudes, parametrized using the Breit-Wigner formalism, and a non-resonant term), which results in model uncertainty, currently estimated to be  $\sim 10^\circ$  on  $\gamma$ . To reduce this, additional studies of the Dalitz plot structure are necessary, and the results using  $D$  mesons coherently produced in  $\psi(3770) \rightarrow D\bar{D}$  at charm-tau factories play a particularly crucial rôle. When one  $D$  meson is tagged as a  $CP$  eigenstate and the other reconstructed as  $K_S \pi^+ \pi^-$ , the Dalitz plot density differs from that in the flavour tagged samples, and the differences are sensitive to the strong phase at each point. Thus, the  $D$  decay model may be verified by fitting the  $CP$  tagged sample, and if this proves impossible, a model-independent technique (dividing the Dalitz plot into bins) can be employed. Additional methods to understand the model uncertainty (eg. using different multibody  $D$  decays) also exist. The understanding of these issues has been advanced through informal discussions between members of various collaborations, and also theorists; it is expected that this will continue to be a fruitful source of progress.

By summer 2006, it is to be expected that the available samples at the  $B$  factories will be approximately double those from CKM2005, and hopefully the combined data sample will exceed  $1 \text{ ab}^{-1}$ . This will allow significant progress in many of the channels discussed above. The precision of the  $\sin(2\beta)$  result will continue to improve, and it should be possible to definitively rule out  $\cos(2\beta) < 0$ . Significant  $CP$  violation effects may be seen in some  $b \rightarrow c\bar{c}d$  channels, and also in  $B_d \rightarrow D^{(*)\pm} \pi^\mp$ . Further progress on the extraction of  $\gamma$  from  $B_u^\pm \rightarrow D^{(*)} K^{(*)\pm}$  is expected. Since the precision of the  $\gamma$  measurement depends on the  $r_B$  values, it is not possible to say with certainty how the error will evolve, but there is some optimism that the  $CP$  violation effects will cross some threshold of significance. Another exciting prospect is that first results from  $B_d \rightarrow D^{(*)} K^{(*)}$  may become available. In addition to other possible new results from BaBar and Belle, the output of CLEO-c will be watched closely by those interested in  $\gamma$ .

Shortly after, attention will increasingly turn to the start up of the LHC. It is clear that despite (and, perhaps, partially because of) the best efforts of the  $B$  factories and the Tevatron experiments, there will be potential for LHCb to make a big impact, in particular in the measurement of  $B_s$  mixing parameters and of  $\gamma$  (in addition to channels outside the scope of this working group). As methods exist to measure both  $\beta$  and  $\gamma$  to within very small theoretical uncertainty, the next generation of  $B$  physics experiments has a promising future. Furthermore, these theoretically clean modes act as Standard Model reference points for other channels (eg. charmless  $B$  decays), with which LHCb and a Super  $B$  Factory may search for new physics.

# 1 Time-Dependent $CP$ Violation Measurements in $B^0 \rightarrow (c\bar{c})K^0$

The measurement of the mixing-induced  $CP$  asymmetry in the so-called gold-plated mode  $B^0 \rightarrow J/\Psi K_S$  is becoming a precision measurement. This served as a motivation to revisit the analysis of this mode within the standard model [1].

It is well known [2] that the time dependent  $CP$  asymmetry

$$a_{CP}^{J/\Psi K_S}(t) = C_{J/\Psi K_S} \cos(\Delta m t) - S_{J/\Psi K_S} \sin(\Delta m t) \quad (1)$$

is very cleanly related to the CKM angle  $\beta$ , since

$$S_{J/\Psi K_S} \approx \sin(2\beta), \quad C_{J/\Psi K_S} \approx 0, \quad (2)$$

where deviations from these relations are expected at the level of a few percent.

The reason for this is summarized as follows. The box diagram shown in fig. 1 leads to a  $\Delta B = 2$  interaction transforming a  $B^0$  into a  $\bar{B}^0$ . Thus the Eigenstates of the Hamiltonian are (to leading order) the combinations

$$|B_{L/H}\rangle = \frac{p|B^0\rangle \pm q|\bar{B}^0\rangle}{\sqrt{|p|^2 + |q|^2}} \quad \text{with} \quad \frac{q}{p} \approx -\frac{M_{12}^*}{|M_{12}|} \quad (3)$$

where  $M_{12}$  is the matrix element of the box diagram contribution between a  $B^0$  and a  $\bar{B}^0$  state. Due to the CKM factors and the large top-quark mass  $M_{12}$  is completely dominated by the top quark. Thus  $M_{12}$  is directly proportional to the CKM phase

$$M_{12}^* \propto (V_{td}V_{tb}^*)^2 \propto e^{-i2\beta} \quad \text{and thus} \quad \frac{q}{p} = e^{-i2\beta} \quad (4)$$

A  $CP$  asymmetry is induced by contributions to a decay which have both different weak and strong phases. Furthermore, the time evolution also induces a phase difference between the two eigenstates  $B_L$  and  $B_H$  which is  $\exp(i\Delta m t)$  and which has the same effect as a strong phase difference and thus also results in a phase difference.

The  $CP$  asymmetry parameters given in (1) are given in terms of the mixing parameters, the decay amplitude  $A(B^0 \rightarrow J/\Psi K_S)$  and its  $CP$  conjugate as

$$C_{J/\Psi K_S} = \frac{1 - |\lambda|^2}{1 + |\lambda|^2} \quad \text{and} \quad S_{J/\Psi K_S} = \frac{2 \text{Im}[\lambda]}{1 + |\lambda|^2} \quad (5)$$

with

$$\lambda = \left(\frac{q}{p}\right) \frac{A(\bar{B}^0 \rightarrow J/\Psi K_S)}{A(B^0 \rightarrow J/\Psi K_S)}. \quad (6)$$



Figure 1: Box diagrams mediating  $\Delta B = \pm 2$  transitions.



Analyzing the possible contributions to the decay  $B^0 \rightarrow J/\psi K_S$  one finds that the decay amplitude contains a tree contribution proportional to  $V_{cb}^* V_{cs}$  which is real in the standard parametrization. Furthermore, the leading penguin contribution is also proportional to the same CKM factor as the tree, while the remaining penguin contribution (due to the up quark) is suppressed by two factors of the Wolfenstein parameter. Thus we have

$$\lambda = -\frac{V_{tb}^* V_{td} V_{cb} V_{cs}^*}{V_{tb} V_{td}^* V_{cb}^* V_{cs}} = -\exp(-2i\beta) \quad (7)$$

leading to (2).

## 1.1 Estimating Corrections to the ‘‘golden relations’’

*Contribution from T. Mannel*

The corrections arise from two sources: (i) corrections to the mixing and (ii) corrections to the decay. The corrections to the mixing amplitude due to contributions which do not carry the phase  $\exp(2i\beta)$  have to be suppressed relative to the leading contribution by a factor  $m_c^2/m_t^2 \sim 10^{-4}$  due to the GIM mechanism. More precise statements can be made by computing the box diagrams of fig. 1 [3, 4, 5]. Since vastly different mass scales are involved, one may make use of effective field theory methods in which case one may compute  $M_{12}$  in terms of the mixing of the time-ordered product of two  $\Delta B = 1$  interactions into local  $\Delta B = 2$  operators of dimension 8. The dim-8 operator relevant for the contributions with a phase different from  $2\beta$  is given by the mixing

$$T^{\Delta B=2} = -\frac{i}{2} \int d^4x T [H^{\Delta B=1}(x)H^{\Delta B=1}(0)] \rightarrow Q_3 = m_c^2(\bar{b}_L\gamma_\mu d_L)(\bar{b}_L\gamma^\mu d_L). \quad (8)$$

which yields contributions with the CKM factor  $(V_{cb}^* V_{cd})^2$  and  $(V_{cb}^* V_{cd})(V_{tb}^* V_{td})$ .

The contributions proportional to  $m_c^2$  shift the imaginary part of the ratio  $M_{12}/|M_{12}|$ , which will contribute to a deviation from the simple relation (2). One obtains

$$\Delta\text{Im} \left[ \frac{M_{12}}{|M_{12}|} \right] = -(2.08 \pm 1.23) \cdot 10^{-4} \quad (9)$$

where the uncertainties are due to the input parameters, which are the CKM parameters and the masses.

The second contribution to the deviation from (2) is much harder to estimate. It originates from the up quark penguin contribution, which induces a different weak phase into the decay. The ratio of matrix elements

$$r := \frac{\langle J/\Psi K_S | H(b \rightarrow u\bar{u}s) | \bar{B}^0 \rangle |V_{ub}| |V_{us}|}{\langle J/\Psi K_S | H(b \rightarrow c\bar{c}s) | \bar{B}^0 \rangle |V_{cb}| |V_{cs}|}, \quad (10)$$

where  $H(b \rightarrow q\bar{q}s)$  denotes the contributions to the effective Hamiltonian due to the  $b \rightarrow q\bar{q}s$  transition, is small due to the ratio of CKM factors. The ratio of decay amplitudes appearing in the parameter  $\lambda$  of (6) can be written in terms of  $r$  as

$$\frac{A(\bar{B}^0 \rightarrow J/\Psi K_S)}{A(B^0 \rightarrow J/\Psi K_S)} = -\frac{1 + r e^{-i\gamma}}{1 + r e^{+i\gamma}} \approx -(1 - 2 i r \sin \gamma). \quad (11)$$

The ratio  $r$  is estimated by using an approach based on naive factorization. The up-quark loop is evaluated perturbatively and yields [6]

$$\begin{aligned} & \langle J/\Psi K_S | H(b \rightarrow u\bar{u}s) | B_q \rangle = \\ & -\frac{G_F}{\sqrt{2}} \langle J/\Psi K_S | \left\{ \frac{\alpha}{3\pi} (\bar{s}b)_{V-A} (\bar{c}c)_V + \frac{\alpha_s}{3\pi} (\bar{s}T^a b)_{V-A} (\bar{c}T^a c)_V \right\} | B_q \rangle \left( \frac{5}{3} - \ln \left( \frac{k^2}{\mu^2} \right) + i\pi \right) \end{aligned} \quad (12)$$

where  $k^2 \sim m_{J/\Psi}^2$  is an average momentum flowing through the up quark loop and  $\mu \sim m_b$  is the typical scale of the process.

The two matrix elements appearing in (12) are estimated by noting that the tree level effective Hamiltonian contains both the color octet and the color singlet matrix elements. It is well known that in naive factorization the color octet contribution vanishes and that the prediction of naive factorization turns out to be too small. Hence we estimate the color octet matrix element by ascribing the difference of the predicted and the the observed rate to this matrix element. In this way we get

$$|\langle J/\Psi K_S | (\bar{s}b)(\bar{c}c) | \bar{B}^0 \rangle_{\text{fact}}| = (3.96 \pm 0.36) \cdot 10^9 \text{ MeV}^3 \quad (13)$$

$$|\langle J/\Psi K_S | (\bar{s}T^a b)(\bar{c}T^a c) | \bar{B}^0 \rangle| = (1.97 \pm 0.64) \cdot 10^8 \text{ MeV}^3 \quad (14)$$

from which we obtain

$$\text{Re}[r] = (-3.62 \pm 1.55) \cdot 10^{-4}, \quad \text{Im}[r] = (-4.48 \pm 1.92) \cdot 10^{-4} \quad (15)$$

where the imaginary part is assumed to be entirely due to the imaginary part of the loop calculated in (12).

The effect on the  $CP$  asymmetry is given as

$$a_{CP}(t) = -(\sin(2\beta) + \Delta S_{J/\Psi K_S}) \sin(\Delta m t) - \frac{\delta}{2} \cos(\Delta m t) \quad (16)$$

and we obtain for the parameter  $\delta$

$$\delta = -(1.02 \pm 0.75) \cdot 10^{-3} \quad (17)$$

The change  $\Delta S_{J/\Psi K_S}$  in the mixing induced  $CP$  asymmetry is given as

$$\Delta S_{J/\Psi K_S} = 2 \sin \gamma \text{Re}[r] \cos(2\beta) - \Delta \text{Im} \left[ \frac{M_{12}}{|M_{12}|} \right] \quad (18)$$

which yields numerically (for  $\sin \gamma = 0.86 \pm 0.12$ )

$$\Delta S_{J/\Psi K_S} = (-2.16 \pm 2.23) \cdot 10^{-4} \quad (19)$$

In summary it turns out that this naive estimate yields a very small correction to the relations (2) from the standard model. However, this statement depends crucially on the way the up-quark penguin contribution is estimated, while the calculation of the  $\Delta B = 2$  mixing is quite reliable.

On the other hand, even if the up-quark penguin contribution is grossly underestimated, the standard model corrections to the simple relations (2) are too small to become visible in the current  $B$ -factory experiments.

## 1.2 A Method to Measure $\phi_1$ Using $\bar{B}^0 \rightarrow D^{(*)}h^0$ With Multibody $D$ Decay

*Contribution from T. Gershon*

The value of  $\sin(2\phi_1)$ , where  $\phi_1$  is one of the angles of the Unitarity Triangle [7] is now measured with high precision:  $\sin(2\phi_1) = 0.731 \pm 0.056$  [8]. However, this measurement contains an intrinsic ambiguity:  $2\phi_1 \longleftrightarrow \pi - 2\phi_1$ . Various methods to resolve this ambiguity have been introduced [9], but they require very large amounts of data (some impressive first results notwithstanding [10]).

A new technique based on the analysis of  $\bar{B}^0 \rightarrow Dh^0$ , followed by the multibody decay of the neutral  $D$  meson, has recently been suggested [11]. Here we use  $h^0$  to denote a light neutral meson, such as  $\pi^0, \eta, \rho^0, \omega$ . The modes  $\bar{B}^0 \rightarrow D_{CP}h^0$ , utilizing the same  $B$  decay but requiring the  $D$  meson to be reconstructed via  $CP$  eigenstates, have previously been proposed as “gold-plated” modes to search for new physics effects [12]. Such effects may result in deviations from the Standard Model prediction that  $CP$  violation effects in  $b \rightarrow c\bar{u}d$  transitions should be very similar to those observed in  $b \rightarrow c\bar{c}s$  transitions, such as  $\bar{B}^0 \rightarrow J/\psi K_S$ . Detailed considerations have shown that the contributions from  $b \rightarrow u\bar{c}d$  amplitudes, which are suppressed by a factor of approximately 0.02 [13], can be taken into account. Consequently, within the Standard Model, studies of  $\bar{B}^0 \rightarrow D_{CP}h^0$  can give a measurement of  $\sin(2\phi_1)$  that is more theoretically clean than that from  $\bar{B}^0 \rightarrow J/\psi K_S$  [14, 15]. However, these measurements still suffer from the ambiguity mentioned above.

In the case that the neutral  $D$  meson produced in  $\bar{B}^0 \rightarrow Dh^0$  is reconstructed in a multibody decay mode, with known decay model, the interference between the contributing amplitudes allows direct sensitivity to the phases. Thus  $2\phi_1$ , rather than  $\sin(2\phi_1)$  is extracted, and the ambiguity  $2\phi_1 \longleftrightarrow \pi - 2\phi_1$  can be resolved. This method is similar to that used to extract  $\phi_3$ , using  $B^\pm \rightarrow DK^\pm$  followed by multibody  $D$  decay [16, 17].

There are a large number of different final states to which this method can be applied. In addition to the possibilities for  $h^0$ , and the various different multibody  $D$  decays which can be used, the method can also be applied to  $\bar{B}^0 \rightarrow D^*h^0$ . In this case, the usual care must be taken to distinguish between the decays  $D^* \rightarrow D\pi^0$  and  $D^* \rightarrow D\gamma$  [60]. Also, if  $h^0$  is not a spinless particle, angular analysis [18] will be required to resolve the contributing amplitudes to  $\bar{B}^0 \rightarrow D^*h^0$ .

A detailed description of the method and the results of a feasibility study are given in [11]. In summer 2005, the Belle Collaboration has presented the first results on  $\phi_1$  using this technique [19].

## 1.3 Measurement of $\cos 2\beta/2\phi_1$ with $B_d^0 \rightarrow J/\psi K^*$

*Contribution from M. Verderi*

The measurement of the sign of  $\cos 2\beta$  provides a direct test of the Standard Model in which  $\cos 2\beta > 0$ . The interference of  $CP$ -odd ( $A_\perp$ ) and  $CP$ -even ( $A_0, A_\parallel$ ) amplitudes in the decay  $B^0 \rightarrow J/\psi K^{*0}; K^{*0} \rightarrow K_S^0 \pi^0$  generates a  $\cos 2\beta$  contribution in the time- and angle-dependent distribution of the decay. This contribution appears as a product of  $\cos 2\beta$  and cosine of strong phases differences. The strong phases themselves are measured up to a two-fold ambiguity leading to a sign ambiguity on the cosine of the strong phases, and hence a sign ambiguity on  $\cos 2\beta$ .

BABAR resolves the strong phases ambiguity pointing out the  $K\pi$   $S$ -wave, beyond the dominant  $K^*(892)$   $P$ -wave, in the  $B \rightarrow J/\psi K\pi$  decay and exploiting the known behaviour of the  $K\pi$   $S$ - $P$  relative phase with  $K\pi$  mass in the  $K^*(892)$  region [20]: among the two strong phases solutions, only one leads to the physical behaviour of the  $K\pi$   $S$ - $P$  relative phase with  $K\pi$  mass.

The  $\cos 2\beta$  parameter is extracted by a time- and angle-dependent analysis of the  $B^0 \rightarrow J/\psi K^{*0}; K^{*0} \rightarrow K_S^0 \pi^0$  decay. The BELLE and BABAR measurements are shown in Table 2. From MonteCarlo studies, BABAR estimates that the non-standard  $\cos 2\beta = -\sqrt{1 - 0.731^2} = -0.67$  solution is excluded at 86% CL.

According to BABAR, the prospect for higher luminosities is that  $\sigma(\cos 2\beta)$  empirically scales as  $\sigma(\cos 2\beta) = 7 \cdot (L/\text{fb}^{-1})^{-1/2}$  for luminosities high enough ( $\gtrsim 100\text{fb}^{-1}$ ). The  $\cos 2\beta$  measurement will be statistically limited for the coming years.

Table 2: BELLE and BABAR measurements of  $\sin 2\beta$  and  $\cos 2\beta$  with  $B^0 \rightarrow J/\psi K^{*0}; K^{*0} \rightarrow K_S^0 \pi^0$ , with both parameters free in the fit and with  $\sin 2\beta$  fixed to world average.

	# events	$\sin 2\beta$	$\cos 2\beta$
BELLE [21]	354	$0.30 \pm 0.32 \pm 0.02$	$0.31 \pm 0.91 \pm 0.10$
		0.731 (fixed)	$0.56 \pm 0.86 \pm 0.11$
BABAR [22]	104	$0.10 \pm 0.57 \pm 0.14$	$3.32^{+0.76}_{-0.96} \pm 0.27$
		0.731 (fixed)	$2.72^{+0.50}_{-0.79} \pm 0.27$

## 2 $CP$ Violation in $b \rightarrow c\bar{c}d$ Transitions

Time-dependent  $CP$  violation in  $B$  decays governed by  $b \rightarrow c\bar{c}d$  transitions have been measured in  $B^0 \rightarrow J/\psi\pi^0$ ,  $D^{*+}D^{*-}$ ,  $D^+D^{*-}$  and  $D^-D^{*+}$  by both Belle and BaBar collaborations. Since the tree diagrams of  $b \rightarrow c\bar{c}d$  transitions contain  $V_{cb}$  and  $V_{cd}$  which have no KM complex phase,  $CP$  violation arises from the complex phase in  $B^0\bar{B}^0$  mixing (*i.e.*  $\phi_1$ ) if neither penguin nor other contributions are substantial. These decays are therefore sensitive to the unitarity angle  $\beta$  and complement the precise measurement of  $\sin(2\beta)$  through  $B^0 \rightarrow (c\bar{c})K^{0(*)}$  decays. The presence of a gluonic penguin contribution with a different weak phase is expected to change the magnitude of the  $CP$  asymmetry by not more than a few percent [23]. However, additional contributions from non-SM processes may lead to shifts as large as  $\Delta\beta \approx 0.6$  in some models [12]. Interference between SM penguin and tree amplitudes can additionally provide some sensitivity to the angle  $\gamma = \arg[-V_{ud}V_{ub}^*/V_{cd}V_{cb}^*]$  [24, 25].

The potential  $b \rightarrow d$  penguin contribution can be probed by other processes. The charge asymmetry between  $B^+ \rightarrow J/\psi\pi^+$  and  $B^- \rightarrow J/\psi\pi^-$  is one possibility, although such an asymmetry also depends on the strong phases. Replacing  $c\bar{c}$  by  $s\bar{s}$ , the  $B \rightarrow \phi\pi$  decay generated by  $b \rightarrow s\bar{s}d$  transition solely takes place via penguin transition, so search for such kind of rare  $B$  decays will give us some information about magnitude of the penguin diagram.

### 2.1 $CP$ Violation in $b \rightarrow c\bar{c}d$ Transitions at Belle

*Contribution from K. Miyabayashi*

$J/\psi\pi^0$  is a  $CP$ -even final state, and therefore the Standard Model (SM) predicts (in the limit of tree-dominance)  $S_{J/\psi\pi^0} = -\sin 2\phi_1$  and  $A_{J/\psi\pi^0} = 0$ . Results from Belle and BaBar are shown in Fig. 2. In the Belle measurement [26], 91 candidates are found from a data sample containing 152 M  $B\bar{B}$  events. Backgrounds are estimated separately for  $B \rightarrow J/\psi X$  and combinatorial. The purity is estimated to be  $86 \pm 10\%$ . The BaBar measurement uses 88 M  $B\bar{B}$  [27]; 49 events are reconstructed in the signal region of which 37 are estimated to be signal.

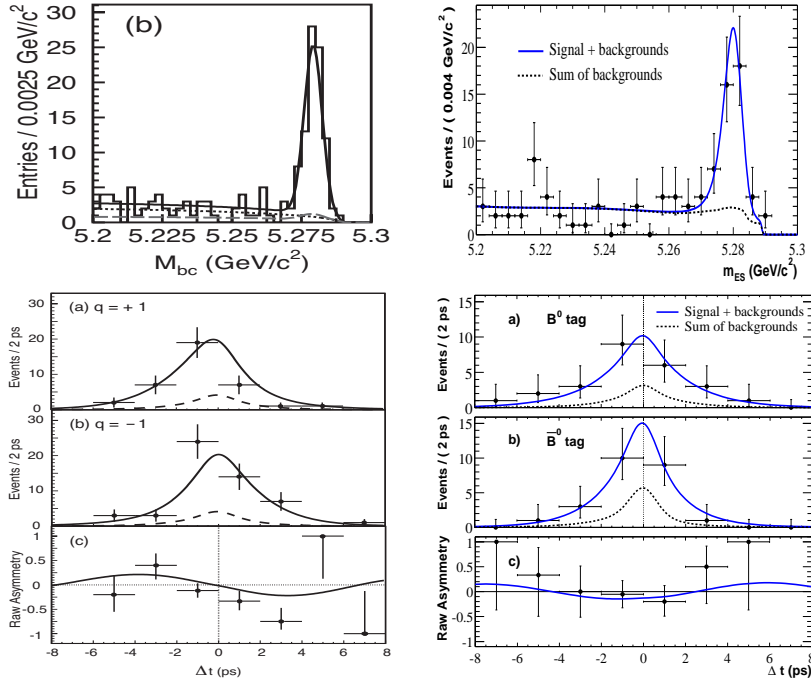


Figure 2: (Top)  $M_{bc}/M_{es}$  distributions from (left) Belle and (right) Babar. (Bottom)  $\Delta t$  distributions and asymmetries. Belle plots are from [26]; BaBar plots are from [27].

The obtained results are (see also Fig. 5)

	$S_{J/\psi\pi^0}$	$A_{J/\psi\pi^0}$
Belle	$-0.72 \pm 0.42(\text{stat}) \pm 0.09(\text{syst})$	$-0.01 \pm 0.29(\text{stat}) \pm 0.03(\text{syst})$
BaBar	$+0.05 \pm 0.49(\text{stat}) \pm 0.16(\text{syst})$	$-0.38 \pm 0.41(\text{stat}) \pm 0.09(\text{syst})$

$B^0 \rightarrow D^{*+}D^{*-}$  has a final state containing two vector mesons, which in general is a combination of  $CP$ -even and  $CP$ -odd. The  $CP$ -odd fraction can be determined by angular analysis of the decay products. Results from BaBar on this analysis are described elsewhere in this document. Based on a dataset corresponding to 152 M  $B\bar{B}$  pairs, Belle reconstructed 194 candidate events with  $67 \pm 7\%$  purity in this decay mode [28]. The  $CP$ -odd fraction is found to be  $0.19 \pm 0.08(\text{stat}) \pm 0.01(\text{syst})$ , and it is taken into account in the subsequent fit to obtain the  $CP$  violation parameters:

$$S_{D^{*+}D^{*-}} = -0.75 \pm 0.56(\text{stat}) \pm 0.12(\text{syst}) \quad (20)$$

$$A_{D^{*+}D^{*-}} = -0.26 \pm 0.26(\text{stat}) \pm 0.06(\text{syst}). \quad (21)$$

These results are shown in Fig. 3.

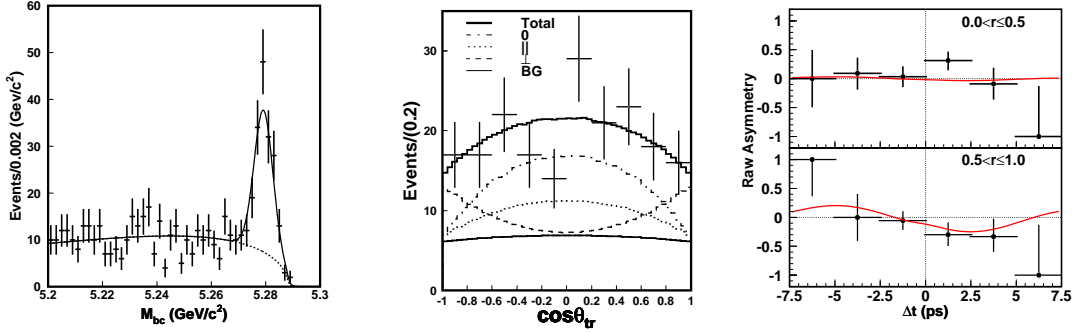


Figure 3: Results of the Belle analysis of  $B^0 \rightarrow D^{*+}D^{*-}$  [28]. (Left to right) Distributions of  $M_{bc}$ ,  $\cos \theta_{tr}$  and raw  $\Delta t$  asymmetry separately for (top) poor and (bottom) good quality tags.

The final states  $D^{*\pm}D^\mp$  are not  $CP$  eigenstates, and hence the phenomenology is more complicated, though the time-dependent observables are still sensitive to  $2\phi_1$ . Results from BaBar on this analysis are described elsewhere in this document. Belle has reconstructed this decay mode with two different methods, full and partial reconstruction [29], using a data set of 152 M  $B\bar{B}$  pairs. The results are summarized in Fig. 5.

All measurements mentioned above are statistically limited, so finding new  $b \rightarrow c\bar{c}d$  decay modes is also important. Both Belle [30] and BaBar [31] collaborations have observed  $B^0 \rightarrow J/\psi\rho^0$  decays; this final state consists of two vector mesons and therefore angular analysis is necessary to extract the  $CP$  composition. Furthermore, the contribution of non-resonant  $B^0 \rightarrow J/\psi\pi^+\pi^-$  decays must be well understood. Recently, the doubly charmed mode  $B^0 \rightarrow D^+D^-$  has been observed by Belle [32]. This is a  $CP$  eigenstate, and looks quite promising for time dependent  $CP$  violation measurements in the near future.

## 2.2 Time-Dependent $CP$ Asymmetries in $B^0 \rightarrow D^{(*)\pm}D^{(*)\mp}$ at Babar

*Contribution from M. Bruinsma*

Using  $(232 \pm 3) \times 10^6 \Upsilon(4S) \rightarrow B\bar{B}$  decays recorded by the BaBar detector [33] at the PEP-II  $e^+e^-$  collider, Babar has measured  $CP$  asymmetries in  $B^0$  decays to the  $CP$  eigenstates  $D^{*+}D^{*-}$  and  $D^+D^-$  and  $CP$  'pseudo'- $CP$ -eigenstates  $D^{*+}D^-$  and  $D^{*-}D^+$ . The results are summarized in Table 3 and are consistent with  $S = -\sin(2\beta)$  and  $C = 0$ , expected in the SM for a tree-level-dominated transition with equal rates for  $B^0 \rightarrow D^{*+}D^-$  and  $B^0 \rightarrow D^{*-}D^+$ .

The vector-vector final state  $D^{*+}D^{*-}$  is predominantly  $CP$ -even, but contains also  $CP$ -odd contributions. The  $CP$ -odd fraction for this decay is measured in a time-integrated angular analysis to be  $R_t = 0.124 \pm 0.044(\text{stat.}) \pm 0.007(\text{syst.})$ . The  $S$  coefficient for  $D^{*+}D^{*-}$  in table 3 is corrected for this  $CP$ -odd dilution. The results for  $D^{*+}D^{*-}$  are preliminary while those for  $D^{*-}D^+$ ,  $D^{*+}D^-$  and  $D^+D^-$  are final[34].

## 2.3 $B_s \rightarrow$ double charm status at CDF

*Contribution from B. Iyutin*

Sample	$N_{\text{sig}}$	Purity	$S$	$C$
$D^{*+}D^{*-}$	396(23)	0.75(2)		$0.04 \pm 0.14(\text{stat.}) \pm 0.02(\text{syst.})$
			$-0.65 \pm 0.26(\text{stat.})_{-0.07}^{+0.09}(R_T) \pm 0.04(\text{syst.})$	
$D^{*+}D^-$	145(16)	0.49(3)	$-0.54 \pm 0.35(\text{stat.}) \pm 0.07(\text{syst.})$	$0.09 \pm 0.25(\text{stat.}) \pm 0.06(\text{syst.})$
$D^{*-}D^+$	126(16)	0.49(3)	$-0.29 \pm 0.33(\text{stat.}) \pm 0.07(\text{syst.})$	$0.17 \pm 0.24(\text{stat.}) \pm 0.04(\text{syst.})$
$D^+D^-$	54(11)	0.37(6)	$-0.29 \pm 0.63(\text{stat.}) \pm 0.06(\text{syst.})$	$0.11 \pm 0.35(\text{stat.}) \pm 0.06(\text{syst.})$

Table 3: Signal yield and purity for each of the  $B^0 \rightarrow D^{(*)\pm}D^{(*)\mp}$  samples, and results for the parameters  $S$  and  $C$  describing the time-dependent  $CP$ -asymmetries. The purity is defined as the fraction of signal events in the region  $m_{ES} > 5.27$  GeV.

With  $243 \text{ pb}^{-1}$  of CDF displaced track trigger [35] data the ratio of branching fractions for fully reconstructed hadronic modes is measured  $Br(B^0 \rightarrow D_s^+ D^-) / Br(B^0 \rightarrow D^- 3\pi)$  where  $D^+ \rightarrow K\pi\pi$  and  $D_s \rightarrow \phi\pi(K^*K, \pi\pi\pi)$ .

The optimization of selection cuts was done maximizing the significance of the signal Monte Carlo over combinatorial background from data. The signal region was blinded.

Monte Carlo simulation is used to determine shapes describing signal and partially reconstructed decays. The shapes were fixed while doing the mass fit (figure 4). Only relative normalizations were allowed to float. The mass of the signal was also allowed to vary as well as parameters describing combinatorial background. Signal yields were obtained integrating over a  $\pm 2.5\sigma$  window, where  $\sigma$  means the fitted signal width.

The analysis efficiency was extracted from signal Monte Carlo. To reduce systematic Monte Carlo mass distribution was fitted and integrated it in a  $2.5\sigma$  window the way it was done for data.

Among the systematic uncertainties an important one is the  $B^0 \rightarrow D^- 3\pi$  sample composition uncertainty. It arises due to the poor knowledge of the  $3\pi$  sub-resonant structure. Cut efficiency uncertainty is assigned due to the difference between data and Monte Carlo distributions for variables we cut on. A fit uncertainty is due to the fit instability with respect to fixed parameters. For  $D_s^- D^+$ , where  $D_s \rightarrow 3\pi$ , there is also a sample composition systematic due to the poor knowledge of  $D_s$  sub-resonant structure. All of these combined are well below the statistical uncertainty.

The ratios of branching fractions corresponding to the three different  $D_s$  modes:

$$\frac{Br(B^0 \rightarrow D_s^+ D^-, D_s \rightarrow \phi\pi)}{Br(B^0 \rightarrow D^- 3\pi)} = 1.95 \pm 0.20(\text{stat}) \pm 0.12(\text{syst}) \pm 0.49(BR_1)$$

$$\frac{Br(B^0 \rightarrow D_s D^+, D_s \rightarrow K^* K)}{Br(B^0 \rightarrow D^- 3\pi)} = 1.83 \pm 0.22(\text{stat}) \pm 0.11(\text{syst}) \pm 0.46(BR_1) \pm 0.17(BR_2)$$

$$\frac{Br(B^0 \rightarrow D_s D^+, D_s \rightarrow \pi\pi\pi)}{Br(B^0 \rightarrow D^- 3\pi)} = 2.46 \pm 0.34(\text{stat}) \pm 0.17(\text{syst}) \pm 0.62(BR_1) \pm 0.34(BR_3)$$

Branching fraction uncertainties are quoted separately:

- $BR_1$  is due to  $Br(D_s \rightarrow \phi\pi)$
- $BR_2$  is due to  $\frac{Br(D_s \rightarrow K^* K)}{Br(D_s \rightarrow \phi\pi)}$

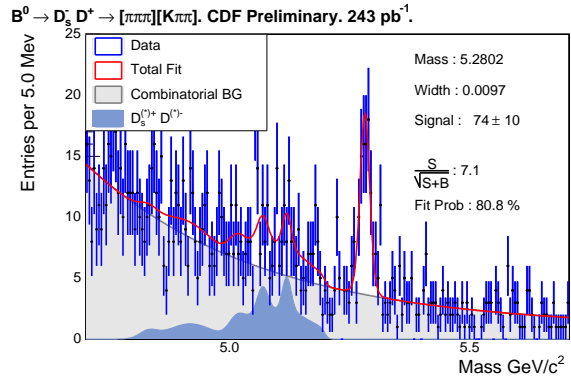
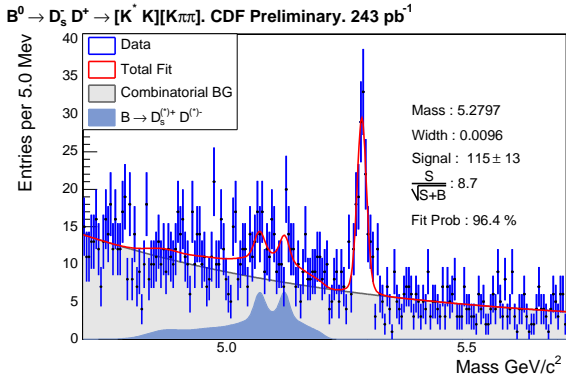
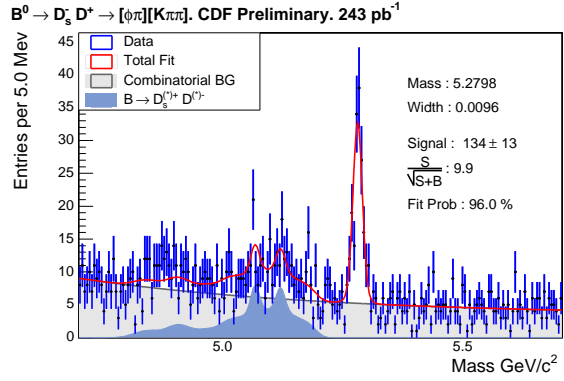
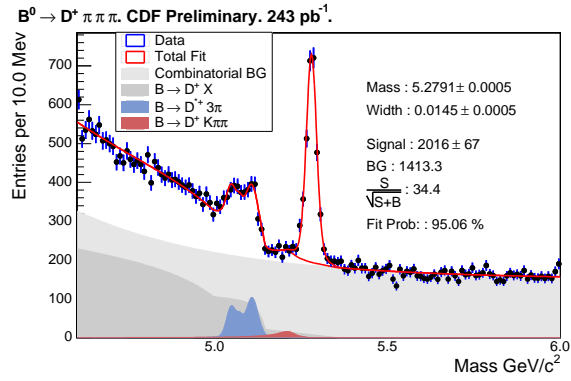


Figure 4: Data fits of  $B^0 \rightarrow D^- 3\pi$  and  $B^0 \rightarrow D_s^- D^+$ ,  $D_s^+ \rightarrow \phi\pi$  (top),  $B^0 \rightarrow D_s^- D^+$ ,  $D_s^+ \rightarrow K^* K$  and  $B^0 \rightarrow D_s^- D^+$ ,  $D_s^+ \rightarrow \pi\pi\pi$  (bottom).



- $BR_3$  is due to  $\frac{Br(D_s \rightarrow \pi\pi\pi)}{Br(D_s \rightarrow \phi\pi)}$

where branching fractions from PDG (2004) were used. In combining results several assumptions were made. The systematic uncertainty for all three modes was considered fully correlated, and “ $BR_2$ ” and “ $BR_3$ ” uncertainties were assumed to be non-correlated. The final value is:

$$\frac{Br(B^0 \rightarrow D_s^+ D^-)}{Br(B^0 \rightarrow D^- 3\pi)} = 2.00 \pm 0.16(NC) \pm 0.12(syst) \pm 0.50(BR_1)$$

where only one number is quoted for the non-correlated error (marked “ $NC$ ”). The current world average from the PDG (2004) is:

$$\frac{Br(B^0 \rightarrow D_s^+ D^-)}{Br(B^0 \rightarrow D^- 3\pi)} = 1.00 \pm 0.39$$

which is consistent with CDF result within  $2\sigma$ . The error on  $D_s \rightarrow \phi\pi$  branching fraction ( $3.6\% \pm 0.9\%$ ), which should be greatly reduced in coming years, dominates the measurement for now. This analysis prepares the way to measure  $Br(B_s \rightarrow D_s D_s)/Br(B^0 \rightarrow D_s^+ D^-)$ .

To summarize this section, time dependent  $CP$  violation in  $b \rightarrow c\bar{c}d$  transitions have been measured using  $B^0 \rightarrow J/\psi\pi^0$  and doubly charmed modes. The measurements performed so far are summarized in Fig. 5. All these measurements are statistically limited. Note that no direct  $CP$  violation has been observed so far. With  $5 \times 10^8$  or  $10^9$   $B\bar{B}$ , we would expect to be able to observe non-zero  $CP$  violation, and in order to check the deviation from  $b \rightarrow c\bar{c}s$  modes, much more data is needed. Therefore, it is interesting to continue to hunt for new decay modes. In order for better understanding of the  $b \rightarrow d$  penguin contribution, it is also important to search for rare decay modes and  $CP$  asymmetries in relevant charged  $B$  decay modes.

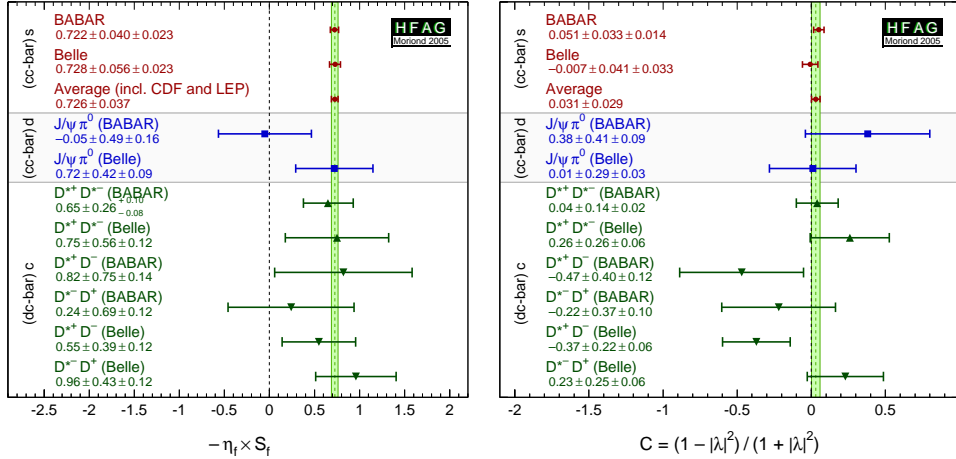


Figure 5: Summary of time-dependent  $CP$  violation measurements in  $b \rightarrow c\bar{c}d$  transitions. (Left)  $-\eta_f S_{fCP}$  where  $\eta_f$  is the  $CP$  eigenvalue of the final state. (Right)  $C_{fCP} = -A_{fCP}$ .

## 2.4 $\gamma$ from $B \rightarrow D^{(*)}\bar{D}^{(*)}$ and $B \rightarrow D_S^{(*)}\bar{D}^{(*)}$

*Contribution from J. Albert*

One can combine information from  $B \rightarrow D^{(*)}\bar{D}^{(*)}$  and  $B \rightarrow D_S^{(*)}\bar{D}^{(*)}$  branching fractions, along with  $CP$  asymmetry measurements in  $B \rightarrow D^{(*)}\bar{D}^{(*)}$ , to obtain information on  $\gamma$  [24, 25] (see also [36]). An extraction of constraints on  $\gamma$  may be obtained by using an  $SU(3)$  relation between the  $B \rightarrow D^{(*)}\bar{D}^{(*)}$  and  $B \rightarrow D_S^{(*)}\bar{D}^{(*)}$  decays. In this technique, the breaking of  $SU(3)$  is parametrized via the ratios of decay constants  $f_{D_S^{(*)}}/f_{D^{(*)}}$ , which are quantities measured in lattice QCD [37]. The quality of the constraint on  $\gamma$  using this technique is highly dependent on the difference in the values of the  $CP$  asymmetries in  $B \rightarrow D^{(*)}\bar{D}^{(*)}$  from the value of  $\sin 2\beta$  as measured in charmonium decays, as this difference is what provides information on the additional weak phase.

## 3 Measurements of $\sin(2\beta + \gamma)/\sin(2\phi_1 + \phi_3)$

The decay modes  $B^0 \rightarrow D^{(*)\mp}\pi^\pm$  have been proposed to measure  $\sin(2\beta + \gamma)$  [38]. In the Standard Model the decays  $B^0 \rightarrow D^{(*)+}\pi^-$  and  $\bar{B}^0 \rightarrow D^{(*)+}\pi^-$  proceed through the  $\bar{b} \rightarrow \bar{u}cd$  and  $b \rightarrow c$  amplitudes  $A_u$  and  $A_c$ , respectively. The relative weak phase between these two amplitudes is  $\gamma$ . When combined with  $B^0\bar{B}^0$  mixing, this yields a weak phase difference of  $2\beta + \gamma$  between the interfering amplitudes.

The decay rate distribution for  $B \rightarrow D^{(*)\pm}\pi^\mp$  is described by an equation similar to 1, where the parameters  $C$  and  $S$  are given by

$$C \equiv 1 - \frac{r^2}{1 + r^2}, \quad S^\pm \equiv \frac{2r}{1 + r^2} \sin(2\beta + \gamma \pm \delta).$$

Here  $\delta$  is the strong phase difference between  $A_u$  and  $A_c$  and  $r \equiv |A_u/A_c|$ . Since  $A_u$  is doubly CKM-suppressed with respect to  $A_c$ , one expects  $r$  to be small of order 2%. Due to the small value of  $r$ , large data samples are required for a statistically significant measurement of  $S$ .

### 3.1 Belle Measurements of $\sin(2\phi_1 + \phi_3)$

*Contribution from F. Ronga*

Belle has probed the  $CP$ -violating parameter  $\sin(2\phi_1 + \phi_3)$  using full reconstruction of  $B^0 \rightarrow D^{(*)}\pi$  decays [39] and partial reconstruction of  $B^0 \rightarrow D^*\pi$  decays [40]. Both analyses are based on a sample of 152 million  $B\bar{B}$  pairs.

Belle expresses the time-dependent decay probabilities for these modes as

$$\begin{aligned} P(B^0 \rightarrow D^{(*)\pm}\pi^\mp) &\approx \frac{1}{8\tau_{B^0}} e^{-|\Delta t|/\tau_{B^0}} [1 \mp \cos(\Delta m \Delta t) - S^\pm \sin(\Delta m \Delta t)] \\ P(\bar{B}^0 \rightarrow D^{(*)\pm}\pi^\mp) &\approx \frac{1}{8\tau_{B^0}} e^{-|\Delta t|/\tau_{B^0}} [1 \pm \cos(\Delta m \Delta t) - S^\pm \sin(\Delta m \Delta t)] \end{aligned} \quad (22)$$

where  $S^\pm = (-1)^L 2R_{D^{(*)}\pi} \sin(2\phi_1 + \phi_3 \pm \delta_{D^{(*)}\pi})$ .  $L$  is the angular momentum of the final state (1 for  $D^*\pi$ ) [15],  $R_{D^{(*)}\pi}$  is the ratio of magnitudes of the suppressed and favoured amplitudes, and  $\delta_{D^{(*)}\pi}$  is their strong phase difference. It is assumed that  $R_{D^{(*)}\pi}$  is small [13].

In the full reconstruction analysis, the following decay chains are reconstructed (charge conjugate modes are included):  $B \rightarrow D^{*+}\pi^-$ ,  $D^{*+} \rightarrow D^0\pi_s^+$ ,  $D^0 \rightarrow K^-\pi^+$ ,  $K^-\pi^+\pi^0$ ,  $D^0 \rightarrow K^-\pi^+\pi^+\pi^-$  and  $B \rightarrow D^+\pi^-$ ,  $D^+ \rightarrow K^-\pi^+\pi^+$ . The event yields are summarized in Table 4.

Decay mode	Candidates	Selected	Purity
$B \rightarrow D\pi$	9711	9351	91%
$B \rightarrow D^*\pi$	8140	7763	96%

Table 4: Number of reconstructed candidates, selected candidates (after tagging and vertexing) and purity, extracted from the fit to  $(\Delta E, M_{bc})$ .

The standard Belle tagging algorithm is used to identify the flavour of the accompanying  $B$  meson. It returns the flavour and a tagging quality  $r$  used to classify events in six bins. The standard Belle vertexing algorithm is then used to obtain the proper-time difference  $\Delta t$ . A fit to the  $\Delta t$  distribution of events in the  $(\Delta E, M_{bc})$  side-band region is performed to get the parameters of the background PDFs. A lifetime fit is performed on all components together to get the resolution parameters; the wrong-tag fractions for the six  $r$  bins are also determined from the data.

The  $S^\pm$  have to be corrected to take into account possible tag-side interference due to tagging on  $B^0 \rightarrow DX$  decays. Effective corrections  $\{S_{\text{tag}}^\pm\}^{\text{eff}}$  are determined for each  $r$  bin by a fit to fully reconstructed  $D^*\ell\nu$  events, where the reconstructed side asymmetry is known to be zero. Finally, a fit is performed to determine  $S^\pm$ , with  $\Delta m$  and  $\tau_{B^0}$  fixed to the world average, and the wrong-tag fractions and  $\{S_{\text{tag}}^\pm\}^{\text{eff}}$  for each  $r$  bin fixed to the values determined previously. We obtain:

$$\begin{aligned}
2R_{D\pi} \sin(2\phi_1 + \phi_3 + \delta_{D\pi}) &= 0.087 \pm 0.054(\text{stat}) \pm 0.018(\text{syst}) \\
2R_{D\pi} \sin(2\phi_1 + \phi_3 - \delta_{D\pi}) &= 0.037 \pm 0.052(\text{stat}) \pm 0.018(\text{syst}) \\
2R_{D^*\pi} \sin(2\phi_1 + \phi_3 + \delta_{D^*\pi}) &= 0.109 \pm 0.057(\text{stat}) \pm 0.019(\text{syst}) \\
2R_{D^*\pi} \sin(2\phi_1 + \phi_3 - \delta_{D^*\pi}) &= 0.011 \pm 0.057(\text{stat}) \pm 0.019(\text{syst})
\end{aligned} \tag{23}$$

The systematic errors come from the uncertainties of parameters that are constrained in the fit and uncertainties on the tagging side asymmetry. The result of the fit for the sub-samples having the best quality flavour tagging is shown on Fig. 6.

The partial reconstruction of  $B \rightarrow D^{*+}\pi_f$ ,  $D^{*+} \rightarrow D^0\pi_s$  is performed by requiring a fast pion  $\pi_f$  and a slow pion  $\pi_s$ , without any requirement on the  $D^0$ . The candidate selection exploits the 2-body kinematics of the decay using 3 variables: the fast pion CM momentum  $p_f^*$ ; the cosine of the angle between the fast pion direction and the opposite of the slow pion direction in the CM ( $\cos \delta_{f,s}$ ); the angle between the slow pion direction and the opposite of the  $B$  direction in the  $D^*$  rest frame ( $\cos \theta_{\text{hel}}$ ). Yields are extracted from a 3D fit to these variables (see Table 5). The flavour of the accompanying  $B$  meson is identified by a fast lepton,  $\ell_{\text{tag}}$ . The proper time  $\Delta t$  is obtained from the  $z$  coordinate of  $\pi_f$  and  $\ell_{\text{tag}}$  constrained to the  $B$ -lifetime smeared beam profile.

The resolution function is modeled by a convolution of three Gaussians whose parameters are determined by a fit to a  $J/\psi \rightarrow \mu^+\mu^-$  sample selected the same way as the signal sample. In order to correct for possible bias due to tiny misalignment in the tracking devices that would mimic  $CP$  violation, the mean of the Gaussian resolution is allowed to be slightly offset. The vertex position is also corrected to account for possible misalignments. A fit to events where the

Mode	Data	Signal	$D^*\rho$	Corr. bkg	Uncorr. bkg
SF	2823	1908	311	—	637
OF	10078	6414	777	928	1836

Table 5: Fit yield for the signal and the various types of background in same-flavour (SF) and opposite-flavour (OF) events.

two pions have same sign is performed to determine the shape of uncorrelated background  $\Delta t$  distribution, while a fit to the  $(p_f^*, \cos \theta_{\text{hel}})$  side-bands provides that of the correlated background. The  $D^*\rho$  component is modeled the same way as the signal, with  $S^\pm$  fixed to zero.

A fit for  $\Delta m$  and  $\tau_{B^0}$  is performed to check the fit procedure. A fit to a  $D^*\ell\nu$  sample selected similarly to the signal sample is performed to check the bias correction. Several MC samples with  $S^\pm \neq 0$  are fitted to check possible fit bias in the extraction of  $S^\pm$ .

An unbinned maximum likelihood fit with  $\Delta m$  and  $\tau_{B^0}$  fixed to the world average, and  $S^\pm$ ,  $\Delta t$  offsets and wrong-tag fractions floated yields:

$$\begin{aligned}
2R_{D^*\pi} \sin(2\phi_1 + \phi_3 + \delta_{D^*\pi}) &= -0.035 \pm 0.041(\text{stat}) \pm 0.018(\text{syst}) \\
2R_{D^*\pi} \sin(2\phi_1 + \phi_3 - \delta_{D^*\pi}) &= -0.025 \pm 0.041(\text{stat}) \pm 0.018(\text{syst})
\end{aligned} \tag{24}$$

The main systematic errors come from the background fractions, the background shapes, the resolution function and the offsets. The result of the fit is shown as asymmetries on Fig. 7. Asymmetries are defined as:

$$\begin{aligned}
A^{\text{SF}} &= (N_{\pi^-\ell^-} - N_{\pi^+\ell^+}) / (N_{\pi^-\ell^-} + N_{\pi^+\ell^+}) \\
A^{\text{OF}} &= (N_{\pi^+\ell^-} - N_{\pi^-\ell^+}) / (N_{\pi^+\ell^-} + N_{\pi^-\ell^+})
\end{aligned}$$

Increase of the available data and addition of more modes in the full reconstruction, as well as tuning of the selection and vertexing on more Monte Carlo and data, will help reduce both statistical and systematic errors. A reduction by a factor 0.3 for the former and 0.5 for the latter is expected with  $1 \text{ ab}^{-1}$ .

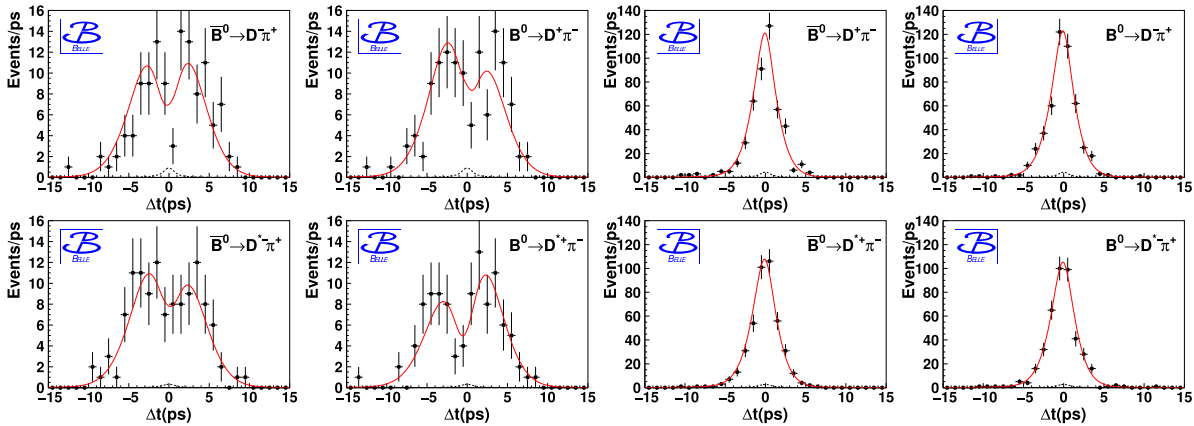


Figure 6:  $\Delta t$  distributions for the  $D\pi$  events (top) and  $D^*\pi$  (bottom) events with the best quality flavour tagging.

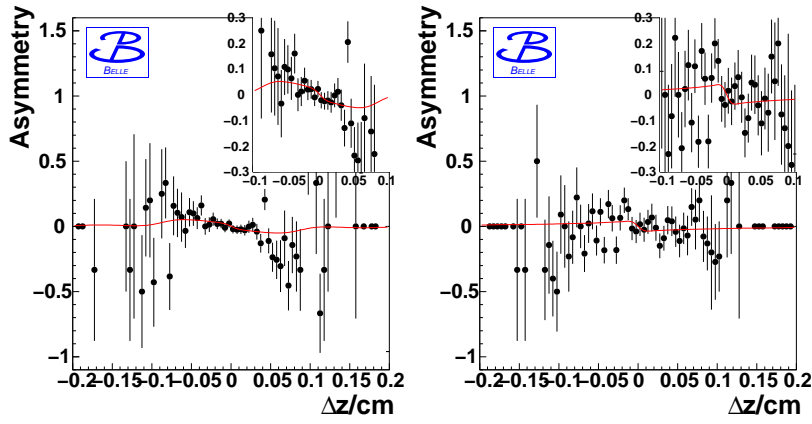


Figure 7: Results of the partial reconstruction fit shown as asymmetries for (left) SF events and (right) OF events. The inset plots magnify the region around  $\Delta z = 0$

## 3.2 Measurements of $\sin(2\beta + \gamma)$ at BaBar

### 3.2.1 Status and Prospects for $CP$ Asymmetry Measurements

*Contribution from S. Ganzhur*

Two different analysis techniques, full reconstruction [41] were used for and partial reconstruction [42] the  $\sin(2\beta + \gamma)$  measurement with  $B^0 \rightarrow D^{(*)\mp}\pi^\pm$ .

The full reconstruction technique is used to measure the  $CP$  asymmetry in  $B^0 \rightarrow D^{(*)\mp}\pi^\pm$  and  $B^0 \rightarrow D^{*\mp}\rho^\pm$  decays. The result with 110 million  $B\bar{B}$  pairs is

$$\begin{aligned}
2r^{D\pi} \sin(2\beta + \gamma) \cos \delta^{D\pi} &= -0.032 \pm 0.031 \pm 0.020 \\
2r^{D\pi} \cos(2\beta + \gamma) \sin \delta^{D\pi} &= -0.059 \pm 0.055 \pm 0.033 \\
2r^{D^*\pi} \sin(2\beta + \gamma) \cos \delta^{D^*\pi} &= -0.049 \pm 0.031 \pm 0.020 \\
2r^{D^*\pi} \cos(2\beta + \gamma) \sin \delta^{D^*\pi} &= +0.044 \pm 0.054 \pm 0.033 \\
2r^{D\rho} \sin(2\beta + \gamma) \cos \delta^{D\rho} &= -0.005 \pm 0.044 \pm 0.021 \\
2r^{D\rho} \cos(2\beta + \gamma) \sin \delta^{D\rho} &= -0.147 \pm 0.074 \pm 0.035,
\end{aligned} \tag{25}$$

where the first error is statistical and the second is systematic. The systematic error for  $B^0 \rightarrow D^{*\mp}\rho^\pm$  includes the maximum bias of asymmetry parameters due to possible dependence of  $r$  on the  $\pi\pi^0$  invariant mass. For the measurement of  $2r \cos(2\beta + \gamma) \sin \delta$  parameter only the lepton-tagged events are used due to a presence of tag-side  $CP$  violation effect [43].

In the partial reconstruction of a  $B^0 \rightarrow D^{*\mp}\pi^\pm$  candidate, only the hard (high-momentum) pion track  $\pi_h$  from the  $B$  decay and the soft (low-momentum) pion track  $\pi_s$  from the decay  $D^{*-} \rightarrow \bar{D}^0\pi_s^-$  are used. Applying kinematic constraints consistent with the signal decay mode, the four-momentum of the non-reconstructed, ‘‘missing’’  $D$  is calculated. Signal events are peaked in the  $m_{miss}$  distribution at the nominal  $D^0$  mass. This method eliminates the efficiency loss associated with the neutral  $D$  meson reconstruction. The  $CP$  asymmetry independent on the assumption on  $r^*$  measured with this technique by *BABAR* using 232 million produced  $B\bar{B}$  pairs is

$$\begin{aligned}
2r^{D^*\pi} \sin(2\beta + \gamma) \cos \delta^{D^*\pi} &= -0.034 \pm 0.014 \pm 0.009 \\
2r^{D^*\pi} \cos(2\beta + \gamma) \sin \delta^{D^*\pi} &= -0.019 \pm 0.022 \pm 0.013,
\end{aligned} \tag{26}$$

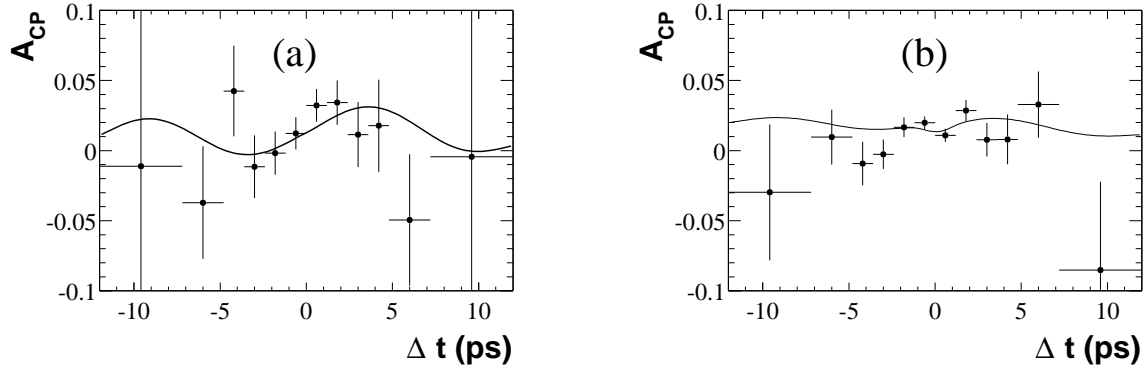


Figure 8: Raw asymmetry for (a) lepton-tagged and (b) kaon-tagged events of  $B^0 \rightarrow D^{*\mp} \pi^\pm$  decay mode using the method of the partial reconstruction. The curves represent the projections of the PDF for the raw asymmetry.

where the first error is statistical and the second is systematic. This measurement deviates from zero by 2.0 standard deviations. Figure 8 shows the raw, time-dependent  $CP$  asymmetry

$$A(\Delta t) = \frac{N_{B^0}(\Delta t) - N_{\bar{B}^0}(\Delta t)}{N_{B^0}(\Delta t) + N_{\bar{B}^0}(\Delta t)}$$

In the absence of background and with high statistics, perfect tagging, and perfect  $\Delta t$  measurement,  $A(\Delta t)$  would be a sinusoidal oscillation with amplitude  $2r \sin(2\beta + \gamma) \cos \delta$ .

Recently it was proposed to consider the  $B^0 \rightarrow D^{(*)\mp} a_{0(2)}^\pm$  decays for measurement of  $\sin(2\beta + \gamma)$  [44]. The decay amplitudes of  $B$  mesons to light scalar or tensor mesons such as  $a_0^+$  or  $a_2^+$ , emitted from a weak current, are significantly suppressed due to the small decay constants  $f_{a_{0(2)}}$ . Thus, the absolute value of the CKM-suppressed and favored amplitudes become comparable and the  $CP$  asymmetry in such decays is expected to be large. However, the theoretical predictions of the branching fractions for  $B^0 \rightarrow D^{(*)\mp} a_{0(2)}^\pm$  is expected of the order of  $(1 \div 4) \cdot 10^{-6}$  [45]. One way to verify the expectations and test a validity of the factorization approach is to measure the branching fractions for the more abundant decay modes  $B^0 \rightarrow D_s^{(*)\pm} a_{0(2)}^\mp$ . Using a sample of about 230 million  $\Upsilon(4S) \rightarrow B\bar{B}$  no evidence for these decays were observed. This allowed one to set upper limits at 90% C.L. on the branching fractions  $B(B^0 \rightarrow D_s^+ a_0^-) < 4.0 \times 10^{-5}$  and  $B(B^0 \rightarrow D_s^+ a_2^-) < 2.5 \times 10^{-4}$ .

The decay modes  $\bar{B}^0 \rightarrow D^{(*)0} \bar{K}^0$  have been proposed for determination of  $\sin(2\beta + \gamma)$  from measurement of time-dependent  $CP$  asymmetries [46, 47, 14, 15]. In the Standard Model the decays of  $B^0$  and  $\bar{B}^0$  mesons into final state  $D^{(*)0} K_S$  proceed through the  $b \rightarrow c$  and  $\bar{b} \rightarrow \bar{u}$  amplitudes, respectively. Due to relatively large  $CP$  asymmetry ( $r \equiv |A(\bar{B}^0 \rightarrow \bar{D}^{(*)0} \bar{K}^0)| / |A(B^0 \rightarrow D^{(*)0} \bar{K}^0)| \approx 0.4$ ) these decay channels look very attractive for such a measurement. Since the parameter  $r$  can be measured by fitting the  $C$  coefficient in time distributions, the measured asymmetry can be interpreted in terms of  $\sin(2\beta + \gamma)$  without additional assumptions. However, the branching fractions of such decays are relatively small  $\sim 5 \cdot 10^{-5}$  and a large data sample is therefore still required. Moreover, the  $B$  decay dynamics can lower the expectation for the ratio  $r$ . The magnitude of this ratio can be probed by measuring the rate for the decays  $\bar{B}^0 \rightarrow D^{(*)0} \bar{K}^{*0}$  and  $\bar{B}^0 \rightarrow \bar{D}^{(*)0} \bar{K}^{*0}$ . From the measured branching fractions [48], one obtains  $r < 0.8$  at the 90% C.L. from a central value of  $r = 0.4 \pm 0.2(stat.) \pm 0.2(syst.)$

### 3.2.2 $2\beta + \gamma$ from $B^0 \rightarrow D^+ K^0 \pi^-$ decays.

*Contribution from F. Polci, M.-H. Schune & A. Stocchi*

The use of the  $B^0 \rightarrow D^+ K^0 \pi^-$  decays for the extraction of  $2\beta + \gamma$  has been proposed in [49]. In these decays the sensitivity to the weak phase  $2\beta + \gamma$  comes from the interference between the Cabibbo allowed and the Cabibbo suppressed amplitudes leading to the same final state through the  $B^0 - \bar{B}^0$  mixing. Here the main advantage comes from the possibility of performing a Dalitz analysis, which allows to reduce the eight fold ambiguity in the determination of  $2\beta + \gamma$  to only a two fold ambiguity [50].

To explore the potentiality of this approach, a study of the sensitivity to  $2\beta + \gamma$  has been performed. The distribution of the invariant masses  $M_{K^0 \pi^-}$  and  $M_{D^+ K^0}$  has been parametrized with a model where the decay amplitude in each point  $i$  of the Dalitz plot is a linear combination with complex parameters of resonances described by Breit-Wigner functions. This model realistically reproduces the distribution obtained by the BaBar collaboration [51].

The time evolution can be written as:

$$P(B^0 \rightarrow D^+ K^0 \pi^-) = \frac{A_{c_i}^2 + A_{u_i}^2}{2} e^{-\Gamma t} \left\{ 1 + \left( \frac{|r_i|^2 - 1}{|r_i|^2 + 1} \right) \cos(\Delta m t) + \left( \frac{2 \text{Im}(r_i)}{|r_i|^2 + 1} \right) \sin(\Delta m t) \right\} \quad (27)$$

where  $A_{c_i}$  ( $A_{u_i}$ ) is the magnitude of the Cabibbo allowed (suppressed) amplitude and  $r_i$  the ratio between the Cabibbo suppressed and the Cabibbo allowed amplitudes which varies across the  $M_{K^0 \pi^-} - M_{D^+ K^0}$  plane. Analogous expressions can be written for  $\bar{B}^0 \rightarrow D^+ K^0 \pi^-$ ,  $B^0 \rightarrow D^- K^0 \pi^+$  and  $\bar{B}^0 \rightarrow D^- K^0 \pi^+$  decays.

. The regions showing the highest sensitivity to  $2\beta + \gamma$  are the ones with interference between  $\bar{B}^0 \rightarrow D^{*0} K^0$  and the Cabibbo suppressed  $\bar{B}^0 \rightarrow \bar{D}^{*0} K^0$  and between  $\bar{B}^0 \rightarrow D^+ K^{*-}$  and the Cabibbo suppressed  $\bar{B}^0 \rightarrow \bar{D}^{*0} K^0$  and it depends on the actual  $D^{*0}$  component.

The conclusion of a feasibility study is that with  $500 \text{ fb}^{-1}$  the relative error will lie between 25% and 50%.

### 3.2.3 $\sin(2\beta + \gamma)$ constraint from $CP$ asymmetries in $B^0 \rightarrow D^{(*)} \pi / \rho$ decays

*Contribution from C. Voena*

The  $CP$  parameters extracted from the time-dependent evolutions of  $B^0 \rightarrow D^{(*)} \pi / \rho$  decays that have been studied at the  $B$ -factory experiments Babar and Belle can be written as:

$$\begin{aligned} a_j &= 2r_j \sin(2\beta + \gamma) \cos \delta_j, \\ b_i &= 2r'_i \sin(2\beta + \gamma) \cos \delta'_i, \\ c_{i,j} &= 2 \cos(2\beta + \gamma) (r_j \sin \delta_j - r'_i \sin \delta'_i). \end{aligned} \quad (28)$$

where  $i$  is the tagging category and  $j$  is the reconstructed  $B$  decay ( $j = D\pi, D^*\pi, D\rho$ ). The parameter  $r_j$  is the ratio of the suppressed over the allowed amplitude contributing to the corresponding decay and  $\delta_j$  is a strong phase. The primed parameters are the corresponding quantities related to  $CP$  violation on the tagging side. We expect a very small asymmetry in these decays,  $r_j$  is expected to be  $\sim 0.02$  (with  $r'_i \leq r_j$ ). In the extraction of  $\sin(2\beta + \gamma)$  we make use of the  $CP$  parameters free of the unknown tag-side interference:

$$\begin{aligned} a_j &= 2r_j \sin(2\beta + \gamma) \cos \delta_j, \\ c_{lep,j} &= 2 \cos(2\beta + \gamma) r_j \sin \delta_j. \end{aligned}$$

For each mode we have two observables and three unknowns, external inputs are therefore needed to extract  $\sin(2\beta + \gamma)$ .  $SU(3)$  symmetry is currently used to estimate the  $r_j$  parameters. The relation (for  $B^0 \rightarrow D^+\pi^-$ ) is:

$$r_{D\pi} = \tan \theta_C \sqrt{\frac{BR(B^0 \rightarrow D_s^+\pi^-) f_D}{BR(B^0 \rightarrow D^-\pi^+) f_{D_s}}} [38] \quad (29)$$

Similar relations have been used for the other two decay modes. Equation 29 has been obtained with two approximations. In the first approximation, the exchange diagram amplitude contributing to the decay  $B^0 \rightarrow D^+\pi^-$  has been neglected and only the tree-diagram amplitude has been considered. No reliable estimate of the exchange term for these decays exists although there are experimental hints that it is suppressed with respect to the tree term. The second approximation involves the use of the ratio of decay constants  $f_D/f_{D_s}$  to take into account  $SU(3)$  breaking effects and assumes factorization. We attribute a 30% relative error to the theoretical assumptions involved in obtaining the value of  $r_j$ .

Using the current experimental inputs we obtain:

$$\begin{aligned} r_{D\pi} &= 0.020 \pm 0.003 \pm 0.006(th.), \\ r_{D^*\pi} &= 0.015^{+0.004}_{-0.006} \pm 0.005(th.), \\ r_{D\rho} &= 0.006 \pm 0.003 \pm 0.002(th.). \end{aligned}$$

It has been suggested by theorists [52] to use the decay  $B^+ \rightarrow D^+\pi^0$  to determine  $r_{D\pi}$  (and similar for the other two modes) making use only of isospin symmetry (and not of  $SU(3)$  symmetry). The measurement of these branching ratios seems however challenging since we expect few events even at high luminosity ( $\sim 6$  in  $500 \text{ fb}^{-1}$ ). Using the current world averages from HFAG for the  $a_j$  and  $c_{lep,j}$  parameter and the  $r_j$  parameters obtained above we determine constraints on  $\sin(2\beta + \gamma)$  [117] using two different statistical approaches: a bayesian [53] approach which gives:

$$2\beta + \gamma = (88^{+40}_{-39})^\circ \quad (30)$$

and a frequentistic [54] approach which gives:

$$|\sin(2\beta + \gamma)| > 0.49 \text{ (0.27) at 68\% (90\%) CL.}$$

Figure shows the corresponding bounds obtained in the unitarity  $(\bar{\rho}, \bar{\eta})$  plane.

Projecting the error on  $2 \text{ ab}^{-1}$ , assuming the same measured central values for the  $a_j$  and  $c_{lep,j}$  parameters and no improvement on the knowledge of  $r_j$  gives an error on  $2\beta + \gamma$  of about  $30^\circ$ .

### 3.2.4 $\sin(2\beta + \gamma)$ from $B^0 \rightarrow D^0 K^{(0/+)}$ decays

*Contribution from V. Sordini, M. Pierini, L. Silvestrini & A. Stocchi*

In terms of the Operator Product Expansion, we can express the amplitudes for the decays of the  $B$  to neutral  $D$ -charged  $K$ :

$$\begin{aligned} A(B^+ \rightarrow \overline{D^0} K^+) &= T + C \\ A(B^+ \rightarrow D^0 K^+) &= \overline{C} + A \end{aligned}$$



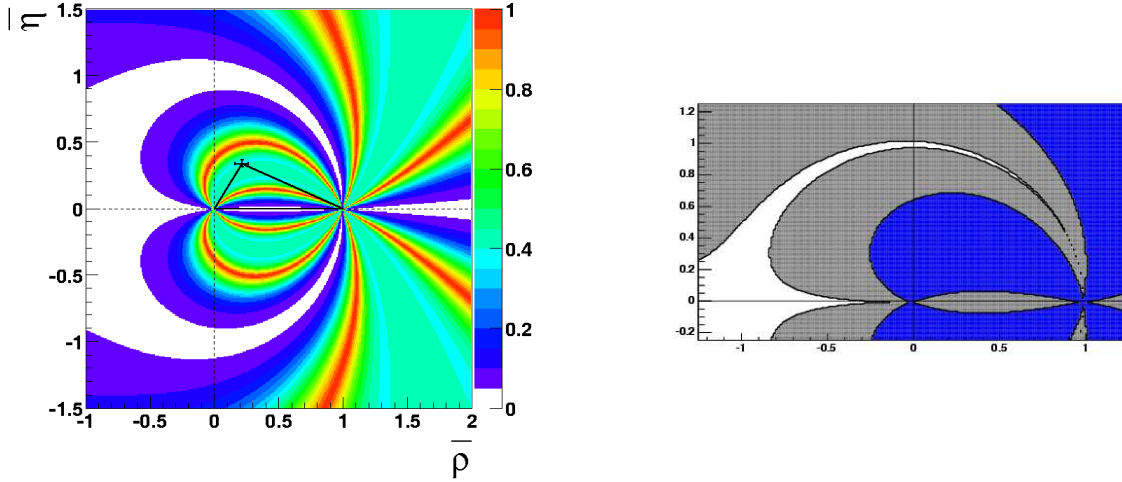


Figure 9: Bound in the unitarity  $(\bar{\rho}, \bar{\eta})$  plane from  $\sin(2\beta + \gamma)$  in the frequentistic (left) and in the bayesian approach (right). For the bayesian approach, the blue region corresponds to the 68% confidence level and the gray region to the 90% confidence level.

where T stays for “tree contribution” ( $T = V_{cs} V_{ub}^* E_1(s, l, c, K, D)$ ), A for “annihilation contribution” ( $A = V_{us} V_{cb}^* A_1(s, l, c, K, D)$ ), C and  $\bar{C}$  are “colour-suppressed contributions” ( $C = V_{cs} V_{ub}^* E_2(c, l, s, D, K)$ ,  $\bar{C} = V_{us} V_{cb}^* E_2(l, c, s, D, K)$ ) The parameters  $E_1, E_2$  and  $A_1$  are renormalization scheme and scale independent. We define  $r_{D^0 K^+}$  as the amplitudes ratio:

$$r_{D^0 K^+} = \frac{|A(B^+ \rightarrow \bar{D}^0 K^+)|}{|A(B^+ \rightarrow D^0 K^+)|}$$

Similarly for the decays of the  $B$  to neutral  $D$ -neutral  $K$  we can write the amplitudes in terms of the same parameters :

$$\begin{aligned} A(B^+ \rightarrow \bar{D}^0 K^0) &= C \\ A(B^+ \rightarrow D^0 K^0) &= \bar{C} \end{aligned}$$

and define the amplitudes ratio:

$$r_{D^0 K^0} = \frac{|A(B^0 \rightarrow \bar{D}^0 K^0)|}{|A(B^0 \rightarrow D^0 K^0)|}$$

C is known since the  $BR(B^+ \rightarrow \bar{D}^0 K^0)$  is measured and writing the two ratios in terms of the OPE parameters

$$\begin{aligned} r_{D^0 K^+} &= \frac{|\bar{C} + A|}{|T + C|} \\ r_{D^0 K^0} &= \frac{|\bar{C}|}{|C|} \end{aligned}$$

we get for  $\bar{C}$  the equation:

$$|\bar{C}| = -A \cos \delta \pm \sqrt{A^2 (\cos^2 \delta - 1) + r_{D^0 K^+}^2 BR(B^+ \rightarrow D^0 K^+)}$$

where the phase space term cancels and  $\delta$  is the strong phase .

There are two solutions for  $|C|$ , these are both acceptable only if:

$$\cos(\delta) < 0 \text{ and } A^2 > r_{D^0 K^+}^2 BR(B^+ \rightarrow D^0 K^+)$$

If we use the actual experimental values:

$$\begin{aligned} BR(B^+ \rightarrow \overline{D^0} K^+) &= (3.7 \pm 0.6) \cdot 10^{-4} \\ BR(B^+ \rightarrow \overline{D^0} K^0) &= (5.0 \pm 1.4) \cdot 10^{-5} \\ BR(B^+ \rightarrow D^+ K^0) &< 5.0 \cdot 10^{-6} \text{ @ 90\% probability} \end{aligned}$$

( the  $BR(B^+ \rightarrow D^+ K^0)$  is useful to determine the annihilation parameter  $A$  since:  $A(B^+ \rightarrow D^+ K^0) = A$  ) and the average for  $r_{D^0 K^+}$  from  $UT_{fit}$  :

$$r_{D^0 K^+} = 0.10 \pm 0.04 \text{ @ 68\% probability}$$

and we decide to accept, in case of ambiguity, both the solutions (the one with the sign + and the one with the sign -), we get :

$$r_{D^0 K^0} = 0.27 \pm 0.18 \text{ ( @ 68\% probability)}$$

Where, of the error on  $r_{D^0 K^0}$ , a contribution of 0.08 is due to the error on  $r_{D^0 K^+}$  and 0.16 to the other uncertainties. For the ratio  $\frac{r_{D^0 K^+}}{r_{D^0 K^0}}$  :

$$\frac{r_{D^0 K^+}}{r_{D^0 K^0}} = 0.43 \pm 0.19 \text{ (@68\%probability)}$$

If we extrapolate the errors on the measurements to a statistics of  $500 \text{ fb}^{-1}$  we would have ambiguity in 7.2% of cases. In this situation we would get:

$$r_{D^0 K^0} = 0.24 \pm 0.15 \text{ ( @ 68\% probability)}$$

Where, of the error on  $r_{D^0 K^0}$ , a contribution of 0.07 is due to the error on  $r_{D^0 K^+}$  and 0.13 to the other uncertainties. For the ratio  $\frac{r_{D^0 K^+}}{r_{D^0 K^0}}$  :

$$\frac{r_{D^0 K^+}}{r_{D^0 K^0}} = 0.44 \pm 0.18 \text{ ( @ 68\%probability)}$$

In principle, if one could determine the ratio  $r_{D^0 K^0}$ , this would be a useful input in the analysis of  $\sin(2\beta + \gamma)$ . We made a study to see the sensitivity to  $\sin(2\beta + \gamma)$ . This study was made assuming the information we get on  $r_{D^0 K^0}$  in the case of **no ambiguity** ( $\sim 93\%$  of cases for  $500 \text{ fb}^{-1}$ ), for which we get an error on  $r_{D^0 K^0}$  of 0.12. Assuming:

$$r_{D^0 K^0} = 0.30 \pm 0.15 \text{ ( @ 68\% probability)}$$

and errors on the observables  $S$  and  $C$  [55]

$$\delta S = 0.6 \quad \delta C = 0.5$$

we get an error of 60% on the determination of  $(2\beta + \gamma)$  through this method. The method doesn't seem much sensitive to  $(2\beta + \gamma)$ : the same exercise made assuming a statistic of  $1 \text{ ab}^{-1}$  and a value of  $r_{D^0 K^0} = 0.40$  returns an error on  $(2\beta + \gamma)$  of 42%.

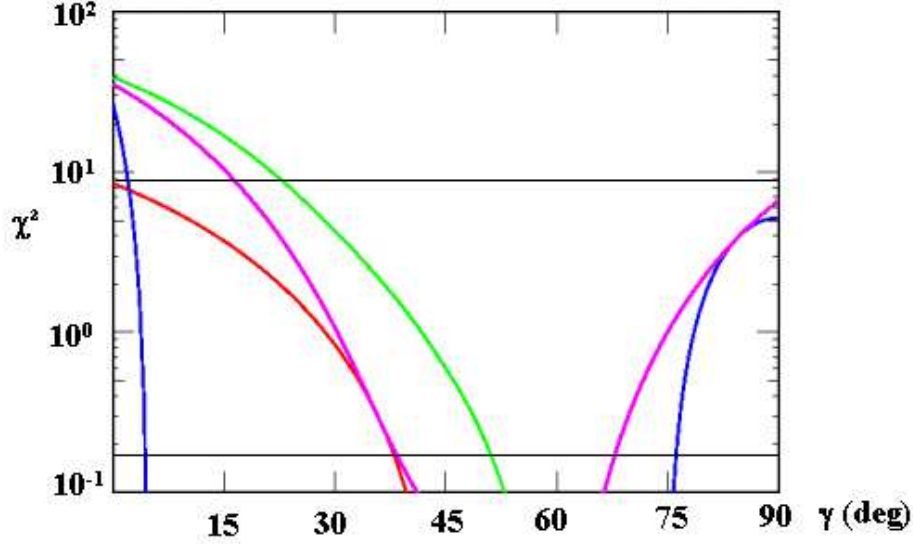


Figure 10:  $\gamma$  determination with incomplete input (i.e. cases when the number of observables is less than the number of unknown parameters). The upper horizontal line corresponds to low-luminosity i.e. around current B-factories whereas the lower horizontal curve is relevant for a SBF. Blue uses all CPES modes of  $D^0$ , red is with only  $K^+\pi^-$  and purple uses combination of the two. Green curve again uses on  $D^0$ ,  $\bar{D}^0 \rightarrow K^+\pi^-$  but now includes  $K^{*-}$  and  $D^{*0}$ ; see text for details.

## 4 Measurements of $\gamma/\phi_3$

### 4.1 Combined Strategies for extraction of a clean $\gamma$

*Contribution from D. Atwood*

A promising feature of clean and precise extraction of  $\gamma$  from  $B \rightarrow KD$  type of modes is that a multitude of strategies exist which are very effective when used in combination[56]. In here we focus on the use of direct  $CP$  from  $B^- \rightarrow "K^- D^0/\bar{D}^0$  though it is also possible to use time dependent  $CP$  violation via  $B^0 \rightarrow "K^0 D^0$ .

Fig 10 illustrates several of the important features. Here  $\chi_{\min}^2$  versus  $\gamma$  is compared for various methods and input data sets. Let us focus first specifically to  $B^- \rightarrow K^- D^0, \bar{D}^0$  with  $D^0, \bar{D}^0$  decays to common modes such as (CPNES)  $K^+\pi^-$  (ADS[57]) or (CPES)  $K_S^0\pi^0$  (GLW[58]). Then for each such common mode (say  $K^+\pi^-$ ) there are basically three unknowns:  $\delta_{st}, r_B$  and  $\gamma$  where  $\delta_{st}$  is the strong phase and  $r_B = Br(B^- \rightarrow K^- \bar{D}^0)/Br(B^- \rightarrow K^- D^0)$  and two observables: the rate for  $B^-$  and for  $B^+$ . Therefore as such we cannot hope to solve for  $\gamma$ . However, as we add another common mode of  $D^0, \bar{D}^0$ , say  $K^+\rho^-$ , then one is adding one new unknown (a strong phase) but 2 more observables. So now there are 4 observables and 4 unknowns and the system, is in principle, soluble though in practice presence of discrete ambiguities complicates the solution. In general for  $N$  such common modes, there will be  $N + 2$  unknowns and  $2N$  observables and as more modes are added  $\gamma$  can be solved for very effectively.

Fig. 10 and Fig. 11 show situation with regard to under-determined and over-determined cases respectively. The upper horizontal line corresponds roughly to the low luminosity i.e.

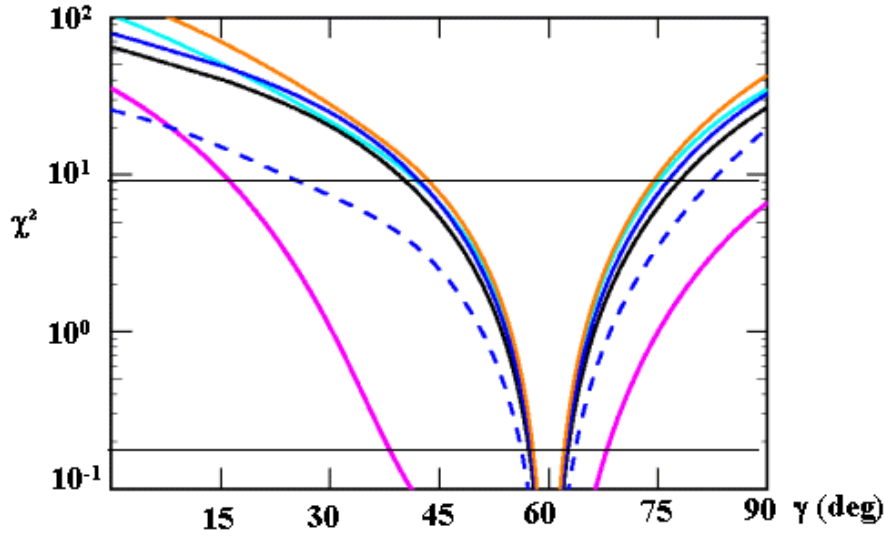


Figure 11:  $\gamma$  extraction with over-determined cases. Purple curve shows the effect of combining GLW (all CPES modes) with one ADS ( $K^+\pi^-$ ) mode; black curve differs from purple only in that it also includes  $D^0$  from  $D^{*0}$ ; blue curves show the effect of properly including the correlated strong phase between  $D^{*0} \rightarrow D^0 + \pi$  and  $D^{*0} \rightarrow D^0 + \gamma$ . Orange curve includes lot more input including Dalitz and multibody modes. see text for details (See also Fig 10).

comparable to the current  $B$ -factories[59] whereas the lower horizontal curve is relevant for a super  $B$ -factory. In Fig. 10 in blue is shown the case when only the input from (GLW) CPES modes of  $D^0$  is used; note all the CPES modes are included here. You see that the resolution on  $\gamma$  then is very poor. In particular, this method is rather ineffective in giving a lower bound; its upper bound is better.

In contrast, a single ADS mode ( $K^+\pi^-$ ) is very effective in so far as lower bound is concerned, but it does not yield an effective upper bound (red).

Note that in these two cases one has only two observables and 3 unknowns. In purple is shown the situation when these two methods are combined Then at least at high luminosity there is significant improvement in attaining a tight upper bound; lower bound obtained by ADS alone seems largely unaffected.

Shown in green is another under determined case consisting of the use of a single ADS mode, though it includes  $K^{*-}$  as well  $D^{*0}$ ; this again dramatically improves the lower bound. From an examination of these curves it is easy to see that combining information from different methods and modes improves the determination significantly[56].

Next we briefly discuss some over determined cases (Fig. 11). In purple all the CPES modes of  $D^0$  are combined with just one doubly cabibbo-suppressed (CPNES) mode. Here there are 4 observables for the 4 unknowns and one gets a reasonable solution at least especially for the high luminosity case.

The black curve is different from the purple one in only one respect; the black one also includes the  $D^{*0}$  from  $B^- \rightarrow K^- D^{*0}$  where subsequently the  $D^{*0}$  gives rise to a  $D^0$ . Comparison of the black one with the purple shows the remarkable improvement by including the  $D^{*0}$ . In this case the number of observables (8) exceeds the number of unknowns (6).

Actually, the  $D^{*0}$  can decay to  $D^0$  via two modes:  $D^{*0} \rightarrow D^0 + \pi$  or  $D^0 + \gamma$ . Bondar and

Gershon [60] have made a very nice observation that the strong phase for the  $\gamma$  emission is opposite that of the  $\pi$  emission. Inclusion (blue curves) of both types of emission increases the number of observables to 12 with no increase in number of unknowns. So this improves the resolving power for  $\gamma$  even more.

The orange curves show the outcome when a lot more input is included; not only  $K^-$ ,  $K^{*-}$ ,  $D^0$ ,  $D^{0*}$  but also Dalitz and multibody decays of  $D^0$  are included. But the gains now are very modest; those once the number of observables exceeds the number of unknowns by a few (say  $O(3)$ ) further increase in input only has a minimal impact.

## 4.2 Measurements of $\gamma$ at BaBar

The measurement of the angle  $\gamma$  of the unitarity triangle through  $B^- \rightarrow D^{(*)}K^{(*)-}$  requires the combination of as many  $B$  and  $D$  modes as possible to reduce the statistical uncertainty. Though the most statistically powerful approach analyzed so far is the one exploiting the Dalitz plot analysis of  $D^0 \rightarrow K_S^0 \pi^- \pi^+$  from  $B^- \rightarrow D^{(*)0} K^-$ , the GLW and ADS methods also provide useful information.

### 4.2.1 BaBar GWL and ADS

*Contribution from M. Rama*

BaBar has studied the decays  $B^\mp \rightarrow D^{(*)0} K^{(*)\mp}$  using  $D^{*0} \rightarrow D^0 \pi^0$  and  $K^{*-} \rightarrow K_S^0 \pi^-$ . The  $D^0$  meson is reconstructed in the CKM-favored modes  $K^- \pi^+$ ,  $K^- \pi^+ \pi^+ \pi^-$  and  $K^- \pi^+ \pi^0$ ; the  $CP+$  eigenstates  $K^- K^+$  and  $\pi^- \pi^+$ ; and the  $CP-$  eigenstates  $K_S^0 \pi^0$ ,  $K_S^0 \phi$ ,  $K_S^0 \omega$ . Figure 12 shows the distributions of  $\Delta E$  of the  $B \rightarrow D^0 K$  events ( $CP+$  and  $CP-$  modes). The signal yields are extracted through a maximum likelihood fit that uses as input  $\Delta E$  and the Cherenkov angle of the bachelor track  $K$ . Similar techniques are used to select  $B \rightarrow D^{*0} K$  and  $B \rightarrow D^0 K^*$  [61, 62, 63, 64]. The measurements of  $A_{CP\pm}$  and  $R_\pm$  allow to constrain the unknowns  $r_b$ ,  $\delta_b$  and the CKM angle  $\gamma$ . The results of the measurements are reported in Table 6, where  $R_{flav} \equiv BF(B^- \rightarrow D^{(*)0} K^-)/BF(B^- \rightarrow D^{(*)0} \pi^-)$ . Particular care is needed when evaluating the systematic uncertainties associated to peculiar sources of background. The  $B^- \rightarrow D_{CP+}^0 K^-$  decays are affected by the charmless 3-body background  $B^- \rightarrow K^- h^- h^+$  ( $h = \pi, K$ ), characterized by the same  $m_{ES}$  and  $\Delta E$  distribution as the signal. The  $B^- \rightarrow K^- \pi^- \pi^+$  and  $B^- \rightarrow K^- K^- K^+$  backgrounds ( $4 \pm 4$  and  $29 \pm 7$  events, respectively) are subtracted from the  $B^- \rightarrow D^0[\rightarrow \pi^- \pi^+] K^-$  and  $B^- \rightarrow D^0[\rightarrow K^- K^+] K^-$  signals ( $18 \pm 7$  and  $75 \pm 13$  events, respectively). Similarly, the  $B^- \rightarrow D^0[\rightarrow K_S^0 a_0] K^{*-}$  is evaluated and subtracted from the  $B^- \rightarrow D^0[\rightarrow K_S^0 \phi] K^{*-}$  signal. In this case, due to the different spin-parity of  $a_0$  with respect to  $\phi$ , the background has an opposite  $CP$  asymmetry with respect to the signal.

On a datasample of 227 million  $\Upsilon(4S) \rightarrow B\bar{B}$  decays we have searched for  $B^- \rightarrow \bar{D}^0 K^-$  followed by  $\bar{D}^0 \rightarrow K^+ \pi^-$ , as well as the charge conjugate sequences. In these processes, the favored  $B$  decay followed by the doubly CKM-suppressed  $D$  decay interferes with the suppressed  $B$  decay followed by the CKM-favored  $D$  decay. The yields of the signal mode and the normalization mode ( $B^- \rightarrow D^0 K^-$  with  $D^0 \rightarrow K^- \pi^+$ ) are extracted through a fit on  $m_{ES}$ , after requiring that the events have a  $\Delta E$  value consistent with zero within the resolution. We find a total of  $4.7_{-3.2}^{+4.0}$  signal events and  $356 \pm 26$  normalization events, that are used to evaluate the charge-integrated ratio  $R_{K\pi} = [B(B^- \rightarrow [K^+ \pi^-]_D K^-) + B(B^+ \rightarrow [K^- \pi^+]_D K^+)]/(2B(B^\mp \rightarrow [K^\mp \pi^\pm]_D K^\mp)) = r_B^2 + r_D^2 + 2r_B r_D \cos \delta_B \cos \gamma$ . The resulting limit is  $\mathcal{R}_{K\pi} < 0.030$  at 90% CL.

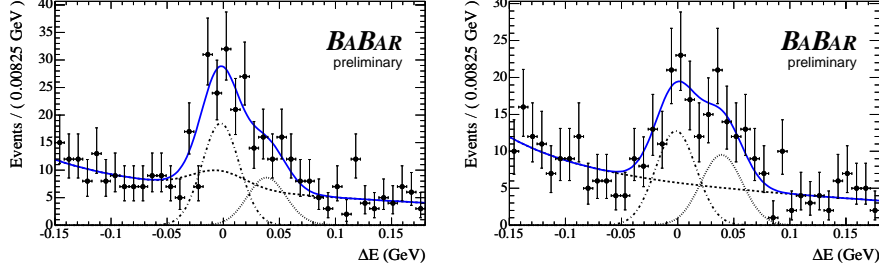


Figure 12: Distributions of  $\Delta E$  for events enhanced in  $B \rightarrow D^0 K$  signal. Left:  $CP+$ ; right:  $CP-$ . Solid curves represent projections of the maximum likelihood fit; dashed-dotted, dotted and dashed curves represent the  $B \rightarrow D^0 K$ ,  $B \rightarrow D^0 \pi$  and background contributions.

Using  $r_D = 0.060 \pm 0.003$  [66], and allowing the variation of  $\gamma$  and  $\delta_B$  on the full range  $0^\circ - 180^\circ$ , we set the limit  $r_B < 0.23$  at 90% CL [65].

Table 6: Measured  $CP$  asymmetries  $A_{CP\pm}$  and ratios  $R_{\pm}$ . The first error is statistical, the second is systematic.

	$B^- \rightarrow D^0 K^-$	$B^- \rightarrow D^0 K^{*-}$	$B^- \rightarrow D^{*0} K^-$
$N_{B\bar{B}} (\times 10^6)$	214	227	123
$A_{CP+}$	$0.40 \pm 0.15 \pm 0.08$	$-0.09 \pm 0.20 \pm 0.06$	$-0.02 \pm 0.24 \pm 0.05$
$A_{CP-}$	$0.21 \pm 0.17 \pm 0.07$	$-0.33 \pm 0.34 \pm 0.10^1$	$1.09 \pm 0.26^{+0.10}_{-0.08}$
$R_+$	$0.87 \pm 0.14 \pm 0.06$	$1.77 \pm 0.37 \pm 0.12$	***
$R_-$	$0.80 \pm 0.14 \pm 0.08$	$0.76 \pm 0.29 \pm 0.06^1$	***

## 5 Measurements of $\gamma/\phi_3$ with $D^0$ Dalitz analysis

The most precise determination of the standard model CKM phase in the long run is provided by the methods based on the interference between  $b \rightarrow c\bar{u}s$  and  $b \rightarrow u\bar{c}s$  [58, 46]. In the case of charged  $B$  decays this means that the interference is between  $B^- \rightarrow DK^-$  followed by  $D \rightarrow f$  decay and  $B^- \rightarrow \bar{D}K^-$  followed by  $\bar{D} \rightarrow f$ , where  $f$  is any common final state of  $D$  and  $\bar{D}$  [58, 46, 60]. Here we will restrict ourselves to the case, where  $f$  is a multibody final state. For concreteness we focus on the following cascade decay [17]

$$B^- \rightarrow DK^- \rightarrow (K_S \pi^- \pi^+)_D K^- . \quad (31)$$

For the  $B$  decay amplitudes we define

$$A(B^- \rightarrow D^0 K^-) \equiv A_B, \quad (32)$$

$$A(B^- \rightarrow \bar{D}^0 K^-) \equiv A_B r_B e^{i(\delta_B - \gamma)}. \quad (33)$$

<sup>1</sup>Additional biases  $\delta A_{CP-} = 0.15 \pm 0.10 \cdot (A_{CP-} - A_{CP+})$  and  $\delta R_- = -0.04_{-0.14}$  are quoted by the authors, reflecting possible interference effects between the  $\phi$  and  $\omega$  resonances and the background.

Here  $\delta_B$  is the difference of strong phases and  $A_B$  is taken to be positive. The same definitions apply to the amplitudes for the  $CP$  conjugate cascade  $B^+ \rightarrow DK^+ \rightarrow (K_S \pi^+ \pi^-)_D K^+$ , except that the weak phase flips the sign  $\gamma \rightarrow -\gamma$  in (33). For the  $D$  meson decay we further define

$$\begin{aligned} A_D(s_{12}, s_{13}) \equiv A_{12,13} e^{i\delta_{12,13}} &\equiv A(D^0 \rightarrow K_S(p_1)\pi^-(p_2)\pi^+(p_3)) \\ &= A(\bar{D}^0 \rightarrow K_S(p_1)\pi^+(p_2)\pi^-(p_3)), \end{aligned} \quad (34)$$

where  $s_{ij} = (p_i + p_j)^2$ , and  $p_1, p_2, p_3$  are the momenta of the  $K_S, \pi^-, \pi^+$  respectively. Note that in the last equation  $CP$  symmetry was used.

Obviously, if  $A_D(s_{12}, s_{13})$  were known, one could extract  $\gamma$  from  $B^\pm \rightarrow DK^\pm$  decay widths. One can measure  $A_D(s_{12}, s_{13})$  from tagged  $D \rightarrow K_S \pi^+ \pi^-$  by modeling it with a sum of Breit-Wigner forms and fitting the parameters from the corresponding Dalitz plot. This is the approach used at present by both BaBar [73] and Belle [74, 75], where the modeling error on extracted value of  $\gamma$  is estimated to be around  $10^\circ$ . In the future this modeling error can be avoided by performing a model independent analysis [17, 72].

Once the function  $A_D(m_-^2, m_+^2)$  is fixed using a model for the  $D^0 \rightarrow K_S \pi^+ \pi^-$  decay, the Dalitz distributions can be fitted simultaneously using the expressions for the two amplitudes and  $r_B, \delta$  and  $\gamma$  can be obtained.

To illustrate the region of the Dalitz plot most sensitive to  $\gamma$  measurement, we show in Fig. 13 the distribution of simulated  $B^- \rightarrow D^0 K^-$  events based on our Dalitz model, where each event is given a weight of  $\frac{d^2 \ln L}{d^2 \gamma}$ . Here  $L$  is the likelihood function described in the following section. The regions of interference between doubly Cabibbo suppressed and Cabibbo allowed decays and  $CP$  eigenstate decays are clearly the most sensitive ones: they exhibit the highest weights.

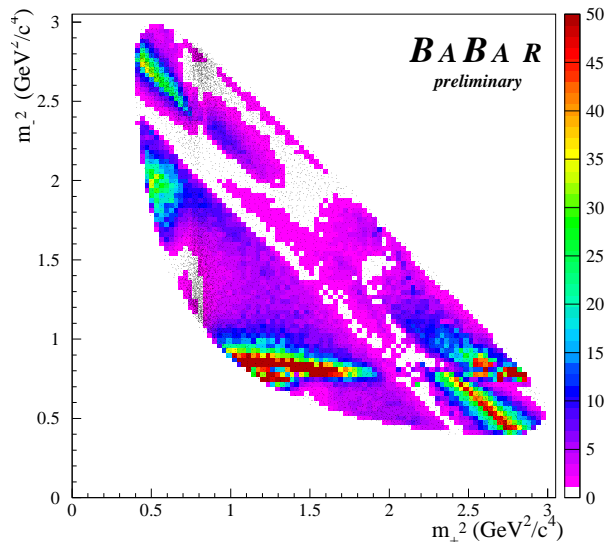


Figure 13:  $\bar{D}^0 \rightarrow K_S \pi^+ \pi^-$  Dalitz distribution of simulated ( $B^+ \rightarrow \bar{D}^0 K^+$ ) events. Each event is given a weight  $\frac{d^2 \ln L}{d^2 \gamma}$ . The weight scale is indicated on the right of the plot. The black points represent the same events with weight equal to unity.

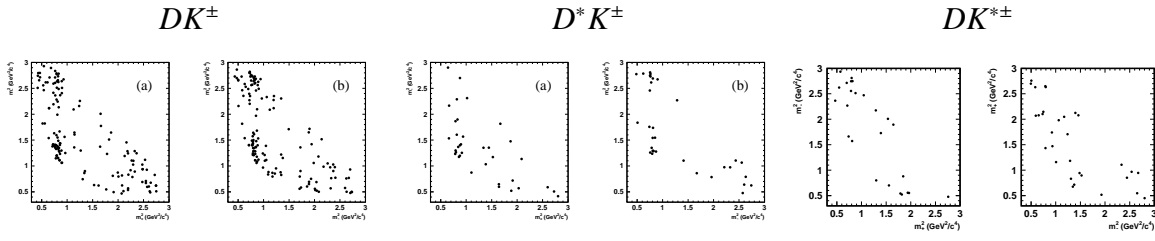


Figure 14: Dalitz distributions from Belle, separately for  $B^+$  and  $B^-$  decays, for (left)  $B^\pm \rightarrow DK^\pm$ , (middle)  $B^\pm \rightarrow D^*K^\pm$ , (right)  $B^\pm \rightarrow DK^{*\pm}$ . In each pair, the left plot contains the  $B^+$  candidates, while the right shows those from  $B^-$ .

## 5.1 Belle Measurement of $\phi_3$ From $B^\pm \rightarrow D^{(*)}K^{(*)\mp}$ , $D \rightarrow K_S\pi^+\pi^-$ Dalitz Analysis

*Contribution from K. Abe*

Belle have measured  $\phi_3$  using the Dalitz analysis method in  $B^\pm \rightarrow D^{(*)}K^{(*)\pm}$  using a data sample of 275 million  $B\bar{B}$  pairs. The subdecays  $D^* \rightarrow D\pi^0$ ,  $K^{*\pm} \rightarrow K_S\pi^\pm$ ,  $D \rightarrow K_S\pi^+\pi^-$  are used. The numbers of candidate events are  $209 \pm 16$  (with a background fraction of  $25 \pm 2\%$ ) for  $B^\pm \rightarrow DK^\pm$ ,  $58 \pm 8$  ( $13 \pm 2\%$ ) for  $B^\pm \rightarrow D^*K^\pm$ , and  $36 \pm 7$  ( $27 \pm 5\%$ ) for  $B^\pm \rightarrow DK^{*\pm}$ . The Dalitz distributions of candidate events are shown in Fig. 14.

We use continuum  $D^{*\pm} \rightarrow [K_S\pi^+\pi^-]_D\pi_s^\pm$  decays to obtain a flavour tagged  $\bar{D}^0 \rightarrow K_S\pi^+\pi^-$  sample and express the  $\bar{D}^0 \rightarrow K_S\pi^+\pi^-$  amplitude as a sum of 18 resonant and one non-resonant amplitudes.

$$f(m_+^2, m_-^2) = \sum_{j=1}^N a_j e^{i\alpha_j} A_j(m_+^2, m_-^2) + b e^{i\beta}. \quad (35)$$

The expected  $\bar{D}^0 \rightarrow K_S\pi^+\pi^-$  Dalitz distribution, with which we compare the data, is then given by

$$p(m_+^2, m_-^2) = \epsilon(m_+^2, m_-^2) \int_{-\infty}^{+\infty} |f(m_+^2 + \mu^2, m_-^2 + \mu^2)|^2 \exp\left(-\frac{\mu^2}{2\sigma_m^2(m_{\pi\pi}^2)}\right) d\mu^2 + B(m_+^2, m_-^2) \quad (36)$$

with efficiency  $\epsilon$ ,  $\pi\pi$  mass resolution  $\sigma_m$ , and background  $B$ . We obtain the parameters of the Dalitz model by minimizing

$$-2\log L = -2 \left[ \sum_{i=1}^n \log p(m_{+,i}^2, m_{-,i}^2) - \log \int_D p(m_+^2, m_-^2) dm_+^2 dm_-^2 \right] \quad (37)$$

with free parameters  $a_j$  and  $\alpha_j$  for each resonance (except for  $K_S\rho$  for which  $a_j = 1$ ,  $\alpha_j = 0$  are reference values),  $b$ ,  $\beta$ , and the masses and widths of  $\sigma_1$  and  $\sigma_2$ . The fit results are listed in Table 7.

The fitting procedure for  $B^\pm \rightarrow D^{(*)}K^{*\pm}$  is similar to that for the  $\bar{D}^0 \rightarrow K_S\pi^+\pi^-$  fit except  $f(m_+^2, m_-^2)$  is replaced with  $f(m_+^2, m_-^2) + r e^{i(\phi_3+\delta)} f(m_-^2, m_+^2)$ . The efficiency, resolution, and background distributions are also replaced with those relevant for the  $B$  decay.

We use  $B^\pm \rightarrow D^{(*)}\pi^\pm$  as control samples to test the analysis procedures. Separate fits to the  $B^+$  and  $B^-$  data give  $r_+ = 0.039 \pm 0.021$ ,  $\theta_+ = 240^\circ \pm 28^\circ$ , and  $r_- = 0.047 \pm 0.018$ ,  $\theta_- = 193^\circ \pm 24^\circ$



Intermediate state	Amplitude	Phase (°)	Fit fraction
$K_S \sigma_1$	$1.57 \pm 0.10$	$214 \pm 4$	9.8%
$K_S \rho^0$	1.0 (fixed)	0 (fixed)	21.6%
$K_S \omega$	$0.0310 \pm 0.0010$	$113.4 \pm 1.9$	0.4%
$K_S f_0(980)$	$0.394 \pm 0.006$	$207 \pm 3$	4.9%
$K_S \sigma_2$	$0.23 \pm 0.03$	$210 \pm 13$	0.6%
$K_S f_2(1270)$	$1.32 \pm 0.04$	$348 \pm 2$	1.5%
$K_S f_0(1370)$	$1.25 \pm 0.10$	$69 \pm 8$	1.1%
$K_S \rho^0(1450)$	$0.89 \pm 0.07$	$1 \pm 6$	0.4%
$K^*(892)^+ \pi^-$	$1.621 \pm 0.010$	$131.7 \pm 0.5$	61.2%
$K^*(892)^- \pi^+$	$0.154 \pm 0.005$	$317.7 \pm 1.6$	0.55%
$K^*(1410)^+ \pi^-$	$0.22 \pm 0.04$	$120 \pm 14$	0.05%
$K^*(1410)^- \pi^+$	$0.35 \pm 0.04$	$253 \pm 6$	0.14%
$K_0^*(1430)^+ \pi^-$	$2.15 \pm 0.04$	$348.7 \pm 1.1$	7.4%
$K_0^*(1430)^- \pi^+$	$0.52 \pm 0.04$	$89 \pm 4$	0.43%
$K_2^*(1430)^+ \pi^-$	$1.11 \pm 0.03$	$320.5 \pm 1.8$	2.2%
$K_2^*(1430)^- \pi^+$	$0.23 \pm 0.02$	$263 \pm 7$	0.09%
$K^*(1680)^+ \pi^-$	$2.34 \pm 0.26$	$110 \pm 5$	0.36%
$K^*(1680)^- \pi^+$	$1.3 \pm 0.2$	$87 \pm 11$	0.11%
non-resonant	$3.8 \pm 0.3$	$157 \pm 4$	9.7%

Table 7: Results of the fit to obtain the parameters of the  $\bar{D}^0 \rightarrow K_S \pi^+ \pi^-$  decay model, from Belle.

for the  $D\pi^\pm$  samples, and  $r_+ = 0.015 \pm 0.042$ ,  $\theta_+ = 169^\circ \pm 186$ , and  $r_- = 0.086 \pm 0.049$ ,  $\theta_- = 280^\circ \pm 30^\circ$  for the  $D^* \pi^\pm$  samples. These results are not inconsistent with the expectation of  $r \sim |V_{ub} V_{cd}^* / V_{cb} V_{ud}^*| \sim 0.01 - 0.02$  although  $\sim 2\sigma$  deviation is possible, which we include in the systematic error.

Fig. 15 shows the results of the fits in terms of  $Re(re^{i\theta}) - Im(re^{i\theta})$  separate  $B^+$  and  $B^-$  fits for  $DK^\pm$ ,  $D^* K^\pm$ , and  $DK^{*\pm}$  samples, respectively.

We use the frequentist technique for determining the confidence region. Here we determine PDFs using a toy Monte Carlo and calculate the confidence level and estimate the true  $(r, \phi_3, \delta)$  and their errors. This procedure removes possible bias which arises from an assumption of  $r$  being positive-definite. For the  $\delta$  and  $\phi_3$ , the difference from unbinned fits are small. However,  $r$  is changed by a small amount as expected. The results are shown in Table. 8.

Systematic errors arise from, i) background fractions and their shapes in the Dalitz plane, ii) efficiency shapes, iii) momentum resolution shapes, and iv) possible bias in the analysis method. In addition, another error is assigned due to the model-dependence of the variation of the complex phase in the  $\bar{D}^0 \rightarrow K_S \pi^+ \pi^-$  amplitude. Furthermore, for the  $DK^{*\pm}$  mode, we include an additional systematic error due to the possible presence of non-resonant  $DK_S \pi$  component which can give interference with different values of  $r$  and  $\delta$ .

When the  $DK^\pm$  and  $D^* K^\pm$  modes are combined, we obtain  $\phi_3 = 68_{-15}^{+14} \pm 13^\circ \pm 11^\circ$ . In the near future, the statistical error can be improved by combining all modes,  $DK^\pm$ ,  $D^*(D\pi)K^\pm$ ,  $DK^{*\pm}$ ,  $D^*(D\gamma)K^\pm$ , and by exploring other  $D$  decay modes such as  $D^0 \rightarrow \pi^+ \pi^- \pi^0$  and  $D^0 \rightarrow K^+ K^- K_S$ . As the data size increases, the experimental systematic error, which is presently dominated by the  $D^{(*)}\pi$  control sample size, will also improve. We hope to improving the  $D^0$

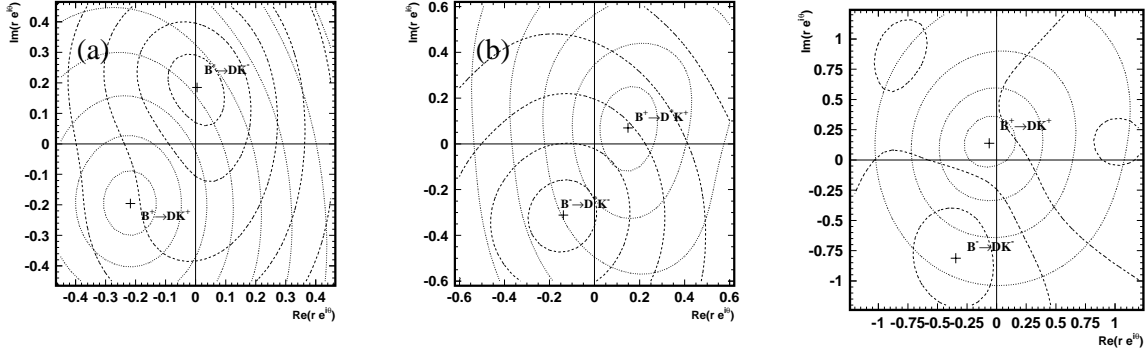


Figure 15: Results from Belle of separate  $B^+$  and  $B^-$  fits in terms of  $Re(re^{i\theta})-Im(re^{i\theta})$  for (left)  $B^\pm \rightarrow DK^\pm$ , (middle)  $B^\pm \rightarrow D^*K^\pm$ , (right)  $B^\pm \rightarrow DK^{*\pm}$ .  $CP$  violation is expected to appear as a relative rotation around the origin of the  $B^+$  and  $B^-$  contours.

	$r$	$\phi_3$ ( $^\circ$ )	$\delta$ ( $^\circ$ )
$DK^\pm$	$0.21 \pm 0.08 \pm 0.03 \pm 0.04$	$64 \pm 19 \pm 13 \pm 11$	$157 \pm 19 \pm 11 \pm 21$
$D^*K^\pm$	$0.12^{+0.16}_{-0.11} \pm 0.02 \pm 0.04$	$75 \pm 57 \pm 11 \pm 11$	$321 \pm 57 \pm 11 \pm 21$
$DK^{*\pm}$	$0.25^{+0.17}_{-0.18} \pm 0.09 \pm 0.04 \pm 0.08$	$112 \pm 35 \pm 9 \pm 11 \pm 8$	$353 \pm 35 \pm 8 \pm 21 \pm 49$

Table 8: Results of the Belle  $B^\pm \rightarrow D^{(*)}K^{(*)\pm}$ ,  $D \rightarrow K_S \pi^+ \pi^-$  measurements.

decay model by studying the  $CP$ -tagged  $D \rightarrow K_S \pi^+ \pi^-$  data from  $\psi(3770) \rightarrow D^0 \bar{D}^0$  at CLEO-c or BES. These data will provide  $|f(m_+^2, m_-^2) \pm f(m_-^2, m_+^2)|^2$  and therefore a direct measurement of the phases, thus dramatically reducing the model uncertainty.

## 5.2 Extracting $\gamma$ from $D$ Dalitz analysis at BaBar

*Contribution from M.H. Schune*

### 5.2.1 The Dalitz Model

The function  $A_D$  has been obtained using the flavour tagged  $D$  meson sample from the continuum decays  $D^{*\pm} \rightarrow D\pi^\pm$ . The Dalitz  $(m_+^2, m_-^2)$  distribution (Fig. 16) is fitted in the context of the isobar formalism described in [76]. In this formalism the amplitude  $f$  can be written as a sum of two-body decay matrix elements and a non-resonant term according to the expression:  $A_D = a_{nr}e^{i\phi_{nr}} + \sum_r a_r e^{i\phi_r} A_S(K_S \pi^- \pi^+ | r)$ . Each term of the sum is parameterized with an amplitude and a phase. We fit the Dalitz distribution with a model consisting of 13 resonances leading to 16 two-body decay amplitudes and phases (Table 9). Of the 13 resonances eight involve a  $K_S$  plus a  $\pi\pi$  resonance and the remaining five are made of a  $(K_S \pi^-)$  resonance plus a  $\pi^+$ . We also include the corresponding doubly Cabibbo-suppressed amplitudes for most of the  $(K_S \pi^-)$   $\pi^+$  decays. All the resonances considered in this model are well established except for the two scalar  $\pi\pi$  resonances,  $\sigma_1$  and  $\sigma_2$ , whose masses and widths are obtained from our sample.

An unbinned maximum likelihood fit is performed to measure the amplitudes  $a_{nr}$ ,  $a_r$  and the

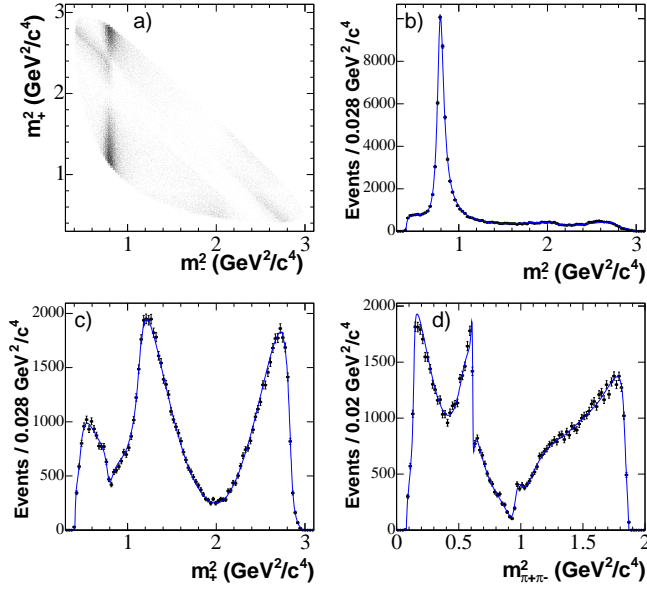


Figure 16: (a)  $D^0 \rightarrow K_S \pi^- \pi^+$  Dalitz distribution from  $D^{*+} \rightarrow D^0 \pi^+$  events, and projections on (b)  $m_-^2$ , (c)  $m_+^2$ , and (d)  $m_{\pi^+\pi^-}^2$ ; from *BABAR*. The curves are the fit projections.

phases  $\phi_{nr}$ ,  $\phi_r$ . components. The results of the fit are shown in Fig. 16. Amplitudes, phases and fit fractions as obtained by the likelihood fit are reported in Table 9.

Resonance	Amplitude	Phase (deg)	Fit fraction
$K^*(892)^-$	$1.781 \pm 0.018$	$131.0 \pm 0.8$	0.586
$K_0^*(1430)^-$	$2.447 \pm 0.076$	$-8.3 \pm 2.5$	0.083
$K_2^*(1430)^-$	$1.054 \pm 0.056$	$-54.3 \pm 2.6$	0.027
$K^*(1410)^-$	$0.515 \pm 0.087$	$154 \pm 20$	0.004
$K^*(1680)^-$	$0.89 \pm 0.30$	$-139 \pm 14$	0.003
$K^*(892)^+$	$0.1796 \pm 0.0079$	$-44.1 \pm 2.5$	0.006
$K_0^*(1430)^+$	$0.368 \pm 0.071$	$-342 \pm 8.5$	0.002
$K_2^*(1430)^+$	$0.075 \pm 0.038$	$-104 \pm 23$	0.000
$\rho(770)$	1 (fixed)	0 (fixed)	0.224
$\omega(782)$	$0.0391 \pm 0.0016$	$115.3 \pm 2.5$	0.006
$f_0(980)$	$0.4817 \pm 0.012$	$-141.8 \pm 2.2$	0.061
$f_0(1370)$	$2.25 \pm 0.30$	$113.2 \pm 3.7$	0.032
$f_2(1270)$	$0.922 \pm 0.041$	$-21.3 \pm 3.1$	0.030
$\rho(1450)$	$0.516 \pm 0.092$	$38 \pm 13$	0.002
$\sigma$	$1.358 \pm 0.050$	$-177.9 \pm 2.7$	0.093
$\sigma'$	$0.340 \pm 0.026$	$153.0 \pm 3.8$	0.013
Non Resonant	$3.53 \pm 0.44$	$127.6 \pm 6.4$	0.073

Table 9: Amplitudes, phases and fit fractions as obtained by the likelihood fit on the tagged  $D$  sample, from *BABAR*.

We estimate the goodness of fit through a  $\chi^2$  test and obtain  $\chi^2 = 3824$  for 3054 – 32 degrees

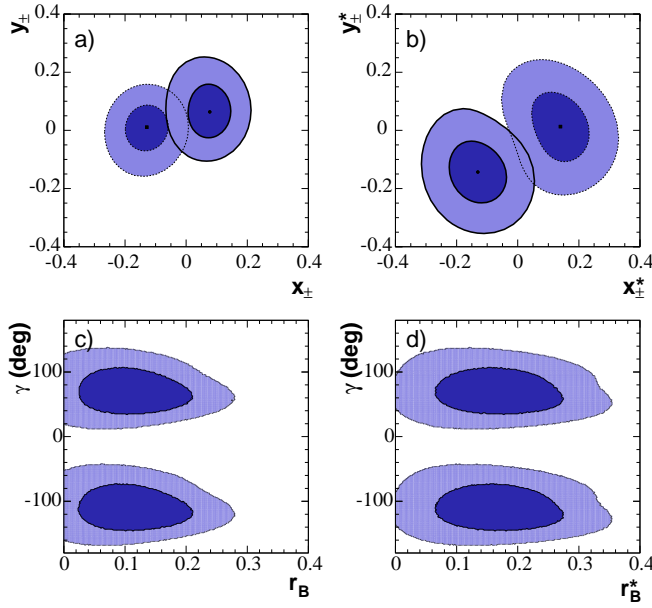


Figure 17: Contours at 68.3% (dark) and 95% (light) confidence level (statistical only) in the  $(x^{(*)}, y^{(*)})$  planes for (a)  $DK^-$  and (b)  $D^*K^-$ , separately for  $B^-$  (thick and solid) and  $B^+$  (thin and dotted). Two-dimensional projections in the  $r_B^{(*)} - \gamma$  planes of the five-dimensional one- (dark) and two- (light) standard deviation regions, for (c)  $DK^-$  and (d)  $D^*K^-$ .

of freedom.

## 5.2.2 Results of the $CP$ fit

BaBar reconstruct the decays  $B^- \rightarrow DK^-$  and  $B^- \rightarrow D^*K^-$  with  $D^* \rightarrow D\pi^0, D\gamma$ .  $B^-$  candidates are formed by combining a mass-constrained  $D^{(*)}$  candidate with a track identified as a kaon [33].

We simultaneously fit the  $B^- \rightarrow D^{(*)}K^-$  samples using an unbinned extended maximum-likelihood fit to extract the  $CP$ -violating parameters along with the signal and background yields.

In the sample of 211 million  $B\bar{B}$  events, the following signal yields are obtained

$$\begin{aligned}
 N(B^- \rightarrow D^0 K^-) &= 261 \pm 19, \\
 N(B^- \rightarrow D^{*0}(D^0 \pi^0) K^-) &= 83 \pm 11, \\
 N(B^- \rightarrow D^{*0}(D^0 \gamma) K^-) &= 40 \pm 8.
 \end{aligned} \tag{38}$$

The results for the  $CP$ -violating parameters  $x_{\pm}^{(*)}$  and  $y_{\pm}^{(*)}$ , are defined as the real and imaginary parts of the complex amplitude ratios  $r_B^{(*)} e^{i(\delta_B^{(*)} \pm \gamma)}$ , respectively.

The  $x_{\pm}^{(*)}$  and  $y_{\pm}^{(*)}$  variables are more suitable fit parameters than  $r_B^{(*)}$ ,  $\delta_B^{(*)}$  and  $\gamma$  because they are better behaved near the origin, especially in low-statistics samples. Figures 17(a,b) show the 68.3% and 95% confidence-level contours (statistical only) in the  $(x^{(*)}, y^{(*)})$  planes for  $DK^-$  and  $D^*K^-$ , and separately for  $B^-$  and  $B^+$ . The separation between the  $B^-$  and  $B^+$  regions in these planes is an indication of direct  $CP$  violation.

The largest contribution to the systematic uncertainties in the  $CP$  parameters comes from the choice of the model used to describe the  $D^0 \rightarrow K_S \pi^- \pi^+$  decay amplitudes. To evaluate this

uncertainty we use the nominal Dalitz model (Table 9) to generate large samples of experiments and we compare experiment by experiment the values of  $x_{\pm}^{(*)}$  and  $y_{\pm}^{(*)}$  obtained from fits using the nominal model and a set of alternative models. Models where one or both of the  $\sigma$  resonances are removed lead to a significant increase in the  $\chi^2$  of the fit. We use the average variations of  $x_{\pm}^{(*)}$  and  $y_{\pm}^{(*)}$  corresponding to this second set of alternative models as the systematic uncertainty due to imperfect knowledge of  $A_D$ .

A frequentist construction of the confidence regions of  $\mathbf{p} \equiv (r_B, r_B^*, \delta_B, \delta_B^*, \gamma)$  based on the constraints on  $x_{\pm}^{(*)}$  and  $y_{\pm}^{(*)}$  has been adopted (see below and Ref. [66]) and allows to extract  $\gamma$ ,  $r_B$ ,  $r_B^*$ ,  $\delta_B$  and  $\delta_B^*$ :

$\gamma = \left(70 \pm 31 \begin{smallmatrix} +12 & +14 \\ -10 & -11 \end{smallmatrix}\right)^\circ$   $[12^\circ, 137^\circ]$ ,  $r_B = 0.118 \pm 0.079 \pm 0.034 \begin{smallmatrix} +0.036 \\ -0.034 \end{smallmatrix}$   $[0, 0.279]$ ,  $r_B^* = 0.169 \pm 0.096 \begin{smallmatrix} +0.030 & +0.029 \\ -0.028 & -0.026 \end{smallmatrix}$   $[0, 0.354]$ ,  $\delta_B = \left(104 \pm 45 \begin{smallmatrix} +17 & +16 \\ -21 & -24 \end{smallmatrix}\right)^\circ$ ,  $\delta_B^* = \left(296 \pm 41 \begin{smallmatrix} +14 \\ -12 \end{smallmatrix} \pm 15\right)^\circ$ . The first error is statistical, the second is the experimental systematic uncertainty and the third reflects the Dalitz model uncertainty. The values inside square brackets indicate the two-standard-deviation intervals.

### 5.3 $\gamma$ extraction in $B^\pm \rightarrow D^{(*)}K^\pm$ Dalitz: a frequentist statistical treatment

*Contribution from N. Neri*

#### 5.3.1 Cartesian coordinates as fit parameters

The likelihood function used for the measurement of the angle  $\gamma$ , reconstructing  $D^0$  three-body decays (such as  $D^0 \rightarrow K_S \pi^+ \pi^-$ ) from  $B^- \rightarrow D^{(*)}K^-$  decays through a Dalitz analysis [17], is affected by biased values and non-Gaussian errors if we fit directly for the parameters  $r_B$ ,  $\gamma$  and  $\delta_B$ . We find that *cartesian coordinates*:

$$\begin{aligned} x_{\pm} &= r_B \cos(\gamma \pm \delta_B) \\ y_{\pm} &= r_B \sin(\gamma \pm \delta_B) \end{aligned}$$

are more suitable set of parameters because they are better behaved near the origin especially in low statistics sample. In addition the cartesian coordinates are largely uncorrelated. If we represent in the  $(x_{\pm}, y_{\pm})$  plane the results for  $B^\pm$  decays, the distance of the two points  $d$  is

$$d = [(x_- - x_+)^2 + (y_- - y_+)^2]^{1/2} = 2r_B |\sin \gamma|.$$

A non null distance means evidence of direct  $CP$  violation.

#### 5.3.2 Frequentist procedure

In the case of a single signal sample<sup>1</sup>  $B^\pm \rightarrow DK^\pm$ , we define a 4-dimensional PDF, of the fit parameter as a function of the true parameter, as:

$$\frac{d^4 P}{d^2 \mathbf{z}_+ d^2 \mathbf{z}_-}(\mathbf{z}_+, \mathbf{z}_- | \mathbf{p}^t) = G_2\left(\mathbf{z}_+; r_B^t \cos(\delta^t + \gamma^t), r_B^t \sin(\delta^t + \gamma^t), \sigma_{x_+}, \sigma_{y_+}, \rho_+\right) \times \\ G_2\left(\mathbf{z}_-; r_B^t \cos(\delta^t - \gamma^t), r_B^t \sin(\delta^t - \gamma^t), \sigma_{x_-}, \sigma_{y_-}, \rho_-\right)$$

<sup>1</sup>A similar procedure has been used for combined measurements of two and three signal  $B^\pm \rightarrow D^{(*)}K^{(*)\pm}$  samples.

where

$$G_2(\mathbf{z}; \mu_x, \mu_y, \sigma_x, \sigma_y, \rho) = \frac{1}{2\pi\sigma_x\sigma_y\sqrt{1-\rho^2}} e^{-\frac{1}{2(1-\rho^2)}\left[\frac{(x-\mu_x)^2}{\sigma_x^2} + \frac{(y-\mu_y)^2}{\sigma_y^2} - \frac{2\rho(x-\mu_x)(y-\mu_y)}{\sigma_x\sigma_y}\right]}$$

and  $\mathbf{z}_\pm = (x_\pm, y_\pm)$  and  $\mathbf{p} = (r_B, \gamma, \delta)$ . The vectors  $\mathbf{z}_\pm^t$  and  $\mathbf{p}^t$ , defined equivalently to  $\mathbf{z}_\pm$  and  $\mathbf{p}$  respectively, are the corresponding parameters in the truth parameter space. The Gaussian widths ( $\sigma_{x_\pm}, \sigma_{y_\pm}$ ) and the correlation distributions ( $\rho_\pm$ ) can be obtained either from Toy MC experiments or from the fit to the data sample itself.

The confidence level  $1 - \alpha$  for each set of true parameters  $\mathbf{p}^t$  is calculated as

$$\alpha(\mathbf{p}^t) = \int_D \frac{d^4P}{d^2\mathbf{z}_+d^2\mathbf{z}_-}(\mathbf{z}_+, \mathbf{z}_-|\mathbf{p}^t) d^2\mathbf{z}_+ d^2\mathbf{z}_-,$$

where the integration domain  $D$  (the confidence region) is given by the condition

$$\frac{d^4P}{d^2\mathbf{z}_+d^2\mathbf{z}_-}(\mathbf{z}_+, \mathbf{z}_-|\mathbf{p}^t) \geq \frac{d^4P}{d^2\mathbf{z}_+d^2\mathbf{z}_-}(\mathbf{z}_+^{\text{data}}, \mathbf{z}_-^{\text{data}}|\mathbf{p}^t),$$

*i.e.* it includes all points in the fit parameter space closer to the truth point than the data point  $\mathbf{z}^{\text{data}}$ . If we are interested in building a 3-dimensional region of joint probability  $1 - \alpha_0$ , then we select only those points for which  $\alpha(\mathbf{p}^t) \leq \alpha_0$ . The 2-dimensional and 1-dimensional contours are then built by projecting the 3-dimensional joint probability regions. The correct coverage of the method has been verified.

Finally, the significance of  $CP$  violation can be determined by finding the confidence level  $1 - \alpha_{CP}$  for the most probable  $CP$  conserving point  $\mathbf{p}_{CP}^t$ , *i.e.* the  $\mathbf{p}^t$  point with  $r_B^t = 0$  or  $\gamma^t = 0$ .

### 5.3.3 Perspectives

A preliminary study has been performed for the  $D^0 \rightarrow K_S K^+ K^-$  decay mode. The  $B^-$  candidate is reconstructed using similar selection of the  $D^0 \rightarrow K_S \pi^- \pi^+$  mode. Using this event yield and a study of the  $D^0 \rightarrow K_S K^\pm K^\mp$  Dalitz plot, toy studies indicate a marginal gain of few percent on the  $\gamma$  uncertainty. However, it is worthwhile noting that the systematic uncertainty due to the Dalitz model will be totally independent of the one of the  $D^0 \rightarrow K_S \pi^- \pi^+$  analysis.

A first analysis of the  $B^- \rightarrow D^0 K^-$  mode using the  $D^0 \rightarrow \pi^+ \pi^- \pi^0$  decay mode has been performed. This channel is affected by a larger background that could dilute the sensitivity to  $\gamma$ . Nevertheless, adding this channel is certainly worthwhile in a strategy of a combined fit with other channels.

Using the present cartesian central values and a Bayesian technique we have computed the expected uncertainty for  $\gamma$  for various integrated luminosities. The systematic uncertainty has been (conservatively) assumed to stay constant. It has been shown that, up to  $500 \text{ fb}^{-1}$ , the result is yet not dominated by the Dalitz model systematic uncertainty. However, in a view of a larger statistics accumulated by  $B$ -factory it is probably worthwhile performing a model independent analysis [17].

## 5.4 Model independent approach

*Contribution from J. Zupan*

The first step in the model independent approach is to partition the Dalitz plot into  $2k$  bins placed symmetrically about the  $12 \leftrightarrow 13$  line. The  $k$  bins lying below the symmetry axis are denoted by index  $i$ , while the remaining bins are indexed with  $\bar{i}$ . The  $\bar{i}$ -th bin is obtained by mirroring the  $i$ -th bin over the axis of symmetry. For bins below the symmetry axis we define

$$c_i \equiv \int_i dp A_{12,13} A_{13,12} \cos(\delta_{12,13} - \delta_{13,12}), \quad (39)$$

$$s_i \equiv \int_i dp A_{12,13} A_{13,12} \sin(\delta_{12,13} - \delta_{13,12}), \quad (40)$$

$$T_i \equiv \int_i dp A_{12,13}^2, \quad (41)$$

where the integrals are done over the phase space of the  $i$ -th bin. The variables  $c_i$  and  $s_i$  contain differences of strong phases and are therefore unknowns in the analysis. The variables  $T_i$ , on the other hand, can be measured from the flavor tagged  $D$  decays, and are assumed to be known inputs into the analysis. The variables  $c_i, s_i$  of the  $i$ -th bin are related to the variables of the  $\bar{i}$ -th bin by

$$c_{\bar{i}} = c_i, \quad s_{\bar{i}} = -s_i, \quad (42)$$

while there is no relation between  $T_i$  and  $T_{\bar{i}}$ .

Together with the information available from the  $B^+$  decay, we arrive at a set of  $4k$  equations

$$\hat{\Gamma}_i^- \equiv \int_i d\hat{\Gamma}(B^- \rightarrow (K_S \pi^- \pi^+)_D K^-) = T_i + r_B^2 T_{\bar{i}} + 2r_B [\cos(\delta_B - \gamma)c_i + \sin(\delta_B - \gamma)s_i], \quad (43)$$

where we display only the first  $k$  equations, while the other expressions for  $\hat{\Gamma}_{\bar{i}}^-, \hat{\Gamma}_i^+, \hat{\Gamma}_{\bar{i}}^+$  can be obtained from the above by  $12 \leftrightarrow 13$  and/or  $\gamma \leftrightarrow -\gamma$  replacements [17]. We have  $2k + 3$  unknowns:  $c_i, s_i, r_B, \delta_B, \gamma$  for  $4k$  observables, so that the set of equations is solvable for  $k \geq 2$ , i.e., if Dalitz plot is divided into at least four bins. The whole approach has been extended also to neutral  $B$  decays [77].

An important input can be provided by charm factories [17, 72]. Namely, the parameters  $c_i$  and  $s_i^2$  describing  $D$  decay can be measured at charm factories working at  $\psi(3770)$ . This greatly reduces the number of unknowns needed to be fit from  $B$  decays (which is the limiting statistical factor). Another observation is that  $c_i, s_i$  are bounded from above and below,  $|s_i|, |c_i| \leq \int_i dp A_{12,13} A_{13,12} \leq \sqrt{T_i T_{\bar{i}}}$ . This can prove useful in the actual implementation of the method. An important question for the implementation of the method is also, how small need the bins be, not to average out sensitivity to  $\gamma$ ? Answer to this question is rather complicated and difficult to answer without a Monte Carlo study.

Another interesting observation is, that to leading order in  $x = \Delta m_D / \Gamma_D, y = \Delta \Gamma_D / (2\Gamma_D)$  CP conserving  $D - \bar{D}$  mixing does not change the formalism [78]. Also, the uncertainty due to CP violation in  $D$  sector is  $\lambda^6 \sim 10^{-4}$  suppressed in SM and therefore completely negligible. However, even these effects can be included in the analysis [78].

## 5.5 Charm phenomenology and extraction of the CKM angle $\gamma$

*Contribution from A.A. Petrov*

The Standard Model is a very constrained system, which implements a remarkably simple and economic description of all  $CP$ -violating processes in the flavor sector by a single  $CP$ -violating parameter, the phase of the CKM matrix. This fact relates all  $CP$ -violating observables in bottom, charm and strange systems and provides an excellent opportunity for searches of physics beyond the Standard Model. One of the major goals of the contemporary experimental  $B$  physics program is an accurate determination of the CKM parameters. As we shall see below, inputs from charm decays are important ingredient in this program, both in the extraction of the angles and sides of the CKM unitarity triangle.

The cleanest methods of the determination of the CKM phase  $\gamma = \arg \left[ -V_{ud}V_{ub}^*/V_{cd}V_{cb}^* \right]$  involve the interference of the  $b \rightarrow c\bar{u}s$  and  $b \rightarrow u\bar{c}s$  quark-level transitions [79]. A way to arrange for an interference of those seemingly different processes was first pointed out in [58, 46]. It involves interference of two *hadronic* decays  $B^+ \rightarrow D^0 K^+ \rightarrow f K^+$  and  $B^+ \rightarrow \bar{D}^0 K^+ \rightarrow f K^+$ , with  $f$  being any common final state for  $D^0$  and  $\bar{D}^0$  decays. Since then, many different methods have been proposed, mainly differing by the  $fK$  final state (i.e. with  $f$  being a  $CP$ -eigenstate or not a  $CP$ -eigenstate) and paths of reaching it: a combination of the Cabibbo-favored (CF) and doubly-Cabibbo suppressed decays (DCSD)  $D^0(\bar{D}^0) \rightarrow K^+\pi^-$  [57], singly-Cabibbo suppressed decays (SCSD)  $D^0(\bar{D}^0) \rightarrow KK^*$  [67], Cabibbo-favored decays employing large  $K^0 - \bar{K}^0$  mixing transitions [17]. For similar methods involving interference of the *initial* state, see [80].

All these methods produce expressions that depend on  $\gamma$  and several hadronic parameters, such as ratios of hadronic amplitudes and strong phases. These parameters cannot be reliably computed at the moment, so their values must be fixed from experimental data. In principle, all of the hadronic parameters in these methods can be obtained from the measurements of  $B$ -decays only. However, accuracy of these methods can be significantly improved if some measurements of charm-related parameters are performed separately. A good example is provided by the original GW method [58, 46], which does not take into account the possibility of relatively large  $D^0 - \bar{D}^0$  mixing [81]. This method relies on the simple triangle amplitude relation

$$\sqrt{2}A(B^+ \rightarrow D_{\pm}K^+) = A(B^+ \rightarrow D^0K^+) \pm A(B^+ \rightarrow \bar{D}^0K^+), \quad (44)$$

which follows from the relation which neglects  $CP$ -violation in charm,

$$\sqrt{2}|D_{\pm}\rangle = |D^0\rangle \pm |\bar{D}^0\rangle. \quad (45)$$

An amplitude  $A(B^+ \rightarrow D_{\pm}K^+)$  is measured with  $D$  decaying to a particular  $CP$ -eigenstate. Neglecting  $D^0 - \bar{D}^0$  mixing, angle  $\gamma$  can then be extracted, up to a discrete ambiguity, from the measurements of  $B^{\pm} \rightarrow f_{CP}K^{\pm}$  and  $B^{\pm} \rightarrow D^0, \bar{D}^0K^{\pm}$ . In particular,

$$\Gamma[B^{\pm} \rightarrow f_{CP}K^{\pm}] \propto 1 + r_B^2 + 2r_B c_{\pm}, \quad (46)$$

where  $c_{\pm} = \cos(\gamma \pm \delta_B)$  and  $r_B$  and  $\delta_B$  are defined from

$$A(B^+ \rightarrow D^0K^+)/A(B^+ \rightarrow \bar{D}^0K^+) = r_B e^{i(\gamma + \delta_B)}, \quad (47)$$

Then,

$$\sin^2 \gamma = \frac{1}{2} \left[ 1 - c_+ c_- \pm \sqrt{(1 - c_+^2)(1 - c_-^2)} \right]. \quad (48)$$

It is easy to see that  $D^0 - \bar{D}^0$  mixing, if not properly accounted for, can affect the results of this analysis. Indeed, taking  $D^0 - \bar{D}^0$  mixing into account results in the modification of the



definitions of  $c_{\pm}$ ,

$$c_{\pm} \rightarrow \cos(\gamma \pm \delta_B) \mp \frac{x}{2r_B} \sin 2\theta_D - \frac{y}{2r_D} \left[ 2\eta_f r_D \cos(\gamma + 2\theta_D \pm \delta_B) + \cos 2\theta_D \right], \quad (49)$$

where

$$x \equiv \frac{m_2 - m_1}{\Gamma}, \quad y \equiv \frac{\Gamma_2 - \Gamma_1}{2\Gamma}, \quad (50)$$

with  $m_{1,2}$  and  $\Gamma_{1,2}$  being the masses and widths of D-meson mass eigenstates  $D_{1,2}$  (which reduce to  $D_{\pm}$  in the  $CP$ -invariance limit),  $\eta_f$  is a  $CP$ -parity of  $f_{CP}$ , and  $\theta_D$  is a  $CP$ -violating phase of  $D^0 - \bar{D}^0$  mixing. It is easy to see that  $y \sim 1\%$  can impact the determination of  $\gamma$  from these modes. Thus, separately constraining  $D^0 - \bar{D}^0$  mixing parameters will be helpful.

The current experimental upper bounds on  $x$  and  $y$  are on the order of a few times  $10^{-2}$ , and are expected to improve significantly in the coming years. As was recently shown [82], in the Standard Model,  $x$  and  $y$  are generated only at second order in  $SU(3)_F$  breaking,

$$x, y \sim \sin^2 \theta_C \times [SU(3) \text{ breaking}]^2, \quad (51)$$

where  $\theta_C$  is the Cabibbo angle. Therefore, predicting the Standard Model values of  $x$  and  $y$  depends crucially on estimating the size of  $SU(3)_F$  breaking. Although  $y$  is expected to be determined by the Standard Model processes, its value can affect the sensitivity to new physics of experimental analyses of  $D$  mixing [83].

Presently, experimental information about the  $D^0 - \bar{D}^0$  mixing parameters  $x$  and  $y$  comes from the time-dependent analyses that can roughly be divided into two categories. First, one can look at the time dependence of  $D \rightarrow f$  decays, where  $f$  is the final state that tags the flavor of the decayed meson. The most popular is the non-leptonic doubly Cabibbo suppressed decay  $D^0 \rightarrow K^+ \pi^-$ . Time-dependent studies allow one to separate the DCSD from the mixing contribution  $D^0 \rightarrow \bar{D}^0 \rightarrow K^+ \pi^-$ ,

$$\begin{aligned} \Gamma[D^0(t) \rightarrow K^+ \pi^-] &= e^{-\Gamma t} |A_{K^+ \pi^-}|^2 \\ &\times \left[ R + \sqrt{R} R_m (y' \cos \phi - x' \sin \phi) \Gamma t + \frac{R_m^2}{4} (y^2 + x^2) (\Gamma t)^2 \right], \end{aligned} \quad (52)$$

where  $R$  is the ratio of DCS and Cabibbo favored (CF) decay rates. Since  $x$  and  $y$  are small, the best constraint comes from the linear terms in  $t$  that are also *linear* in  $x$  and  $y$ . A direct extraction of  $x$  and  $y$  from Eq. (52) is not possible due to unknown relative strong phase  $\delta_D$  of DCS and CF amplitudes [84], as  $x' = x \cos \delta_D + y \sin \delta_D$ ,  $y' = y \cos \delta_D - x \sin \delta_D$ . As discussed below, this phase can be measured independently [81, 85, 86]. Second,  $D^0$  mixing can be measured by comparing the lifetimes extracted from the analysis of  $D$  decays into the  $CP$ -even and  $CP$ -odd final states. This study is also sensitive to a *linear* function of  $y$  via

$$\frac{\tau(D \rightarrow K^- \pi^+)}{\tau(D \rightarrow K^+ K^-)} - 1 = y \cos \phi - x \sin \phi \left[ \frac{R_m^2 - 1}{2} \right]. \quad (53)$$

Time-integrated studies of the semileptonic transitions are sensitive to the *quadratic* form  $x^2 + y^2$  and are not competitive with the analyses discussed above.

Charm factories (ChF) such as CLEO-c and BES-III introduce new *time-independent* methods that are sensitive to a linear function of  $y$ . There, one can use the fact that heavy meson

pairs produced in the decays of heavy quarkonium resonances have the useful property that the two mesons are in the  $CP$ -correlated states [87],

$$|D\bar{D}^0\rangle_L = \frac{1}{\sqrt{2}} \left\{ |D^0(k_1)\bar{D}^0(k_2)\rangle + (-1)^L |D^0(k_2)\bar{D}^0(k_1)\rangle \right\}, \quad (54)$$

where  $L$  is the relative angular momentum of two  $D$  mesons,  $CP$  properties of the final states produced in the decay of  $\psi(3770)$  are anti-correlated, one  $D$  state decayed into the final state with definite  $CP$  properties immediately identifies or tags  $CP$  properties of the state “on the other side.” That is to say, if one state decayed into, say  $\pi^0 K_S$  with  $CP = -1$ , the other state is “ $CP$ -tagged” as being in the  $CP = +1$  state. By tagging one of the mesons as a  $CP$  eigenstate, a lifetime difference may be determined by measuring the leptonic branching ratio of the other meson. Its semileptonic *width* should be independent of the  $CP$  quantum number since it is flavor specific, yet its *branching ratio* will be inversely proportional to the total width of that meson. Since we know whether this  $D(k_2)$  state is tagged as a ( $CP$ -eigenstate)  $D_\pm$  from the decay of  $D(k_1)$  to a final state  $S_\sigma$  of definite  $CP$ -parity  $\sigma = \pm$ , we can easily determine  $y$  in terms of the semileptonic branching ratios of  $D_\pm$ . This can be expressed simply by introducing the ratio

$$R_\sigma^L = \frac{\Gamma[\psi_L \rightarrow (H \rightarrow S_\sigma)(H \rightarrow Xl^\pm\nu)]}{\Gamma[\psi_L \rightarrow (H \rightarrow S_\sigma)(H \rightarrow X)] Br(H^0 \rightarrow Xl\nu)}, \quad (55)$$

where  $X$  in  $H \rightarrow X$  stands for an inclusive set of all final states. A deviation from  $R_\sigma^L = 1$  implies a lifetime difference. Keeping only the leading (linear) contributions due to mixing,  $y$  can be extracted from this experimentally obtained quantity,

$$y \cos \phi = (-1)^L \sigma \frac{R_\sigma^L - 1}{R_\sigma^L}. \quad (56)$$

Theoretical predictions of  $x$  and  $y$  within and beyond the Standard Model span several orders of magnitude [88]. Roughly, there are two approaches, neither of which give very reliable results because  $m_c$  is in some sense intermediate between heavy and light. The “inclusive” approach is based on the operator product expansion (OPE). In the  $m_c \gg \Lambda$  limit, where  $\Lambda$  is a scale characteristic of the strong interactions,  $\Delta M$  and  $\Delta\Gamma$  can be expanded in terms of matrix elements of local operators [89]. Such calculations yield  $x, y < 10^{-3}$ . The use of the OPE relies on local quark-hadron duality, and on  $\Lambda/m_c$  being small enough to allow a truncation of the series after the first few terms. The charm mass may not be large enough for these to be good approximations, especially for nonleptonic  $D$  decays. An observation of  $y$  of order  $10^{-2}$  could be ascribed to a breakdown of the OPE or of duality. The “exclusive” approach sums over intermediate hadronic states, which may be modeled or fit to experimental data [90]. Since there are cancellations between states within a given  $SU(3)$  multiplet, one needs to know the contribution of each state with high precision. However, the  $D$  is not light enough that its decays are dominated by a few final states. While most studies find  $x, y < 10^{-3}$ , Refs. [90] obtain  $x$  and  $y$  at the  $10^{-2}$  level by arguing that  $SU(3)_F$  violation is of order unity, but the source of the large  $SU(3)_F$  breaking is not made explicit. It was shown that phase space effects alone provide enough  $SU(3)_F$  violation to induce  $y \sim 10^{-2}$  [82]. Large effects in  $y$  appear for decays close to  $D$  threshold, where an analytic expansion in  $SU(3)_F$  violation is no longer possible. Thus, theoretical calculations of  $x$  and  $y$  are quite uncertain, and the values near the current experimental bounds cannot be ruled out.

Another example of a method that will benefit from the separately performed charm decay measurements is the ADS method [57]. In its original form, it seeks to obtain  $\gamma$  from two sets of

measurements,  $B^\pm \rightarrow D^0(\rightarrow K^\mp \pi^\pm)K^\pm$ , i.e. use decays of  $D$  into non- $CP$ -eigenstate final states,

$$\begin{aligned} R_{ADS} &= \frac{\Gamma(B^- \rightarrow D^0_{\rightarrow K^+\pi^-} K^-) + \Gamma(B^+ \rightarrow D^0_{\rightarrow K^-\pi^+} K^+)}{\Gamma(B^- \rightarrow D^0_{\rightarrow K^-\pi^+} K^-) + \Gamma(B^+ \rightarrow D^0_{\rightarrow K^+\pi^-} K^+)} \\ &= r_D^2 + 2r_B r_D \cos \gamma \cos(\delta_B + \delta_D) + r_B^2, \end{aligned} \quad (57)$$

$$\begin{aligned} A_{ADS} &= \frac{\Gamma(B^- \rightarrow D^0_{\rightarrow K^+\pi^-} K^-) - \Gamma(B^+ \rightarrow D^0_{\rightarrow K^-\pi^+} K^+)}{\Gamma(B^- \rightarrow D^0_{\rightarrow K^-\pi^+} K^-) + \Gamma(B^+ \rightarrow D^0_{\rightarrow K^+\pi^-} K^+)} \\ &= 2r_B r_D \cos \gamma \cos(\delta_B + \delta_D) / R_{ADS}, \end{aligned} \quad (58)$$

where one parameterizes the ratio of a DCS to CF decays,  $A(D^0 \rightarrow K^+\pi^-)/A(D^0 \rightarrow K^-\pi^+) = r_D e^{i\delta_D}$ . The accuracy of this method will be greatly improved if  $r_D$  and  $\delta_D$  are measured separately. While the separate measurement of  $r_D$  is already available, determination of  $\delta_D$  will become possible at the charm factories at Cornell and Beijing. This allows one to measure  $\cos \delta_D$ . In order to see this, let us write a triangle relation,

$$\sqrt{2}A(D_\pm \rightarrow K^-\pi^+) = A(D^0 \rightarrow K^-\pi^+) \pm A(\bar{D}^0 \rightarrow K^-\pi^+), \quad (59)$$

which follows from the fact that, in the absence of  $CP$ -violation in charm, mass eigenstates of the neutral  $D$  meson coincide with its  $CP$ -eigenstates, as in Eq. (45). This implies a relation for the branching ratios,

$$1 \pm 2 \cos \delta_D \sqrt{r_D} = 2 \frac{Br(D_\pm \rightarrow K^-\pi^+)}{Br(D^0 \rightarrow K^-\pi^+)}, \quad (60)$$

where we used the fact that  $r_D \ll \sqrt{r_D}$  and neglected  $CP$  violation in mixing, which could undermine the  $CP$ -tagging procedure by splitting the  $CP$ -tagged state on one side into a linear combination of  $CP$ -even and  $CP$ -odd states. Its effect, however, is completely negligible here. Notice that the phase  $\delta_D$  in Eq. (60) is the same as the one that appears in Eq. (52). Now, if both decays of  $D_+$  and  $D_-$  are measured,  $\cos \delta_D$  can be obtained from the asymmetry

$$\cos \delta_D = \frac{Br(D_+ \rightarrow K^-\pi^+) - Br(D_- \rightarrow K^-\pi^+)}{2 \sqrt{r_D} Br(D^0 \rightarrow K^-\pi^+)}. \quad (61)$$

Both Eqs. (60) and (61) can be used to extract  $\delta_D$  at ChF. Similar measurements are possible for other  $D$  decays [91].

One potential problem in measuring the strong phase this way is the need for high-statistics measurement which might not be possible at CLEO-c, provided if phase turns out to be small. One indication of that is the fact that  $A(D^0 \rightarrow K^+\pi^-) = \lambda^2 A(\bar{D}^0 \rightarrow K^+\pi^-) = \lambda^2 A(D \rightarrow K^-\pi^+)$  in the flavor SU(3) limit, which implies that  $\delta_D = 0$  in this limit. Therefore, calculation of the value of  $\delta_D$  is equivalent to computation of an SU(3)-breaking correction. This, however, does not imply that it is very small [82], as SU(3) breaking in charm decays can be significant.

Another possibility would be to use other common modes of  $D^0$  and  $\bar{D}^0$ , such as  $D \rightarrow K^{*+}\pi^-, \rho^- K^+, \rho^+ \pi^-$ , etc. The same arguments leading to Eq. (61) can be applied there as well and the resulting equation would look identical. One added benefit is that SU(3) symmetry arguments alone do not force the strong phase to be zero, so its value could in principle be larger. One can speculate that if the chiral symmetry in QCD is realized in the ‘‘vector’’ mode [92], then  $A(D^0 \rightarrow K^{*+}\pi^-) = \lambda^2 A(D^0 \rightarrow K^{*-}\pi^+)$  in the limit of ‘‘vector’’ SU(3)<sub>L</sub> × SU(3)<sub>R</sub> symmetry, so the relevant strong phase is still zero. It is however not clear if this realization of chiral symmetry is relevant to charm decays (except, may be in the large  $N_c$  limit). In any case, vector symmetry is badly broken in  $D$  decays [92], so the resulting strong phase can still be large. Clearly, only experimental measurements would settle these issues.

## 5.6 CLEO-c Impact on $\gamma/\phi_3$ Measurements

*Contribution from D. Asner*

The CLEO-c research program [93] consists of studies of hadronic, semileptonic and leptonic charm meson decay which include measurements of doubly-Cabibbo processes, studies of charm Dalitz plot analyses, and tests for physics beyond the Standard Model including searches for charm mixing. Precision determination of  $\gamma/\phi_3$  depends upon constraints on charm mixing amplitudes, measurements of doubly-Cabibbo suppressed amplitudes and relative phases, and studies of charm Dalitz plots tagged by flavor or  $CP$  content.

The CLEO-c physics program [93] includes a variety of measurements that will improve the determination of  $\gamma/\phi_3$  from the  $B$ -factory experiments. The total number of charm mesons accumulated at CLEO-c will be much smaller than the samples already accumulated by the  $B$ -factories. However, the quantum correlations in the  $\psi(3770) \rightarrow D\bar{D}$  system provide a unique laboratory in which to study charm.

### 5.6.1 Components of CLEO-c Physics Program Pertinent to $\gamma/\phi_3$

Neutral flavor oscillation in the  $D$  meson system is highly suppressed within the Standard Model. The time evolution of a particle produced as a  $D^0$  or  $\bar{D}^0$ , in the limit of  $CP$  conservation, is governed by four parameters:  $x = \Delta m/\Gamma$  and  $y = \Delta\Gamma/2\Gamma$  which characterize the mixing matrix,  $\delta$  the relative strong phase between Cabibbo favored (CF) and doubly-Cabibbo suppressed (DCS) amplitudes and  $R_D$  the DCS decay rate relative to the CF decay rate. The mixing rate  $R_M$  is defined as  $\frac{1}{2}(x^2 + y^2)$  [94]. Standard Model based predictions for  $x$  and  $y$ , as well as a variety of non-Standard Model expectations, span several orders of magnitude [95]. It is reasonable to expect that  $x \approx y \approx 10^{-3}$  in the Standard Model. The mass and width differences  $x$  and  $y$  can be measured in a variety of ways. The most precise limits are obtained by exploiting the time-dependence of  $D$  decays [94]. Time-dependent analyses are not feasible at CLEO-c; however, the quantum-coherent  $D^0\bar{D}^0$  state provides time-integrated sensitivity to  $x, y$  at  $O(1\%)$  level and  $\cos\delta \sim 0.1$  [93, 85] in  $1\text{ fb}^{-1}$  of  $\psi(3770) \rightarrow D\bar{D}$ . Although CLEO-c does not have sufficient sensitivity to observe Standard Model charm mixing the projected sensitivity in  $1\text{ fb}^{-1}$  at  $\psi(3770)$  compares favorably with current experimental results; see Fig. 1 in Ref. [94].

### 5.6.2 Targeted Analyses

Measurements of each of the four parameters that describe  $CP$  conserving mixing can in principle be determined individually by a series of “targeted” analyses. The techniques and projected sensitivities in  $1\text{ fb}^{-1}$  are described briefly in the subsections that follow. Greater detail can be found in Ref. [93].

**$R_M$**  The measurement of  $R_M$  can be determined unambiguously by considering the decays  $\psi(3770) \rightarrow (K^-\pi^+)(K^-\pi^+)$  and  $\psi(3770) \rightarrow (\ell^\pm(KX))(\ell^\mp(KX))$ . The hadronic final state cannot be produced from DCS decay due to a quantum statistics argument - the  $C$ -odd initial state cannot produce the symmetric final state required by Bose statistics if both the  $D^0$  and  $\bar{D}^0$  decay into the same final state ( $K\pi$ ). A fit utilizing six constraints make this channel effectively background free. The double semileptonic channel has fewer constraints due to the two neutrinos. The number of “right-sign”  $(K^-\pi^+)(K^+\pi^-)$  and  $(\ell^\pm(KX))(\ell^\mp(KX))$  events in the two channels combined produced in  $1\text{ fb}^{-1}$  is expected to be  $\sim 20,000$  corresponding to  $\sqrt{2R_M} < 1.7\%$  @95% Confidence Level (C.L.).

**cos  $\delta$**  Final states where one  $D$  decays to  $K\pi$  and the other to a  $CP$  eigenstate can be used to probe  $\cos \delta$ . The  $CP$ -even eigenstates accessible to CLEO-c include  $K^+K^-$ ,  $\pi^+\pi^-$  and  $K_S^0\pi^0\pi^0$  and the  $CP$ -odd eigenstates include  $K_S^0\pi^0$ ,  $K_S^0\eta$ ,  $K_S^0\omega$ ,  $K_S^0\phi$ , and  $K_S^0\eta'$ . The  $CP$  content of the  $K_S^0\pi^+\pi^-$  and  $\pi^+\pi^-\pi^0$  Dalitz plots will also be utilized. Sensitivity to  $\cos \delta \sim 1/(2\sqrt{R_D N})$  where  $N$ , the total number of  $CP$  tagged  $K\pi$ , will be  $\sim 9200$  and  $R_D$  is already well measured, thus leading to an expected precision of  $\pm 0.09$  in  $\cos \delta$ .

**y** Tagging one of the  $D$  mesons as a  $CP$  eigenstate,  $y$  can be determined by measuring the flavor specific branching ratios of the other meson. The flavor tag width is independent of the  $CP$  quantum number; however the branching ratio is inversely proportional to the total width. Consequently, charm threshold experiments have time-integrated sensitivity to  $y$ . Neglecting factors related to DCS decays (described in detail in Ref. [96]), we can construct the ratio

$$\frac{2\Gamma[\psi \rightarrow (D \rightarrow CP)(D \rightarrow \text{flavor})]}{\Gamma[\psi \rightarrow (D \rightarrow CP)(D \rightarrow X)Br(D \rightarrow \text{flavor})]} \sim (1 \pm y) \quad (62)$$

where  $X$  represents an inclusive set of all states. A positive  $y$  would make the above ratio  $> 1$  for  $CP+$  tags.

The decay  $D^0 \rightarrow K_S^0\pi^+\pi^-$  is measured with a Dalitz plot analysis to proceed through intermediate states that are  $CP+$  eigenstates, such as  $K_S^0 f_0$ ,  $CP-$  such as  $K_S^0 \rho$  and flavor eigenstates such as  $K^{*-}\pi^+$  [97]. The presence of mixing through  $y$  would introduce an intensity modulation across the Dalitz plot as a function of the  $CP$  of the contributing amplitudes. The sensitivity at CLEO-c to  $y$  with Dalitz plot analyses has not yet been fully evaluated. Preliminary estimates suggests a limit of  $y \sim \text{few\%}$  @95% C.L. is attainable with the CLEO-c data.

**x** Separate measurement of  $y$  and  $R_M$  as outlined above allow the value  $x$  to be determined. The upper limit on  $R_M$  corresponds to a limit of  $|x| < 1.7\%$  @95% C.L..

**$R_D$**  Although  $R_D$  is determined by the ratio of  $(K^-\pi^+)(K^-\ell^+\nu)$  to  $(K^-\pi^+)(K^+\ell^-\bar{\nu})$  up to corrections that are second order in  $x$  and  $y$ , a more precise measurement is attainable using a  $D^{*+}$  tag to measure  $D^0 \rightarrow K^+\pi^-$  relative to  $D^0 \rightarrow K^-\pi^+$  [94].

### 5.6.3 Comprehensive Analysis

The comprehensive analysis simultaneously determines mixing and doubly-Cabibbo suppressed parameters by examining various single tag and double tag rates. Due to quantum correlations in the  $C = -1$  and  $C = +1$   $D^0\bar{D}^0$  pairs produced in the reactions  $e^+e^- \rightarrow D^0\bar{D}^0(\pi^0)$  and  $e^+e^- \rightarrow D^0\bar{D}^0\gamma$ , respectively, the time-integrated  $D^0\bar{D}^0$  decay rates are sensitive to interference between amplitudes for indistinguishable final states. This size of this interference is governed by the relevant amplitude ratios and can include contributions from  $D^0$ - $\bar{D}^0$  mixing.

We consider in the comprehensive analysis the following categories of final states:

- $f$  or  $\bar{f}$ : hadronic states that can be reached from either  $D^0$  or  $\bar{D}^0$  decay but that are not  $CP$  eigenstates. An example is  $K^-\pi^+$ , which results from Cabibbo-favored  $D^0$  transitions or doubly Cabibbo-suppressed  $\bar{D}^0$  transitions. We include in this category Cabibbo-suppressed transitions as well as self-conjugate final states of mixed  $CP$ , such as  $K_S^0\pi^+\pi^-$ .
- $\ell^+$  or  $\ell^-$ : semileptonic or purely leptonic final states, which, in the absence of mixing, tag unambiguously the flavor of the parent  $D$ .
- $S_+$  or  $S_-$ :  $CP$ -even and  $CP$ -odd eigenstates, respectively.

Table 10: Estimated uncertainties (statistical and systematic, respectively) for different  $C$  configurations, with  $r_D$  and branching fractions to  $CP$  eigenstates constrained to the world averages.

Parameter	Value	$\Gamma_{D^0\bar{D}^0}^{C=-1} = 3 \times 10^6$	$\Gamma_{D^0\bar{D}^0}^{C=+1} = 3 \times 10^6$	$\Gamma_{D^0\bar{D}^0}^{C=-1} = 10 \cdot \Gamma_{D^0\bar{D}^0}^{C=+1} = 3 \times 10^6$
$y$	0	$\pm 0.015 \pm 0.008$	$\pm 0.007 \pm 0.003$	$\pm 0.012 \pm 0.005$
$x_2$	0	$\pm 0.0006 \pm 0.0006$	$\pm 0.0003 \pm 0.0003$	$\pm 0.0006 \pm 0.0006$
$\cos \delta$	1	$\pm 0.15 \pm 0.04$	$\pm 0.13 \pm 0.05$	$\pm 0.13 \pm 0.03$
$x \sin \delta$	0	—	$\pm 0.010 \pm 0.003$	$\pm 0.024 \pm 0.005$

We calculate decay rates for  $D^0\bar{D}^0$  pairs to all possible combinations of the above categories of final states in Ref. [96], for both  $C = -1$  and  $C = +1$ , reproducing the work of Refs. [85, 87]. Such  $D^0\bar{D}^0$  combinations, where both  $D$  final states are specified, are referred to as double tags (or DT). In addition, we calculate rates for single tags (or ST), where either the  $D^0$  or  $\bar{D}^0$  is identified and the other neutral  $D$  decays generically. Any DT event also contains two ST decays, and ST rates are obtained by summing the corresponding DT rates.

Experimental measurements of  $D^0$  branching fractions rely on determining yields of ST decays assuming knowledge of the luminosity and  $D^0\bar{D}^0$  cross section. If, in addition, one also measures DT yields, then the luminosity and  $D^0\bar{D}^0$  cross section need not be known [98, 99, 100]. However, in correlated  $D^0\bar{D}^0$  decay, the ST and DT rates no longer depend solely on the branching fractions of interest; the rates are modified by  $x$ ,  $y$ , and the magnitudes and phases of various amplitude ratios. Therefore, one must correct the measured ST and DT yields in order to extract the branching fractions. Conversely, as shown in Ref. [96], using these yields, it is possible to determine simultaneously the mixing and amplitude ratio parameters as well as the relevant branching fractions. The estimated uncertainties on the fit parameters based on approximately  $3 \times 10^6$   $D^0\bar{D}^0$  pairs are presented in Table 10 using efficiencies and background levels similar to those found at CLEO-c.

#### 5.6.4 Dalitz Plot Analyses

A Dalitz plot analysis of multibody final states measures amplitudes and phases rather than the decay rates. A better understanding of final state interactions in exclusive weak decays is needed in order to elucidate the origin of  $CP$  violation in the  $B$  sector [17]. Currently, the most important three-body decay for  $\gamma/\phi_3$  determination is  $D^0 \rightarrow K_S^0\pi^+\pi^-$ . Recently Babar [101] and Belle [75] have reported  $\gamma = (70 \pm 3_{-10-11}^{+12+14})^\circ$  and  $\phi_3 = (77_{-19}^{+17} \pm 13 \pm 11)^\circ$ , respectively, where the third error is the systematic error due to modeling of the Dalitz plot. A fit which includes only established resonances, similar to that of CLEO [97] which used Breit-Wigner (BW) line shapes, provides very poor description of the data. An improved description requires the inclusion of two ad-hoc  $\pi\pi$   $S$ -wave resonances which account for  $\sim 10\%$  of the fit area.

It may be possible to reduce the systematic error due to model uncertainty by using the K-matrix formalism to describe the  $\pi\pi$   $S$ -wave contribution to  $D^0 \rightarrow K_S^0\pi^+\pi^-$ . The FOCUS collaboration has used a hybrid BW/K-Matrix model where the higher spin resonances are described using BW line shapes and the  $\pi\pi$   $S$ -wave is parameterized using the K-matrix model of Anisovich and Sarantsev [102] to describe  $D^+ \rightarrow \pi^+\pi^-\pi^+$  [103]. Similarly, the CLEO collaboration has searched for  $\pi\pi$   $S$ -wave in  $D^0 \rightarrow \pi^+\pi^-\pi^0$  [104] following the K-matrix formalism of Au, Morgan, and Pennington [105]. Currently, the CLEO collaboration is considering K-matrix

descriptions of both the  $\pi\pi$   $S$ -wave and the  $K\pi$   $P$ -wave contributions to  $D^0 \rightarrow K_S^0 \pi^+ \pi^-$ . This more sophisticated description of the  $K_S^0 \pi^+ \pi^-$  decay may lead to a smaller systematic error in the determination of  $\gamma/\phi_3$ .

Both  $D^0$  and  $\bar{D}^0$  populate the Dalitz plots  $K_S^0 \pi^+ \pi^-$ ,  $\pi^+ \pi^- \pi^0$ ,  $K^+ K^- \pi^0$  and  $K_S^0 K^\pm \pi^\mp$  and so can be used in the determination of  $\gamma/\phi_3$  which exploit the interference between  $b \rightarrow c\bar{u}s$  ( $B^- \rightarrow D^0 K^-$ ) and  $b \rightarrow u\bar{c}s$  ( $B^- \rightarrow \bar{D}^0 K^-$ ) where the former process is real and the later is  $\propto e^{-i\gamma}$  [106]. Studying  $CP$  tagged Dalitz plots allows a model independent determination of the relative  $D^0$  and  $\bar{D}^0$  phase across the Dalitz plot. Consider  $D^0 \rightarrow K_S^0 \pi^+ \pi^-$  decay which proceeds through intermediate states that are  $CP+$  eigenstates, such as  $K_S^0 f_0$ ,  $CP-$  such as  $K_S^0 \rho$  and flavor eigenstates such as  $K^{*-} \pi^+$  [97]. The Dalitz plots for  $\psi(3770) \rightarrow D^0 \bar{D}^0 \rightarrow S_+ K_S^0 \pi^+ \pi^-$  and  $\psi(3770) \rightarrow D^0 \bar{D}^0 \rightarrow S_- K_S^0 \pi^+ \pi^-$  will be distinct and the Dalitz plot for the untagged sample  $\psi(3770) \rightarrow D^0 \bar{D}^0 \rightarrow X K_S^0 \pi^+ \pi^-$  will be different from that observed with uncorrelated  $D$  mesons from continuum production at  $\sim 10$  GeV [97]. The CLEO collaboration will perform a simultaneous fit to  $CP+$ ,  $CP-$ , and flavor tag samples with BW/K-matrix hybrid models. A good fit will validate Dalitz plot model and is expected to reduce the model dependent systematic error on the  $\gamma/\phi_3$  measurements to a few degrees. If a good model cannot be constructed, a model independent result can be obtained from a binned analysis of the  $CP$  tag and flavor tag Dalitz plots. It is noteworthy that, although the statistical sample is smaller, the negligible  $\pi\pi$   $S$ -wave contribution to  $D \rightarrow \pi^+ \pi^- \pi^0$  may lead to a better decay model and smaller uncertainty on  $\gamma/\phi_3$  relative to that obtained with  $D \rightarrow K_S^0 \pi^+ \pi^-$ .

### 5.6.5 Summary

CLEO-c measurements are important inputs for each of the methods proposed to determine  $\gamma/\phi_3$ . The Gronau-London-Wyler and Atwood-Dunietz-Soni methods will benefit from improved mixing parameters and DCS parameters, respectively. The Dalitz plot method will benefit from improved models of three-body charm decay.

The quantum correlated  $D^0 \bar{D}^0$  system from the decay of  $\psi(3770)$  provides time-integrated sensitivity to the mixing parameters  $x$  and  $y$  and the doubly-Cabibbo suppressed parameters  $R_D$  and  $\delta$ . Targeted analyses will provide the first measurement of  $\cos \delta$  and sensitivity to  $R_M$  and  $y$  competitive with  $B$ -factory measurements. A comprehensive analysis of single tag and double tag yields allows simultaneous determination of hadronic and semileptonic branching fractions, mixing parameters, and doubly-Cabibbo suppressed parameters with sensitivity similar to the collection of targeted analyses.

The decays  $B^- \rightarrow D^{(*)} K^{-(*)}$  followed by a three-body decay of the  $D$  such as  $K_S^0 \pi^+ \pi^-$  or  $\pi^+ \pi^- \pi^0$  currently provide the greatest sensitivity to the CKM angle  $\gamma/\phi_3$ . The precision of these measurements will eventually be limited by the understanding of the  $D \rightarrow K_S^0 \pi^+ \pi^-$  Dalitz plot. K-matrix descriptions of the  $\pi\pi$   $S$ -wave may yield improved models of charm Dalitz plots and these models will be tested using the  $CP$  tagged sample of charm decays at CLEO-c. The model uncertainty, which is currently  $\pm 10^\circ$ , may be reduced to a few degrees with sufficient data.

## 5.7 $B_c$ Mesons: Another Probe of $CP$ Violation

*Contribution from R. Fleischer*

Many strategies to explore  $CP$  violation through the “conventional” charged  $B_u$  and the neutral  $B_{d,s}$  mesons were proposed in the literature. There is, however, another species of  $B$

mesons, the  $B_c$ -meson system, which consists of  $B_c^+ \sim c\bar{b}$  and  $B_c^- \sim b\bar{c}$ . These mesons were observed by the CDF collaboration through their decay  $B_c^+ \rightarrow J/\psi \ell^+ \nu_\ell$ , with the following mass and lifetime [107]:

$$M_{B_c} = (6.40 \pm 0.39 \pm 0.13) \text{ GeV}, \quad \tau_{B_c} = (0.46_{-0.16}^{+0.18} \pm 0.03) \text{ ps.} \quad (63)$$

Recently, D0 reported the measurement of  $B_c^+ \rightarrow J/\psi \mu^+ X$  [108], yielding

$$M_{B_c} = (5.95_{-0.13}^{+0.14} \pm 0.34) \text{ GeV}, \quad \tau_{B_c} = (0.448_{-0.096}^{+0.123} \pm 0.121) \text{ ps.} \quad (64)$$

Moreover, there is now also evidence for the decay  $B_c^+ \rightarrow J/\psi \pi^+$  from the CDF collaboration [109], allowing the extraction of

$$M_{B_c} = (6.2870 \pm 0.0048 \pm 0.0011) \text{ GeV.} \quad (65)$$

As run II of the Tevatron will provide further insights into  $B_c$  physics and a huge number of  $B_c$  mesons will be produced at the LHC, the natural question arises whether insights into  $CP$  violation can also be obtained from  $B_c$ -meson decays. In order to address this question, we have to consider non-leptonic  $B_c$  decays, as in the case of the exploration of  $CP$  violation through decays of the conventional  $B_{u,d,s}$  mesons. Since the  $B_c$  mesons are charged particles, i.e. do not exhibit mixing effects, we have obviously to rely on direct  $CP$  violation. It is well-known that the extraction of  $\gamma$  from such effects suffers from hadronic uncertainties, and that an elegant solution of this problem is offered in the case of the  $B_u^\pm$  mesons through the ‘‘triangle approach’’ illustrated in Fig. 18 [58].

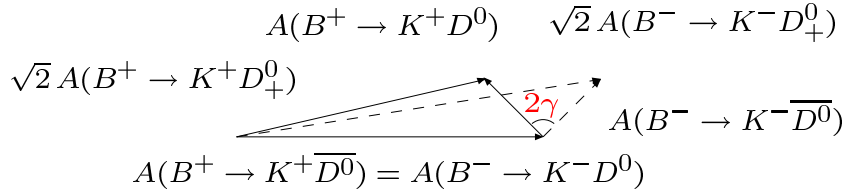


Figure 18: The extraction of  $\gamma$  from  $B^\pm \rightarrow K^\pm\{D^0, \bar{D}^0, D_\pm^0\}$  decays.

In the  $B_c$ -meson system, such a strategy for the determination of  $\gamma$  is offered by the decays  $B_c^\pm \rightarrow D_s^\pm D$ , which are the  $B_c$ -meson counterparts of the  $B_u^\pm \rightarrow K^\pm D$  modes used in the conventional triangle method [58], and satisfy the following amplitude relations [110]:

$$\sqrt{2}A(B_c^+ \rightarrow D_s^+ D_+^0) = A(B_c^+ \rightarrow D_s^+ D^0) + A(B_c^+ \rightarrow D_s^+ \bar{D}^0) \quad (66)$$

$$\sqrt{2}A(B_c^- \rightarrow D_s^- D_+^0) = A(B_c^- \rightarrow D_s^- \bar{D}^0) + A(B_c^- \rightarrow D_s^- D^0), \quad (67)$$

with

$$A(B_c^+ \rightarrow D_s^+ \bar{D}^0) = A(B_c^- \rightarrow D_s^- D^0) \quad (68)$$

$$A(B_c^+ \rightarrow D_s^+ D^0) = A(B_c^- \rightarrow D_s^- \bar{D}^0) \times e^{2i\gamma}. \quad (69)$$

At first sight, everything is completely analogous to the  $B_u^\pm \rightarrow K^\pm D$  case [58]. However, there is an important difference [111, 112], which becomes obvious by having a look at the corresponding Feynman diagrams: in the  $B_c^\pm \rightarrow D_s^\pm D$  system, the amplitude with the rather



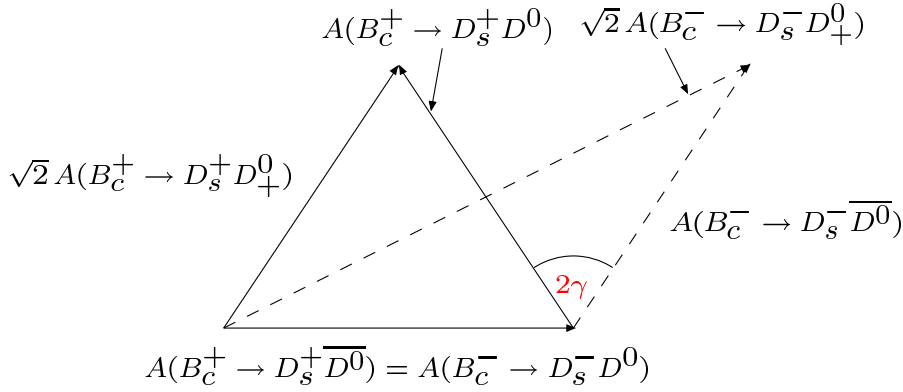


Figure 19: The extraction of  $\gamma$  from  $B_c^\pm \rightarrow D_s^\pm \{D^0, \bar{D}^0, D_+^0\}$  decays.

small CKM matrix element  $V_{ub}$  is *not* colour-suppressed, while the larger element  $V_{cb}$  comes with a colour-suppression factor. Therefore, we obtain

$$\left| \frac{A(B_c^+ \rightarrow D_s^+ D^0)}{A(B_c^+ \rightarrow D_s^+ \bar{D}^0)} \right| = \left| \frac{A(B_c^- \rightarrow D_s^- \bar{D}^0)}{A(B_c^- \rightarrow D_s^- D^0)} \right| \approx \frac{1}{\lambda} \frac{|V_{ub}|}{|V_{cb}|} \times \frac{a_1}{a_2} \approx 0.4 \times 3 = O(1), \quad (70)$$

and conclude that the two amplitudes are similar in size. In contrast to this favourable situation, in the decays  $B_u^\pm \rightarrow K^\pm D$ , the matrix element  $V_{ub}$  comes with the colour-suppression factor, resulting in a very stretched triangle. The extraction of  $\gamma$  from the  $B_c^\pm \rightarrow D_s^\pm D$  triangles is illustrated in Fig. 19, which should be compared with the squashed  $B_u^\pm \rightarrow K^\pm D$  triangles shown in Fig. 18. Another important advantage is that the interference effects arising from  $D^0, \bar{D}^0 \rightarrow \pi^+ K^-$ , which were pointed out in the context of the  $B_u^\pm \rightarrow K^\pm D$  case in [57], are practically unimportant for the measurement of  $\text{BR}(B_c^+ \rightarrow D_s^+ D^0)$  and  $\text{BR}(B_c^+ \rightarrow D_s^+ \bar{D}^0)$  since the  $B_c$ -decay amplitudes are of the same order of magnitude. This feature implies also that the sensitivity to  $D^0$ - $\bar{D}^0$  mixing, which provides a nice avenue for new physics to enter these triangle strategies [113], is considerably smaller than in the  $B_u$  case [112].

Consequently, the  $B_c^\pm \rightarrow D_s^\pm D$  decays provide – from the theoretical point of view – the ideal realization of the “triangle” approach to determine  $\gamma$  [111]. On the other hand, the practical implementation still appears to be challenging, although detailed experimental feasibility studies for LHCb are strongly encouraged. Using a relativistic quark model [114], which predicts the branching ratios for  $B^+ \rightarrow \bar{D}^0 e^+ \nu_e$ ,  $B^+ \rightarrow K^+ \bar{D}^0$  and  $B^+ \rightarrow D_s^+ \bar{D}^0$  in good accordance with experiment, the branching ratios for non-leptonic  $B_c$  decays were recently predicted, yielding in fact a pattern in nice accordance with (70) [114]. In another study [115], also semi-leptonic  $B_c$  decays were investigated, which give a nice testing ground.

In addition to  $CP$  violation, there are several other interesting aspects of  $B_c$  physics. Since these mesons are the lowest lying bound states of two heavy quarks,  $\bar{b}$  and  $c$ , the QCD dynamics of the  $B_c^+$  mesons is similar to quarkonium systems, such as  $b\bar{b}$  and  $\bar{c}c$ , which are approximately non-relativistic. However, there is an important difference: as the  $B_c$  mesons contain open flavour, they are stable under strong interactions. The quarkonium-like  $B_c$  mesons provide an important laboratory to explore exciting topics such as heavy-quark expansions (HQE), non-relativistic QCD (NRQCD) or factorization in a setting that is complementary to “conventional” weak hadron decays [116], and should provide further valuable insights into the interplay of strong and weak interactions.

## 5.8 Extraction of $\gamma$ at LHCb with a Combined $B_s \rightarrow D_s^\pm K^\mp$ and $B_d \rightarrow D^\pm \pi^\mp$ Analysis

*Contribution from G. Wilkinson*

### 5.8.1 Introduction

The potential of  $B_s \rightarrow D_s^\pm K^\mp$ ,  $B_d \rightarrow D^\pm \pi^\mp$  and  $B_d \rightarrow D^\pm \pi^\mp$  decays for extracting the CKM angle  $\gamma$  is well known [116]. An analysis based on any of these modes in isolation, however, suffers from the problem of discrete ambiguities, and in the case of  $B_d$  decays, of difficulties posed by very small interference effects. This report explains how a combined analysis of, for example,  $B_s \rightarrow D_s^\pm K^\mp$  and  $B_d \rightarrow D^\pm \pi^\mp$  under the assumption of U-spin symmetry, circumvents these problems. This strategy was proposed in [117] and is here explored in the context of the expected performance in these decays at LHCb.

### 5.8.2 Formalism

From measuring the two flavour tagged decay modes,  $B_s \rightarrow D_s^+ K^-$ , as a function of proper time,  $t$ , the  $CP$  asymmetry  $A_{CP}(D_s^+ K^-)(t)$  may be constructed:

$$A_{CP}(D_s^+ K^-)(t) \equiv \frac{B_s \rightarrow D_s^+ K^-(t) - \overline{B}_s \rightarrow D_s^+ K^-(t)}{B_s \rightarrow D_s^+ K^-(t) + \overline{B}_s \rightarrow D_s^+ K^-(t)}.$$

This has the following dependence:

$$A_{CP}(D_s^+ K^-)(t) = \frac{C_s \cos \Delta m_s t + S_s \sin \Delta m_s t}{\cosh(\Delta \Gamma_s t/2) - A_{\Delta \Gamma_s} \sinh(\Delta \Gamma_s t/2)},$$

where  $\Delta m_s$  and  $\Delta \Gamma_s$  are the mass and lifetime difference between the heavy and light  $B_s$  eigenstates, which for the purposes of this discussion are assumed to be known. The three observables  $C_s$ ,  $S_s$  and  $A_{\Delta \Gamma_s}$  can then be fitted from the data. (In doing this the full flavour untagged statistics may be used to fix  $A_{\Delta \Gamma_s}$ .) From performing an equivalent analysis for the  $D_s^- K^+$  final state three additional observables,  $\overline{C}_s$ ,  $\overline{S}_s$  and  $\overline{A}_{\Delta \Gamma_s}$ , can be obtained. The observables depend on the underlying physics parameters in the following manner:

$$C_s, (\overline{C}_s) = -(+)\left(\frac{1 - r_s^2}{1 + r_s^2}\right), \quad (71)$$

$$S_s, (\overline{S}_s) = \frac{2r_s \sin(\phi_s + \gamma + (-)\delta_s)}{1 + r_s^2}, \quad (72)$$

$$A_{\Delta \Gamma_s}, (\overline{A}_{\Delta \Gamma_s}) = -\frac{2r_s \cos(\phi_s + \gamma + (-)\delta_s)}{1 + r_s^2}. \quad (73)$$

Here  $r_s$  is the ratio of amplitudes between the interfering tree diagrams,  $\delta_s$  is a possible  $CP$  conserving strong phase difference between the diagrams and  $\phi_s$  is the  $CP$  violating weak phase associated with the  $B_s$ - $\overline{B}_s$  oscillations, believed to be very small in the Standard Model. It is assumed that  $\phi_s$  can be constrained from other measurements, such as those in  $B_s \rightarrow J/\psi \phi$  decays.

Measurement of the six observables  $C_s$ ,  $\overline{C_s}$ ,  $S_s$ ,  $\overline{S_s}$ ,  $A_{\Delta\Gamma_s}$  and  $\overline{A_{\Delta\Gamma_s}}$  allows  $r_s$ ,  $\delta_s$  and  $\gamma$  to be determined. The same information may be extracted by making a simultaneous event-by-event fit to the four decay distributions.

Exactly parallel relations hold in the  $B_d$  system, for analysis of  $B_d \rightarrow D^\pm\pi^\mp$  or  $B_d \rightarrow D^{*\pm}\pi^\mp$  decays. In this case however, the negligible width splitting between the mass eigenstates, means that there are effectively only four observables:  $C_d$ ,  $\overline{C_d}$ ,  $S_d$  and  $\overline{S_d}$ . These observables depend on  $r_d$ ,  $\phi_d$  (measured from  $B_d \rightarrow J/\psi K^0$  and equal to  $2\beta$  in the Standard Model),  $\delta_d$  and  $\gamma$ . Note that the value of these observables will in general be different between  $B_d \rightarrow D^\pm\pi^\mp$  and  $B_d \rightarrow D^{*\pm}\pi^\mp$ , firstly because of the possibility of different values of  $r_d$  and  $\delta_d$  for the two cases, and secondly because the  $l = 1$  state of the  $B_d \rightarrow D^{*\pm}\pi^\mp$  decay introduces some sign flips in expressions 72 and 73 (see [117] for more details).

### 5.8.3 LHCb Event Yields and Performance

LHCb has reported simulation studies of  $B_s \rightarrow D_s^\pm K^\mp$  and  $B_d \rightarrow D^{*\pm}\pi^\mp$  in [118]. The results are summarised here, together with estimates from a preliminary study of  $B_d \rightarrow D^\pm\pi^\mp$ .

The isolation of  $B_s \rightarrow D_s^\pm K^\mp$  decays is experimentally challenging, because of the low branching ratio and background from the order-of-magnitude more prolific  $B_s \rightarrow D_s^\pm\pi^\mp$  decay mode. The LHCb trigger system gives good performance for fully hadronic modes and selects  $B_s \rightarrow D_s^\pm K^\mp$  events with an efficiency of 30%. The  $\pi - K$  discrimination of the RICH system reduces the  $B_s \rightarrow D_s^\pm\pi^\mp$  contamination to  $\sim 10\%$ . It is estimated that the experiment will accumulate 5.4k events per year of operation (with a year defined as  $2 \text{ fb}^{-1}$  of integrated luminosity), with a background to signal level of  $< 0.5$ . The excellent  $\sim 40 \text{ fs}$  proper time precision provided by the silicon Vertex Locator will ensure that - provided  $\Delta m_s$  is not far in excess of expectation - the  $B_s$  oscillations will be well resolved, and hence the  $CP$  asymmetries can be measured. It is estimated that the statistical precision on  $\gamma$  from this channel alone will be  $14^\circ$  for  $2 \text{ fb}^{-1}$ , assuming  $\Delta m_s = 20 \text{ ps}^{-1}$ ,  $\Delta\Gamma_s/\Gamma_s = -0.10$  and taking plausible values of  $\gamma$  and  $\delta_s$ .

The channel  $B_d \rightarrow D^{*\pm}\pi^\mp$  has been investigated through the sub-decay  $D^{*\pm} \rightarrow D^0(\rightarrow K\pi)\pi^\pm$ , in which it is estimated 206k events will be accumulated per year, with a background to signal level  $< 0.3$ . Earlier studies using inclusive  $D^0$  decays [119] suggest that these statistics can be increased still further.

Studies are underway to investigate the feasibility of reconstructing  $B_d \rightarrow D^\pm\pi^\mp$ , with  $D^\pm \rightarrow K^\pm\pi^\mp\pi^\pm$ . The preliminary indications are that 210k events will be collected each year, with a background to signal ratio of around 0.3.

### 5.8.4 Extraction of $\gamma$ from modes in isolation

In extracting  $\gamma$  from the observables of a single decay mode, two problems are encountered, one general, and one specific to the  $B_d$  decays.

1. The extraction of  $\gamma$  from  $S_{s(d)}$  and  $\overline{S_{s(d)}}$  yields 8 possible solutions. The same is true of calculating  $\gamma$  from  $A_{\Delta\Gamma_s}$  and  $\overline{A_{\Delta\Gamma_s}}$ . Figure 20 illustrates this by plotting all possible solutions for  $\gamma$  and  $\delta_s$  in the case where the true values are assumed to be  $\gamma = 60^\circ$  and  $\delta = 60^\circ$ . Therefore the study of  $B_d \rightarrow D^\pm\pi^\mp$  or  $B_d \rightarrow D^{*\pm}\pi^\mp$  in isolation results in an 8-fold ambiguity for  $\gamma$ . The extra observables available in the  $B_s$  system mean that in principle there is only a 2-fold ambiguity, but in practice measurement errors may make it difficult to exclude local minima coming from the additional bogus solutions. This

problem will be accentuated if the magnitude of  $\Delta\Gamma_s/\Gamma_s$  is small, hence making  $A_{\Delta\Gamma_s}$  and  $\overline{A_{\Delta\Gamma_s}}$  difficult to measure.

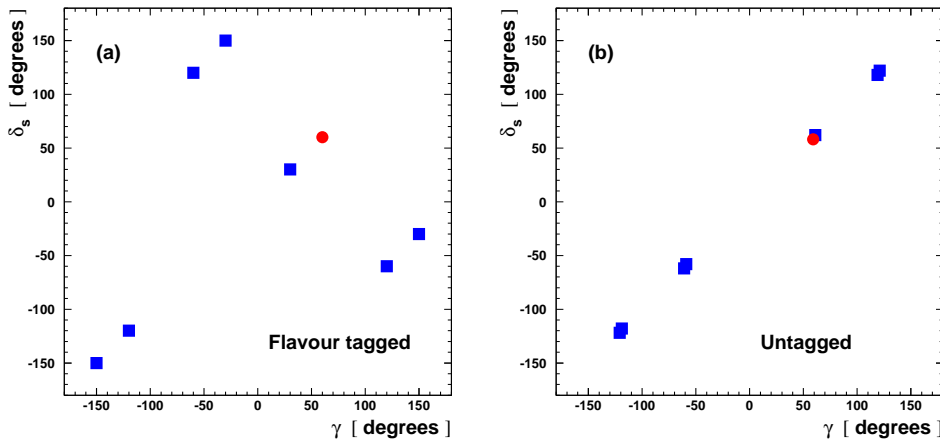


Figure 20: Valid solutions for  $\delta_s$  and  $\gamma$  for (a) the flavour tagged  $S_s$ ,  $\overline{S_s}$  observables and (b) the untagged  $A_{\Delta\Gamma_s}$ ,  $\overline{A_{\Delta\Gamma_s}}$  observables. In both cases there are eight solutions (although, in the case of (b), these are two-fold degenerate). The solid circle indicates the true solution  $\gamma = 60^\circ$ ,  $\delta_s = 60^\circ$ .

- As is clear from expressions 72 and 73, extracting  $\gamma$  from  $S_{s(d)}$  and  $\overline{S_{s(d)}}$ , or  $A_{\Delta\Gamma_s}$  and  $\overline{A_{\Delta\Gamma_s}}$  require that  $r_{s(d)}$  be known. From comparing the CKM elements in the interfering diagrams it is expected that  $r_s \sim 0.4$  and  $r_d \sim 0.02$ . Therefore  $|C_s|$  will be significantly different from 1, and measurements of  $C_s$  and  $\overline{C_s}$  will allow  $r_s$  to be extracted from the data – indeed this is what is done in the present LHCb simulation studies. This will not be possible, however, for  $r_d$ . Instead this parameter has to be set using external assumptions [120]. These assumptions introduce a troublesome systematic error to the analysis.

Both of these problems may be tackled by making a combined analysis of U-spin related  $B_d$  and  $B_s$  modes.

### 5.8.5 A Combined U-Spin Analysis of $B_s \rightarrow D_s^\pm K^\mp$ and $B_d \rightarrow D^\pm \pi^\mp$

The decays  $B_s \rightarrow D_s^\pm K^\mp$  and  $B_d \rightarrow D^\pm \pi^\mp$  are identical under U-spin symmetry, *ie.* the exchange of  $d$  and  $s$  quarks. This symmetry allows the observables in both decays to be combined in a manner to yield certain relations, which then give  $\gamma$  under the assumption that the a priori unknown hadronic contributions to the observables are identical in both channels. These unknowns are the strong phases  $\delta_d$  and  $\delta_s$ , and  $a_d$  and  $a_s$ , the hadronic contributions to  $r_d$  and  $r_s$ , defined by  $r_{d,s} = a_{d,s} f_{d,s}^{\text{CKM}}$ , where the CKM factors,  $f_{d,s}^{\text{CKM}}$ , are easily calculable.

The following analysis follows the strategy proposed in [117]. The example plots and numbers assume the scenario  $\gamma = 60^\circ$ ,  $\delta_{d,s} = 60^\circ$ ,  $a_{d,s} = 1$ ,  $\phi_d = 47^\circ$  and  $\phi_s = 0^\circ$ . The experimental contours assume that in one year LHCb can measure  $S_d$  and  $\overline{S_d}$  with an uncertainty of 0.014, and  $S_s$  and  $\overline{S_s}$  with an uncertainty of 0.14 (results consistent with the performance figures quoted in section 5.8.3). It is also useful to assume that in the early year of operation the analysis can benefit from studies of  $B_d \rightarrow D^\pm \pi^\mp$  made at the  $B$ -factories. Taking existing measurements [39],

and scaling to  $2500 \text{ fb}^{-1}$  to represent a plausible  $B$ -factory integrated luminosity in 2008 gives an error on  $S_d$  and  $\overline{S}_d$  of 0.014.

Using expression 72, the sine observables for the  $B_s$  and  $B_d$  channels may be combined to give the following exact relations:

$$\left( \frac{a_s \cos \delta_s}{a_d \cos \delta_d} \right) = -\frac{1}{R} \left( \frac{\sin(\phi_d + \gamma)}{\sin(\phi_s + \gamma)} \right) \left( \frac{S_s + \overline{S}_s}{S_d + \overline{S}_d} \right), \quad (74)$$

$$\left( \frac{a_s \sin \delta_s}{a_d \sin \delta_d} \right) = -\frac{1}{R} \left( \frac{\cos(\phi_d + \gamma)}{\cos(\phi_s + \gamma)} \right) \left( \frac{S_s - \overline{S}_s}{S_d - \overline{S}_d} \right). \quad (75)$$

Here  $R = \left( \frac{1-\lambda^2}{\lambda^2} \right) \left( \frac{1+r_d^2}{1+r_s^2} \right)$ , where  $\lambda$  is the sine of the Cabibbo angle. Because  $r_d \ll 1$   $R \approx \frac{1-\lambda^2}{\lambda^2(1+r_s^2)}$  and hence these relations may be exploited without the need to measure  $r_d$ . In the limit of full U-spin symmetry, the left hand sides of equations 74 and 75 are equal to unity, and both relations give a determination of  $\gamma$ .

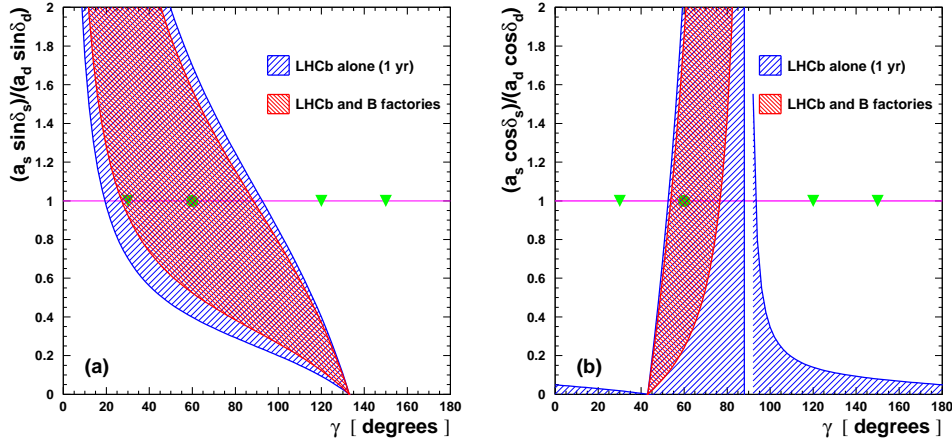


Figure 21: Contours formed from (a) expression 74 and (b) expression 75 showing the 1 sigma contours for one year of LHCb data, and one year of LHCb data together with the measurements which may be available from the  $B$ -factories by 2008. The solid circle indicates the true solution; the inverted solid triangles indicate fake solutions from an analysis of  $B_s \rightarrow D_s^\pm K^\mp$  alone. Exact U-spin symmetry corresponds to a value of unity for the ordinate in both plots.

Fig. 21 show the one sigma contours which will be obtained with one year of LHCb operation, together with the improvement possible if  $B$ -factory data are also included. The ambiguous solutions from the ‘conventional’ analysis are indicated. It can be seen that these bogus solutions are disfavoured by the combined analysis. There is, however, a mirror solution at  $-180^\circ + \gamma$  outside the region of the plots. This possibility can be rejected either by making assumptions about the orientation of the unitarity triangle, or by noting that such a solution is accompanied by a very sizable strong phase difference, which is unlikely to be the case.

The precision achievable on  $\gamma$  is in general different for the two expressions. In the chosen scenario, relation 75 gives the best result, returning an uncertainty of  $\sigma_\gamma = {}_{-7}^{+16}$  degrees. In the

one year analysis the contribution of the  $B$ -factory data is significant. With five years of data, the precision improves to  $5^\circ$ .

The plots also allow any biases from U-spin breaking effects to be assessed. It can be seen that relation 75 has the steepest contour and hence exhibits the best robustness. For example, a 20% deviation in  $a_s \cos \delta_s / a_d \cos \delta_d$  from unity leads to a  $3^\circ$  bias in  $\gamma$ .

In order to further assess the reliability the  $\gamma$  extraction, the U-spin dependence may be weakened. This can be done by combining relations 74 and 75 into a single expression which involves *either*  $\delta_d$  and  $\delta_s$  *or*  $a_s$  and  $a_d$ . For example, the latter exercise yields the equation

$$\frac{a_s}{a_d} = \pm \frac{1}{R} \frac{\sin 2(\phi_d + \gamma)}{\sin 2(\phi_s + \gamma)} \sqrt{\frac{(S_s^+)^2 \cos^2(\phi_s + \gamma) + (S_s^-)^2 \sin^2(\phi_s + \gamma)}{(S_d^+)^2 \cos^2(\phi_d + \gamma) + (S_d^-)^2 \sin^2(\phi_d + \gamma)}}. \quad (76)$$

It is now possible to determine  $\gamma$  by demanding that  $a_s = a_d$ , but making no assumption about  $\delta_d$  and  $\delta_s$ . With this approach, the statistical precision from five years of data is about 6 degrees. Again the dependence is sufficiently steep that deviations in  $a_s/a_d$  from unity coming from U-spin breaking give relatively small biases in the result.

It should be emphasised that these analyses only make use of the flavour tagged observables in  $B_s \rightarrow D_s^\pm K^\mp$  and  $B_d \rightarrow D^\pm \pi^\mp$ . If the magnitude of  $\Delta\Gamma_s$  is sufficiently large, then measurements of the untagged observables  $A_{\Delta\Gamma_s}$  and  $\bar{A}_{\Delta\Gamma_s}$  will provide additional information which will help further in the exclusion of ambiguous solutions, and add to the ultimate precision on  $\gamma$ .

### 5.8.6 Conclusions

LHCb will accumulate large samples of  $B_s \rightarrow D_s^\pm K^\mp$ ,  $B_d \rightarrow D^{*\pm} \pi^\mp$  and  $B_d \rightarrow D^\pm \pi^\mp$  events. Independently each of these channels may be used to extract the CKM angle  $\gamma$ , although in the case of the  $B_d$  channels this requires making assumptions about  $r_d$ , the relative magnitude of the interfering tree diagrams. When using the flavour-tagged observables alone, this  $\gamma$  determination carries with it an 8-fold ambiguity, which compromises the usefulness of the measurement.

A combined analysis of  $B_s \rightarrow D_s^\pm K^\mp$  and  $B_d \rightarrow D^\pm \pi^\mp$  under the assumption of U-spin symmetry allows the true solution to be isolated with only a 2-fold ambiguity. Plausible assumptions about the size of the strong phase difference or the orientation of the unitarity triangle allow the remaining bogus solution to be excluded. This U-spin analysis has the further benefit of exploiting the  $B_d$  data without the need to know  $r_d$ .

The intrinsic precision of the combined analysis is competitive with other approaches. For example, in the example scenario considered, a  $5^\circ$  uncertainty is achievable after five years of operation. The combined analysis does not make use of the untagged observables available in  $B_s \rightarrow D_s^\pm K^\mp$ , which provide additional information which will improve the precision still further.

The systematic error associated with the assumption of U-spin symmetry can be transparently assessed through studying the contours associated with the measurements. In some cases these offer a very robust  $\gamma$  extraction. Furthermore, a variety of separate  $\gamma$  determinations may be performed, each with different U-spin symmetry assumptions. Comparison between the results will help in assigning the systematic error.

Finally, an analogous exercise can be performed from considering the U-spin related channels  $B_d \rightarrow D^{*\pm} \pi^\mp$  and  $B_s \rightarrow D_s^{*\pm} K^\mp$ . The reconstruction of the latter channel at LHCb is under investigation.

## 6 Summary & (near) Outlook for $\beta$ & $\gamma$

*Contribution from A. Soni*

While the direct measurement of  $\beta$  are now in a “matured” stage since the post- $B$ -factory era of first determinations in 2001-2, past year has seen significant progress in extracting  $\gamma$ . Of course, the errors are still rather large but we expect reduction of these to take place quite rapidly in the near future. Table 11 summarizes the current status and the prospects for the next few years for  $\beta$  and  $\gamma$ .

Table 11: Summary of status and prospects for  $\beta$  &  $\gamma$ ; luminosity per experiment is given in units of  $10^8 B\bar{B}$  pairs. Note current central values,  $\beta = 0.725$  &  $\gamma = 69^\circ$ . IEE is irreducible experimental error and ITE is irreducible theory error

Qty	CKM05	SUM06	End08	IEE05	ITE
Lumin/(expt)	2	5	10		
$\delta(\sin 2\beta)$	0.037	0.028	0.02	0.02	0.001
$\delta\gamma^\circ$	$\pm 13 \pm 9 \pm 13$	$\pm 9 \pm 6 \pm 7$	5 to 2	?	.05

On  $\beta$  the current error of 0.037[121] should decrease to about 0.02 in about 3 years but after that the currently estimated irreducible experimental error (IEE), which both BABAR & BELLE agree to be around 0.02 (see talks by Browder and Lange), will start to become the limiting factor. Since the irreducible theory error (ITE) on  $\beta$  is estimated to be  $\approx 0.01$ [1](and talk by Mannel) it is important that effort is put into reducing the IEE so that it is comparable to ITE.

Regarding  $\gamma$ , so far the  $B \rightarrow DK$  with Dalitz analysis of the multi-body mode  $D^0 \rightarrow K_s \pi^+ \pi^-$  proposed by [17] and independently in [16] has been very successful. Using about  $3 \times 10^8$   $B$ -pairs BELLE gets  $\gamma = 68 \pm 15 \pm 13 \pm 11^\circ$  (see talk by Abe), where the first error is statistical, the second is experimental systematics and the third is modelling error of the Dalitz study. BABAR’s combined use of GLW[58, 46], ADS [57] and this multi-body mode in about  $2 \times 10^8$   $B$ -pairs leads to  $\gamma = 70 \pm 31 \pm 12 \pm 13^\circ$  (see talk by Schune). Combining these we arrive at the current error on  $\gamma$  in the Table 11 of about  $\pm 13 \pm 9 \pm 13$ . We think it is a bit too premature to add the modelling and the systematic errors in quadrature to the statistical error; especially the modelling error ought to be left separate for now. Prospects for appreciably reducing the error on  $\gamma$  in the next three years or so seems to be excellent; there are many reasons for this optimism. In fact it is well known there are many common modes CPES(GLW), single-Cabibbo suppressed [67] (CPNES & CPES) as well as double Cabibbo suppressed ones [57] (CPNES & CPES). With increasing luminosity from about  $10^8$  to about  $10^9$   $B$ -pairs as more and more of these channels get added to the analysis, it is anticipated that the statistical error on  $\gamma$  will reduce faster than  $1/\sqrt{N}$ . This is the basis for guess-estimating the error in 2006 to get around  $\pm 9 \pm 6 \pm 7$ . As we enter the era of  $1 \text{ ab}^{-1}/\text{expt}$  around 2008 then we expect the error on  $\gamma$  to be around 5 to 2 degrees. Input from charm factories can help a lot in reducing the error on  $\gamma$  (see talks by Asner, Atwood and Petrov). The optimistic error of  $2^\circ$  may well be plausible by 2008 if sufficient information from charm factory is forthcoming.

Another important way to get these angles is, of course, by studying time-dependent (i.e. MIXCP) CP violation via  $B^0 \rightarrow D^{0(*)} K^0$ . Once again, all the common decay modes of  $D^0$

and  $\bar{D}^0$  can be used just as in the case of direct CP studies involving  $B^\pm$  decays. Therefore, needless to say input from charm factory also becomes desirable for MIXCP studies of  $B^0 \rightarrow D^{0(*)}K^0$ . It is important to stress that this method give not only the combinations of the angles ( $2\beta + \gamma \equiv \alpha - \beta + \pi$ ) but also in addition this is another way to get  $\beta$  cleanly [69, 14, 11]. In fact whether one uses  $B^\pm$  with DIRCP or  $B^0 - \bar{B}^0$  with TDCP these methods are very clean with (as indicated above) the ITE of  $\approx 0.01$ . However, the TDCP studies for getting  $\gamma$  (with the use of  $\beta$  as determined from  $\psi K_s$ ) is less efficient than with the use of DIRCP involving  $B^\pm$ . However, once we go to luminosities  $\geq 1 \text{ ab}^{-1}$  then the two methods for  $\gamma$  should become competitive. This method for getting  $\beta$  is significantly less efficient than from the  $\psi K_s$  studies [69].



## References

- [1] H. Boos, T. Mannel and J. Reuter, Phys. Rev. D **70**, 036006 (2004).
- [2] I. I. Y. Bigi and A. I. Sanda, Nucl. Phys. B **193**, 85 (1981).
- [3] J. S. Hagelin, Nucl. Phys. B **193**, 123 (1981).
- [4] A. J. Buras, W. Slominski, H. Steger, Nucl. Phys. B **245**, 369 (1984); Nucl. Phys. B **238**, 529 (1984).
- [5] S. Herrlich and U. Nierste, Nucl. Phys. B **476**, 27 (1996).
- [6] M. Bander, D. Silverman, A. Soni, Phys. Rev. Lett. **43**, 242 (1979).
- [7] For a review of  $CP$  violation phenomenology, see D. Kirkby and Y. Nir in S. Eidelman *et al.*, Phys. Lett B **592**, 1 (2004).
- [8] B. Aubert *et al.* (BABAR Collaboration), Phys. Rev. Lett. **94**, 161803 (2005); K. Abe *et al.* (Belle Collaboration), Phys. Rev. D **71**, 072003 (2005); Erratum-ibid. D **71**, 079903 (2005).
- [9] Ya. Azimov *et al.*, JETP Lett. **50**, 447 (1989), Phys. Rev. D **42**, 3705 (1990), Z Phys. A **356**, 437 (1997); B. Kayser, NSF-PT-97-2, hep-ph/9709382; H.R. Quinn, T. Schietinger, J.P. Silva, A.E. Snyder, Phys. Rev. Lett. **85**, 5284 (2000); Yu. Grossman, H. Quinn, Phys. Rev. D **56**, 7259 (1997); J. Charles, A. Le Yaouanc, L. Oliver, O. Pène, J.-C. Raynal, Phys. Lett. B **425**, 375 (1998); Erratum-ibid. B **433**, 441 (1998); T.E. Browder, A. Datta, P.J. O'Donnell, S. Pakvasa, Phys. Rev. D **61**, 054009 (2000); J. Charles, A. Le Yaouanc, L. Oliver, O. Pène, J.-C. Raynal, Phys. Rev. D **58**, 114021 (1998). See also [10] and references therein.
- [10] B. Aubert *et al.* (BABAR Collaboration), Phys. Rev. D **71**, 032005 (2005).
- [11] A. Bondar, T. Gershon and P. Krokovny, Phys. Lett. B **624**, 1 (2005). Similar methods were proposed in D. Atwood and A. Soni, Phys. Rev. D **68**, 033009 (2003) and M. Gronau, Y. Grossman, N. Shuhmaher, A. Soffer and J. Zupan, Phys. Rev. D **69**, 113003 (2004).
- [12] Yu. Grossman, M.P. Worah, Phys. Lett. B **395** 241 (1997).
- [13] D.A. Suprun, C.-W. Chiang and J.L. Rosner, Phys. Rev. D **65**, 054025 (2002).
- [14] R. Fleischer, Phys. Lett. B **562**, 234 (2003).
- [15] R. Fleischer, Nucl. Phys. B **659**, 321 (2003).
- [16] A. Poluektov *et al.* (Belle Collaboration), Phys. Rev. D **70**, 072003 (2004).
- [17] A. Giri, Y. Grossman, A. Soffer and J. Zupan, Phys. Rev. D **68**, 054018 (2003).
- [18] I. Dunietz *et al.*, Phys. Rev. D **43**, 2193 (1991).
- [19] K. Abe *et al.* (Belle Collaboration), BELLE-CONF-0546, hep-ex/0507065.

- [20] E-135 Collaboration (LASS Collaboration), D. Aston *et al.*, Nucl. Phys. **B296**, 493 (1988).
- [21] R. Itoh *et al.* (Belle Collaboration), Phys. Rev. Lett. **95**, 091601 (2005).
- [22] B. Aubert *et al.* (BABAR Collaboration), Phys. Rev. D **71**, 032005 (2005).
- [23] Z.Z. Xing, Phys. Rev. D **61**, 14010 (2000); X-Y. Pham and Z.Z. Xing, Phys. Lett. B **458**, 375 (1999).
- [24] A. Datta and D. London, Phys. Lett. B **584**, 81 (2004).
- [25] J. Albert, A. Datta, and D. London, Phys. Lett. B **605**, 335 (2005).
- [26] S. U. Kataoka *et al.* (Belle Collaboration), Phys. Rev. Lett. **93**, 261801 (2004).
- [27] B. Aubert *et al.* (BABAR Collaboration), Phys. Rev. Lett. **91**, 061802 (2003).
- [28] H. Miyake *et al.* (Belle Collaboration), Phys. Lett. B. **91**, 34 (2005).
- [29] T. Aushev *et al.* (Belle Collaboration), Phys. Rev. Lett. **93**, 201802 (2004).
- [30] K. Abe *et al.* (Belle Collaboration), BELLE-CONF-0441, hep-ex/0408107.
- [31] B. Aubert *et al.* (BABAR Collaboration), Phys. Rev. Lett. **90**, 091801 (2003).
- [32] G. Majumder *et al.* (Belle Collaboration), Phys. Rev. Lett. **95**, 041803 (2005).
- [33] B. Aubert *et al.* (BABAR Collaboration), Nucl. Instrum. Meth. A **479**, 1 (2002).
- [34] B. Aubert *et al.* (BABAR Collaboration), Phys. Rev. Lett. **95**, 131802 (2005)
- [35] D. Acosta *et al.*, Phys. Rev. D **71**, 032001 (2005).
- [36] R. Fleischer, Eur. Phys. J. C **10**, 299 (1999).
- [37] J. Simone, invited talk at *Lattice 2004*, Fermilab, June 2004:  
<http://lqcd.fnal.gov/lattice04/presentations/paper252.pdf>
- [38] R.G. Sachs, Enrico Fermi Institute Report, EFI-85-22 (1985) (unpublished); I. Dunietz and R.G. Sachs, Phys. Rev. D **37**, 3186 (1988) [E: Phys. Rev. D **39**, 3515 (1989)]; I. Dunietz, Phys. Lett. B **427**, 179 (1998); P.F. Harrison and H.R. Quinn, ed., SLAC-R-504 (1998), Chap. 7.6.
- [39] T. Sarangi, K. Abe *et al.* (Belle Collaboration), Phys. Rev. Lett. **93**, 031802 (2004).
- [40] T. Gershon *et al.* (Belle Collaboration), Phys. Lett. B 624, **11** (2005).
- [41] B. Aubert *et al.* (BABAR Collaboration), Phys. Rev. Lett. **92**, 251801 (2004).
- [42] B. Aubert *et al.* (BABAR Collaboration), Phys. Rev. Lett. **92**, 251802 (2004).
- [43] O. Long, M. Baak, R.N. Cahn, and D. Kirkby, Phys. Rev. D **68**, 034010 (2003).
- [44] M. Diehl, G. Hiller, Phys. Lett. B **517**, 125 (2001).

- [45] M. Diehl, G. Hiller, JHEP **0106**, 067 (2001).
- [46] M. Gronau and D. London, Phys. Lett. B **253**, 483 (1991).
- [47] B. Kayser and D. London, Phys. Rev. D **61**, 116013 (2000); A.I. Sanda, DPNU-01-19, hep-ph/0108031. See also [57].
- [48] B. Aubert *et al.* (BABAR Collaboration), BABAR-CONF-04/006, hep-ex/0408052.
- [49] R. Aleksan, T. C. Petersen and A. Soffer, Phys. Rev. D **67**, 096002 (2003).
- [50] R. Aleksan and T. C. Petersen, eConf **C0304052**, WG414 (2003), hep-ph/0307371.
- [51] B. Aubert *et al.* (BABAR Collaboration), Phys. Rev. Lett. **95**, 171802 (2005).
- [52] I. Dunietz, Phys. Lett. B **427**, 179 (1998).
- [53] <http://www.utfit.org>
- [54] B. Aubert *et al.* (BABAR Collaboration), Phys. Rev. D **71**, 112003 (2005).
- [55] Sh. Rahatlou, private communication.
- [56] D. Atwood and A. Soni, Phys. Rev. D **71**, 013007 (2005).
- [57] D. Atwood, I. Dunietz and A. Soni, Phys. Rev. Lett. **78**, 3257 (1997); Phys. Rev. D **63**, 036005(2001).
- [58] M. Gronau and D. Wyler, Phys. Lett. B **265**, 172 (1991).
- [59] S. Hashimoto *et al.*, KEK-REPORT-2004-4, hep-ex/0406071; J. Hewett *et al.*, SLAC-R-709, hep-ph/0503261.
- [60] A. Bondar and T. Gershon, Phys. Rev. D **70**, 091503(R) (2004).
- [61] B. Aubert *et al.* (BABAR Collaboration), Phys. Rev. Lett. **92**, 202002 (2004).
- [62] B. Aubert *et al.* (BABAR Collaboration), SLAC-PUB-10655, hep-ex/0408082.
- [63] B. Aubert *et al.* (BABAR Collaboration), Phys. Rev. D **71**, 031102 (2005).
- [64] B. Aubert *et al.* (BABAR Collaboration), SLAC-PUB-10639, hep-ex/0408069.
- [65] B. Aubert *et al.* (BABAR Collaboration), BABAR-CONF-04/13, hep-ex/0408028.
- [66] Particle Data Group, S. Eidelman *et al.*, Phys. Lett. **B592**, 1 (2004).
- [67] Y. Grossman, Z. Ligeti and A. Soffer, Phys. Rev. D **67**, 071301 (2003). M. Gronau, Phys. Lett. B **557**, 198 (2003).
- [68] N. Sinha, Phys. Rev. D **70**, 097501 (2004)
- [69] B. Kayser and D. London, Phys. Rev. D **61**, 116013 (2000). D. Atwood and A. Soni, Phys. Rev. D **68**, 033009 (2003).

- [70] R. Aleksan, I. Dunietz and B. Kayser, *Z. Phys. C* **54**, 653 (1992).
- [71] M. Gronau, *Phys. Rev. D* **58**, 037301 (1998).
- [72] D. Atwood and A. Soni, *Phys. Rev. D* **68**, 033003 (2003).
- [73] B. Aubert *et al.* (BABAR Collaboration), BABAR-CONF-04/043, hep-ex/0408088.
- [74] K. Abe *et al.* (Belle Collaboration), BELLE-CONF-0476, hep-ex/0411049.
- [75] K. Abe *et al.* (Belle Collaboration), BELLE-CONF-0502, hep-ex/0504013.
- [76] S. Kopp *et al.* (CLEO Collaboration), *Phys. Rev. D* **63**, 092001 (2001); H. Muramatsu *et al.* (CLEO Collaboration), *Phys. Rev. Lett.* **89**, 251802 (2002); Erratum-ibid: **90** 059901 (2003).
- [77] M. Gronau, Y. Grossman, N. Shuhmaher, A. Soffer and J. Zupan, *Phys. Rev. D* **69**, 113003 (2004).
- [78] Y. Grossman, A. Soffer, J. Zupan, work in progress.
- [79] D. Atwood, these proceedings; Y. Grossmann, these proceedings.
- [80] A. F. Falk and A. A. Petrov, *Phys. Rev. Lett.* **85**, 252 (2000); A. F. Falk, *Phys. Rev. D* **64**, 093011 (2001).
- [81] J. P. Silva and A. Soffer, *Phys. Rev. D* **61**, 112001 (2000).
- [82] A. F. Falk, Y. Grossman, Z. Ligeti and A. A. Petrov, *Phys. Rev. D* **65**, 054034 (2002).
- [83] S. Bergmann, Y. Grossman, Z. Ligeti, Y. Nir, A.A. Petrov, *Phys. Lett. B* **486**, 418 (2000).
- [84] A. F. Falk, Y. Nir and A. A. Petrov, *JHEP* **9912**, 019 (1999).
- [85] M. Gronau, Y. Grossman and J. L. Rosner, *Phys. Lett. B* **508**, 37 (2001).
- [86] E. Golowich and S. Pakvasa, *Phys. Lett. B* **505**, 94 (2001).
- [87] D. Atwood and A. A. Petrov, *Phys. Rev. D* **71**, 054032 (2005).
- [88] A. A. Petrov, eConf **C030603**, MEC05 (2003), hep-ph/0311371; H. N. Nelson, in *Proc. of the 19th Intl. Symp. on Photon and Lepton Interactions at High Energy LP99* ed. J.A. Jaros and M.E. Peskin, UCSB HEP 99-08, hep-ex/9908021; see also A. Datta, D. Kumbhakar, *Z. Phys. C* **27**, 515 (1985); A. A. Petrov, *Phys. Rev. D* **56**, 1685 (1997); E. Golowich and A. A. Petrov, *Phys. Lett. B* **427**, 172 (1998).
- [89] H. Georgi, *Phys. Lett. B* **297**, 353 (1992); T. Ohl, G. Ricciardi and E. Simmons, *Nucl. Phys. B* **403**, 605 (1993); I. Bigi and N. Uraltsev, *Nucl. Phys. B* **592**, 92 (2001).
- [90] J. Donoghue, E. Golowich, B. Holstein and J. Trampetic, *Phys. Rev. D* **33**, 179 (1986); L. Wolfenstein, *Phys. Lett. B* **164**, 170 (1985); P. Colangelo, G. Nardulli and N. Paver, *Phys. Lett. B* **242**, 71 (1990); T.A. Kaeding, *Phys. Lett. B* **357**, 151 (1995).
- [91] J. L. Rosner and D. A. Suprun, *Phys. Rev. D* **68**, 054010 (2003).

- [92] H. Georgi, Nucl. Phys. B **331**, 311 (1990); H. Georgi and F. Uchiyama, Phys. Lett. B **238**, 395 (1990).
- [93] R.A. Briere *et al.*, CLNS-01-1742 (2001).
- [94] D. Asner, in Review of Particle Physics, Phys. Lett. B **592**, 1 (2004).
- [95] A. A. Petrov, *Proceedings of Flavor Physics and CP Violation* (2003).
- [96] D. Asner and W. Sun, Phys. Rev. D **73**, 034024 (2006).
- [97] H. Muramatsu *et al.* (CLEO Collaboration), Phys. Rev. Lett. **89**, 251802 (2002). [Erratum-*ibid.* **90**, 059901 (2003).]
- [98] R.M. Baltrusaitis *et al.* (MARK III Collaboration), Phys. Rev. Lett. **56**, 2140 (1986).
- [99] J. Adler *et al.* (MARK III Collaboration), Phys. Rev. Lett. **60**, 89 (1988).
- [100] Q. He *et al.* (CLEO Collaboration), Phys. Rev. Lett. **95**, 121801 (2005).
- [101] B. Aubert *et al.* (BABAR Collaboration), Phys. Rev. Lett. **95**, 121802 (2005).
- [102] V.V. Anisovich and A.V. Sarantsev, Eur. Phys. A **16**, 229 (2003).
- [103] J. M. Link *et al.* (FOCUS Collaboration), Phys. Lett. B **585**, 200 (2004).
- [104] D. Cronin-Hennessy *et al.* (CLEO Collaboration), Phys. Rev. D **72**, 031102 (2005).
- [105] K. L. Au, D. Morgan, and M. R. Pennington, Phys. Rev. D **35**, 1633 (1987).
- [106] I. I. Y. Bigi and A. I. Sanda, Phys. Lett. B **211**, 213 (1988).
- [107] F. Abe *et al.* (CDF Collaboration), Phys. Rev. Lett. **81**, 2432 (1998).
- [108] D0Note 4539-CONF (August 2004).
- [109] CDF Note 7438 (February 2005).
- [110] M. Masetti, Phys. Lett. B **286**, 160 (1992).
- [111] R. Fleischer and D. Wyler, Phys. Rev. D **62**, 057503 (2000).
- [112] R. Fleischer, Phys. Rep. **370**, 531 (2002).
- [113] C.C. Meca and J.P. Silva, Phys. Rev. Lett. **81**, 1377 (1998); J.P. Silva and A. Soffer, Phys. Rev. D **61**, 112001 (2000).
- [114] M.A. Ivanov, J.G. Körner and O.N. Pakhomova, Phys. Lett. B **555**, 189 (2003).
- [115] M.A. Ivanov, J.G. Körner and P. Santorelli, Phys. Rev. D **71**, 094006 (2005).
- [116] For an overview of these channels' potential at the LHC see P. Ball *et al.*, CERN-TH-2000-101, hep-ph/0003238, in CERN report on *Standard Model Physics (and more) at the LHC*, CERN, Geneva, 2000.

- [117] R. Fleischer, Nucl. Phys. B **671**, 459 (2003).
- [118] The LHCb Collaboration, *LHCb Reoptimized Detector Design and Performance*, CERN-LHCC-2003-030.
- [119] J. Rademacker, *Measuring the CKM Angle  $\gamma$  with  $B_d \rightarrow D^{*\pm} \pi^\mp$* , CERN-LHCb-2001-153.
- [120] For an overview of strategies, see Cecilia Voena's talk at this conference.
- [121] Heavy Flavor Averaging Group,  
hep-ex/0412073 and <http://www.slac.stanford.edu/xorg/hfag>.